Impact of Fatigue on Corticomuscular Coupling and EEG Microstates during Human-Robot Interaction and Physical Exercise

By

SHADIYA ALINGAL MEETHAL

School of Physics, Engineering and Computer Science
UNIVERSITY OF HERTFORDSHIRE

submitted to the University of Hertfordshire in partial fulfilment of the requirements of the degree of Doctor of Philosophy

MAY 2023

This thesis is dedicated to my parents Abdul Majeed Alingal Meethal and Jameela Chomath Paramba for their endless love, encouragement and prayers that have been a constant source of strength, enabling me to overcome challenges and pursue my dreams.

ACKNOWLEDGEMENTS

I would like to express my sincere gratitude to my principal supervisor Dr Farshid Amirabdollahian for his invaluable guidance, mentorship, expertise and constant encouragement throughout this research. His insightful feedback, constructive criticism, and unwavering support have been instrumental in shaping this thesis. I would also like to personally thank him for his understanding and flexibility, which allowed me to strike a balance between my research and family responsibilities.

My sincere thanks also go to my second supervisor Dr Volker Steuber for his invaluable contributions to my academic journey. I am deeply grateful for the time and expertise he dedicated to thoroughly reviewing my thesis drafts and publications.

I would like to thank my colleagues in Robotic Research Group, in particular Udeshika Dissanayake, Vignesh Velmurugan, Mohamad Reza Shahabian Alashti, Mohammad Hossein Bamorovat Abadi, and Mubashir Ahmad for helping with my research work and providing a pleasant atmosphere during my research in University. Also, I would like to thank all the participants who took part in my studies for their valuable time and feedback. I would also like to thank all my friends who helped me to recruit participants for the experiments.

Special thanks to the research degree administrators for guiding me through the University processes. I am immensely grateful to the two exceptional women Dr Ajisa Muthayil Ali and Dr Sherna Salim who have always motivated me in my research. Their encouragement, kind words, and motivation have been invaluable in times of self-doubt and challenges.

I am incredibly grateful to my dear husband Azeemsha and my lovely daughter Farha for their support and patience. I would also like to acknowledge the financial support provided by the University of Hertfordshire, UK. The work reported in this thesis was supported by the research studentship from the School of Computer Science, University of Hertfordshire, and sincere thanks to the school for the support.

AUTHOR'S DECLARATION

I declare that the work in this dissertation was carried out in accordance with the requirements of the University's Regulations and Code of Practice for Research Degree Programmes and that it has not been submitted for any other academic award. Except where indicated by specific reference in the text, the work is the candidate's own work. Work done in collaboration with, or with the assistance of, others, is indicated as such. Any views expressed in the dissertation are those of the author.

SIGNED: SHADIYA ALINGAL MEETHAL DATE: 31/05/2023

Abstract

Human movements are controlled by the Central Nervous System. Motor dysfunction and sensory-motor deficits result in restricted use of the upper extremities in stroke patients, leading to difficulty in carrying out daily activities. Human-robot interaction (HRI) in rehabilitation can provide individualised, task oriented therapy to patients for fast recovery. The key goals of rehabilitation strategies are to enhance the functional ability and cognitive performance of stroke patients in an optimised way. Therapy can often benefit from assessing progress. Nine Hole Peg Test (NHPT) is one of the widely used tests for assessing upper extremity impairment whose only outcome measure is the time for completion of the task.

Coordination between EEG and EMG signals plays a vital role in movement control. EEG-EMG coherence is considered capable of measuring the control of spinal motor neurons by the cerebral cortex. It helps to understand how the brain controls muscle movement and also the effects of muscle movement on brain function hence can give more insight into fatigue. EEG microstates are recurrent scalp potential configurations that remain stable for a short period of time. The analysis of EEG microstates can help to identify the background neuronal activity at the millisecond level. Analysing EEG-EMG coherence and EEG microstates on a person performing NHPT under fatigue conditions will help us to have a better understanding of underlying neuronal activities.

To explore these an experiment was conducted with 8 healthy participants while interacting with a robot-assisted NHPT. The experiment involved two trials of NHPT, then a fatiguing exercise which was then followed by two more trials of NHPT. EEG-EMG coherence was examined for pre fatigue and post fatigue trials of NHPT. EEG microstates analysis was conducted for resting state conditions, NHPT trial, and also during physical exercise. The analysis of EEG-EMG coherence showed an increase in corticomuscular coupling with fatigue. The increased EEG-EMG coherence suggests that the functional coupling between the brain and muscles becomes stronger with fatigue. Three distinct microstates were observed for the different physical states of participants. Changes were assessed by utilising microstate parameters such as occurrence, coverage, duration, and global explained variance. It was found that the coverage of some microstates is impacted by fatigue in all the experimental stages used for analysis. These results support the involvement of different neural assemblies but also highlight the potential that physical fatigue can be observed and identified by assessing changes in microstate parameters.

TABLE OF CONTENTS

List of Tables

List of Figures

Figure **Page**

GLOSSARY

CMC Corticomuscular coupling.

CNS Central nervous system.

ECR Extensor carpi radialis.

ED Extensor digitorum.

EEG Electroencephalogram.

EMG Electromyogram.

EOG Electrooculogram.

ERD Event Related Desynchronisation.

FCR Flexor carpi radialis.

HRI Human-robot interaction.

MUAP Motor Unit Action Potential.

NHPT Nine Hole Peg Test.

CHAPTER 1

INTRODUCTION

Stroke is the second most common cause of death in the world and 7% of all deaths in the UK are caused by stroke. Stroke is a condition where the blood supply to the brain is disrupted, resulting in oxygen starvation, brain damage and loss of function. One in six people worldwide will have a stroke in their lifetime [67]. Stroke causes a greater range of disabilities than any other condition. Over three-quarters of stroke survivors report arm weakness, which makes their daily living activities difficult [99]. Stroke survivors often suffer from long-term functional impairment and cognitive deficits that diminish their quality of life and pose challenges in personal and social relationships. Motor dysfunction and sensory-motor deficits result in restricted use of the upper extremities in stroke patients, leading to difficulties in carrying out daily living activities.

Human-robot interaction (HRI) is a rapidly growing field that has the potential to transform many aspects of our lives. One of the main areas where HRI is currently being explored is in the field of healthcare. Robots are being developed to assist with tasks such as surgery, patient care, and rehabilitation. Robot-assisted therapy is increasingly accepted as a part of rehabilitative care following stroke.

Human-robot interactions have emerged as a promising field in the development of innovative solutions for upper limb rehabilitation. HRI technology is used to enhance the recovery process in patients with upper limb impairments by providing targeted, task-oriented therapy[12]. Robotic devices are capable of monitoring the patient's movements and providing feedback to encourage proper technique to achieve optimal performance[171][115]. HRI technology can also improve the engagement and motivation of patients during the rehabilitation process. Robots can be designed to provide interactive and engaging feedback during the therapy session, making the experience more enjoyable for the patient[133]. Additionally, robotic devices can collect data on the patient's progress, which can be used to provide personalised treatment plans[98]. Overall, the integration

of HRI technology in upper limb rehabilitation has the potential to improve outcomes and reduce the burden on healthcare providers.

The primary objectives of rehabilitation strategies for stroke patients are to optimise and comprehensively enhance functional ability and cognitive performance. Knowledge of neurological factors behind activities and assessments of stroke patients will help to design better rehabilitation strategies. In therapy, progress is usually evaluated by various assessment techniques. The Nine Hole Peg Test (NHPT) is one of the widely used tests for measuring fine motor dexterity. A reliable outcome measure of NHPT is the time taken to complete placing nine pegs into nine holes [185]. Performance metrics that can assess the quality of fine motor tasks can be gathered with the help of haptic devices.

Damage to the corticospinal system can lead to a diminished ability to voluntarily activate motor units, causing a lack of coordination and strength in muscle activation due to the impaired communication between the brain and the muscles[96]. Stroke patients, as a result of their diminished muscular and cognitive abilities, are susceptible to experiencing fatigue during their rehabilitation exercises. Previous research in our group explored the possibility of using electroencephalogram (EEG) and electromyogram (EMG) features individually as potential fatigue indicators during human-robot interaction[139][47]. The coordination between EEG and EMG signals plays an important role in movement control. The EEG-EMG coherence is considered capable of measuring the control of spinal motor neurons by the cerebral cortex[126]. Understanding the correlation between the brain and muscles can be a powerful tool in enhancing therapies focused on restoring coordination between them. Studying the coherence better helps to understand how the brain controls muscle movement and also the effects of muscle movement on brain function, hence it has the potential to provide some insights on mechanisms underlying fatigue[106].

EEG microstates are able to reflect individual high-level aspects of cognition and information processing[101]. Changes in the scalp electric field configuration imply changes in the distribution of underlying neural generators. This means that different microstate topographies at any time reflect the neural network activity predominating at that time[196].

1.1 Scope of the Thesis

The principal aim of this research is to understand the neurophysiological correlates of fatigue while interacting with a robotic rig and during physical exercise.By exploring the underlying neural and muscular activity associated with fatigue, this study aims to provide valuable insights for the development of more effective rehabilitation strategies. The research methodology employed in this study includes the utilisation of a haptic device, specifically the Geomagic Touch, to administer the NHPT within an embedded reality environment. A g.tec data acquisition system was used to gather EEG and EMG signals from the participants. To gain a deeper understanding

of the neurophysiological correlates of fatigue, two aspects, the EEG-EMG coherence and EEG microstates, are analysed in this study. These analyses will shed light on the coherence between the brain activity and the muscle activation, as well as provide insights into the dynamic patterns of brain activity during fatigue inducing tasks. A subjective assessment of muscle fatigue was also conducted by providing appropriate pre/post-fatigue questionnaires. This subjective evaluation provides complementary information to the objective neurophysiological measurements, enhancing the overall understanding of the fatigue experienced by participants.

Given that this experiment involved healthy participants, its implications extend beyond the scope of stroke rehabilitation, encompassing broader dimensions and applications in various fields. The results of this study aid in injury prevention by identifying and addressing potential risks associated with inappropriate exercise intensity. Moreover, it allows for the optimization of training intensity, empowering runners to enhance their fitness efficiently while minimising the likelihood of overexertion-related injuries.

1.2 Research Questions

The main hypothesis behind this research was:

"Fatigue can be detected and assessed by analysing alterations in neurophysiological parameters during interaction with a robotic rig and physical exercise". The ultimate goal of this research is to understand the link between fatigue and EEG-EMG coherence/EEG microstates in the context of human-robot interaction and physical activity which can help in developing optimised HRI approaches for personalised post-stroke therapy.

This leads to the following research questions which are explored in this thesis.

1.2.1 Research Question 1

How does physical fatigue alter the coherence between EEG and EMG for healthy participants while performing a robot-assisted NHPT?

EEG-EMG coherence has been studied for the pathophysiology of movement disorders[151], as an index of fatigue[66][175][140], and biomarker for motor recovery[93][87][192]. However, none of these studies explored corticomuscular coherence in the context of NHPT. Past research has indicated a high and significant correlation between upper limb muscles and brain activity during motor tasks[142][59]. Thus coordination between the brain and muscles plays a significant part in a person while performing NHPT.

In this research, EEG signals from sixteen electrode locations and EMG signals from three upper limb muscles were collected while a person performs a haptic NHPT. Analysing EEG-EMG coherence provides a comprehensive understanding of the participant's neural and muscular responses during the haptic NHPT task. Fatigue was induced in participants through a repetitive

wrist flexion-extension task using a dumbbell. To explore the impact of fatigue, EEG-EMG coherence was calculated for pre fatigue and post fatigue NHPT.

1.2.2 Research Question 2

Does fatigue impact EEG microstate parameters while interacting with a robotic rig and physical exercise?

EEG microstates represent the momentary organisation of neural activity within specific brain regions and are thought to reflect underlying functional brain networks. Few studies have addressed EEG microstates related to fatigue [173][104], stroke[197][189][63], and exhaustive exercises[199][162][163]. The existing literature already established the influence of muscle fatigue on the modulation of brain activity[55][165][26]. Analysis of EEG microstates can help in better understanding of temporal dynamics of functional brain networks. Most of the studies related to EEG microstates deal with resting state microstates. Here, an attempt is made to perform the analysis of microstates for EEG data acquired from a person while performing the NHPT, before and after a fatiguing condition that is induced using a wrist dumbbell exercise.

1.3 Thesis Layout

The following outlines the contents of each chapter and demonstrates how they contribute to supporting the research questions.

- Chapter 2 presents the literature review which examines existing scholarly work and research relevant to the thesis topic. It analyses previous studies, theories, and concepts to establish a theoretical foundation for the current research. The chapter discusses different topics including electroencephalography, electromyogram, fatigue, stroke rehabilitation, EEG-EMG coherence, EEG microstates, rehabilitation robotics and NHPT.

- Chapter 3 highlights the experiment design, participant demographics, data collection methods, and fatigue exercise used in the study. It ensures the study is conducted in a rigorous and systematic manner. This chapter supports the research questions by providing a clear framework for data collection and analysis.

- Chapter 4 addresses research question 1 by analysing the EEG-EMG coherence. This chapter details the EEG and EMG data preparation and also the analysis of EEG-EMG coherence pre and post fatigue. The analysis indicated an enhancement in corticomuscular coupling as a result of fatigue. The results also demonstrated the difference in coupling between different upper limb muscles and the motor cortex, in the context of the task set for this experiment.

- Chapter 5 explains the microstate analysis to address research question 2. It details the different steps involved in microstate analysis and also describes the three different microstates observed for resting state, NHPT trial and dumbbell exercise. Fatigue induced changes in microstate parameters in these three experiment states are also discussed. Alterations in microstate parameters were observed after the physical fatigue. A decline in the coverage, duration and global explained variance of some microstates was observed as a result of fatigue.
- Chapter 6 summarises the main findings of the study and reflects on the significance of the research and discusses its implications for the theory, practice, and further research.

CHAPTER 2

BACKGROUND

This chapter provides the background information required to support this research. This includes details about the basics of EEG, EMG, corticomuscular coupling, microstates, rehabilitation robotics and fatigue.

2.1 Stroke rehabilitation

Approximately 15-17 million people experience stroke annually worldwide, and roughly one-third of them become permanently disabled[53]. Stroke patients frequently encounter significant physical and mental impairments that considerably affect their everyday existence[82]. Typically, stroke occurs when a blood clot forms in a blood vessel in the brain or when a vessel ruptures and spills blood into the surrounding brain tissue. This can cause damage to some of the nerve cells that connect, resulting in partial paralysis on one side of the body[53]. Rehabilitation training is often necessary for stroke patients to recover lost motor functions. The primary goal of stroke rehabilitation is to help individuals regain as much independence as possible. Rehabilitation can also help stroke survivors manage any long-term effects of the stroke, such as muscle weakness, spasticity (muscle stiffness), or cognitive deficits.

Literature indicates that brain injury can disrupt motor control by reducing the transmission of nerve impulses to the spinal cord, resulting in an impaired responsiveness of motor units. This leads to inadequate muscle activation and control, ultimately impacting motor coordination and altering the pattern of muscle contractions[58][46]. Rehabilitation can help to minimise the damage caused by injury. Multiple researchers have established a correlation between muscle activity and brain activity during the execution of a task-specific activity[72][157][182].

A typical stroke rehabilitation process involves a cyclical approach that includes four stages: (1) assessment to determine the patient's needs and quantify their extent; (2) goal setting to

establish practical and achievable targets for improvement; (3) intervention to aid in achieving the set goals; and (4) reassessment to evaluate the progress made in reaching the agreed-upon goals[97]. The most prevalent form of impairment resulting from a stroke is motor impairment, which limits mobility and muscle movement.

The recovery process for stroke patients is influenced by several factors. Due to the neuromuscular adaptation to a standardised outpatient regimen of exercise, the recovery will reach a plateau often by three months post-stroke onset and most certainly by six months[169][132]. There are studies which emphasise the importance of initiating rehabilitation at an early stage[10]. The high intensity training has more impact on recovery compared to low intensity training at all stages post-stroke. Patients who received high-intensity training showed improved responsiveness even when the treatment was delayed by two years, as compared to those who received low-intensity interventions[10].

Individuals who underwent repetitive task training after experiencing a stroke demonstrated enhanced progress in performing functional activities[54]. Engaging in repeated practice of challenging movement tasks leads to increased cortical representations of the practised movement in the brain. Studies have demonstrated that increased task repetition following a stroke can induce cortical changes and promote functional improvement[27][105][88]. Stroke patients who received repetitive finger tracking training showed improved tracking accuracy and grasp and release function accompanied by cortical reorganisation[27]. Cortical reorganisation and rehabilitation outcomes are positively associated with repetitive task-specific practice[68][174]. A systematic review of the improvement in strength as a result of repetitive training demonstrated a positive impact on muscle strength improvement[44]. This leads to an improvement in functional activity.

After a stroke, the upper extremities are usually more affected than the lower extremities. Individuals with a compromised upper limb often face challenges in performing numerous activities of daily living, such as reaching and grasping objects [83]. While it is crucial to aim for the restoration of upper limb (UL) function in post-stroke patients, the extent of disability may make it harder to achieve complete motor function recovery. Assistive technologies, such as prosthetic limbs and devices can help in restoring movement or can electrically stimulate muscles to induce contractions in the limbs. Long-term implanted systems or surface electrodes can restore paralysed or atrophied muscles with neuromuscular electrical stimulation (NMES)[6]. Wearable sensors can be used in the inpatient stroke and acute rehabilitation setting and have the potential to develop an automated system to quantify the dose of individual rehabilitation therapy[9]. The exact mechanisms of neurological recovery after a stroke are not fully understood. However, fast motor recovery can be achieved by the intervention of more than one therapeutic technique. The rehabilitation of neural pathways heavily relies on cerebral plasticity, which can be influenced by specific therapeutic upper limb exercises in stroke patients[6]. Using a feedback system in a rehabilitative environment will help in achieving faster and better functional outcomes[111].

2.2 Anatomy of human brain

The brain can be segmented into three parts: the cerebrum, cerebellum, and brain stem. The cerebrum, which contains both the left and right hemispheres of the brain, is responsible for a wide range of functions, including movement initiation, sensory information processing and regulating emotional and behavioural expression. The outer layer of the cerebrum is referred to as the cerebral cortex. Voluntary movements of muscles are coordinated by the cerebellum and the motor cortex. Involuntary functions such as respiration, heart regulation, and biorhythms are controlled by the brainstem[148]. Synchronisation of neocortical neurons is achieved with the help of the brain stem and thalamus. The primary origin of the EEG are these layers of cortical neurons[168]. The lateral view of the human brain is presented in Figure 2.1. It can be seen that the cerebral hemisphere is divided into four lobes which are the frontal lobe, the parietal lobe, the temporal lobe, and the occipital lobe.

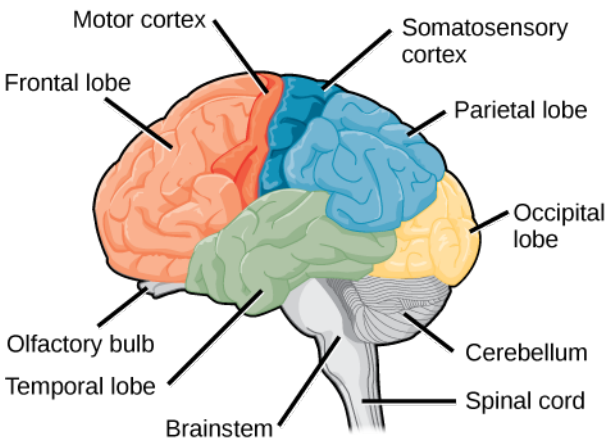

Figure 2.1: Four lobes of human brain[172]

The frontal lobe is the foremost section of the cerebral hemisphere. The frontal lobe houses the motor cortex and olfactory bulb. The olfactory bulb helps in processing smells. The motor cortex is a crucial component for planning and executing movement. The motor cortex comprises different regions that correspond to various muscle groups. Cognitive functions such as maintaining attention, speech, and decision-making are also controlled by neurons in the frontal lobe. The parietal lobe located in the upper region of the brain is responsible for processing two primary functions - somatosensation (touch sensations like pain, pressure, heat, and cold) and proprioception (the sense of body part orientation in space)[172]. The parietal lobe also helps in interpreting language and vision. The main function of the occipital lobe which is located at the back of the brain is to help in seeing, recognizing, and identifying the visual world. The temporal lobe is located anterior to the occipital lobe and posterior to the frontal lobe[135]. The primary function of the temporal lobe is the processing and interpreting of sounds. The medial surface of the temporal lobe helps in processing memory formation[73]. EEG collected from different parts

of the brain provides means for identifying numerous neurological disorders and other anomalies within the human body.

2.3 Electroencephalography (EEG)

Electroencephalography is one of the most powerful techniques which helps to study the electrical activity of the brain[35]. The electrical activity of the brain can be recorded with the help of placing sensor electrodes on the scalp. With its high temporal resolution, EEG provides the opportunity to investigate the cortical and subcortical brain activity and observe the dynamic behaviour of neuronal networks across the entire brain[19][153]. Richard Caton is credited with the first recorded instances of neurophysiologic activity in animals in 1875, while the recording of electrical brain activity in humans did not occur until 50 years later. In 1924, Hans Berger, a German psychiatrist, was the first to develop EEG techniques for use on humans[107]. The excellent temporal resolution of EEG makes it a valuable tool for investigating the timing and coordination of neural events underlying various cognitive and sensory processes.

2.3.1 Origin of EEG

The central nervous system (CNS) comprises nerve cells and glial cells. Nerve cells contain axons, dendrites, and cell bodies, and can transmit information over long distances in response to stimuli. Action potentials and postsynaptic potentials contribute to the electrical activities of neurons. An action potential (AP) is an electrical impulse transmitted by a nerve, caused by the flow of ions across the neuronal membrane. This temporary change in the membrane potential travels along the axon in one direction, typically initiated in the axon hillock close to the cell body. The depolarisation of the membrane potential produces a spike, followed by repolarisation and a return to resting state. Most nerve action potentials last about one millisecond[148]. An example of the action potential is shown in Figure 2.2. Various types of stimuli can initiate APs, with sensory nerves responding to a range of modalities such as chemical, light, electricity, pressure, and touch. Action potentials upon arriving at synapse result in the release of a chemical substance which changes the permeability of the postsynaptic membrane of the next neuron. A difference in potential is created as a result of ion movements across the membrane. An excitatory postsynaptic potential (EPSP) is generated due to the influx of positive ions into the neuron, while an influx of negative ions or an efflux of positive ions creates an inhibitory postsynaptic potential (IPSP) and the neuron becomes hyperpolarised. The summation of synchronously generated postsynaptic potentials contributes to the EEG [15].

2.3.2 EEG Frequency bands

A normal EEG recording displays voltage values along the vertical axis and time along the horizontal axis, producing a nearly real-time visualisation of current cerebral activity. The

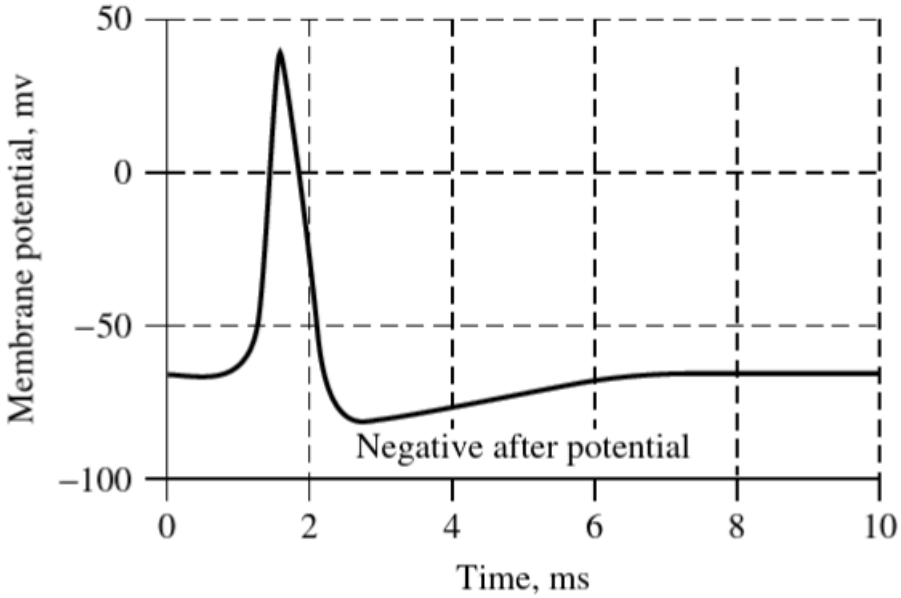

Figure 2.2: An example of action potential[148]

amplitude and frequency of EEG signals change from person to person depending upon their cognitive state. Based on the frequency ranges brain waves are categorised into five types: delta, theta, alpha, beta, and gamma[148]. Delta waves are the slowest of all brain waves which lie in the range 0.5-4Hz. These are mainly present in EEGs of deep sleep and are most often found in infants and young children. Suppression of this wave can lead to poor sleep and inability to revitalise the brain[1]. The frequency of theta waves ranges from 4Hz to 7.5Hz and are associated with drowsiness, deep meditation and daydreaming. Theta oscillations are prominent in infants and young children but rarely observed in healthy adults[129]. Strong theta activity in a waking adult may be caused by various pathological problems[148]. Alpha rhythms, which appear in the frequency range 8Hz-13Hz, are normally associated with relaxed wakefulness. The alpha frequencies transiently increase immediately after eye closure and are often attenuated with eye opening[168]. Brain rhythms in the frequency range of 13-30Hz with a voltage less than 30μV are termed beta waves. Beta waves are the normal wake-up rhythm of the brain associated with active thinking, attention, or solving specific problems. Rhythmical beta activity is mainly found in the frontal and central regions[148]. The gamma band, the highest frequencies of EEG typically includes frequencies above 30 Hz. Gamma waves are modulated by sensory input and are associated with a broad range of cognitive phenomena such as working memory and attention[74].

During physical motor execution and mental motor imagery, a relative power decrease/increase can be observed in the electroencephalogram within a specific frequency band. This phenomenon

is widely utilised for the purpose of brain-computer interfaces (BCI) and is known as Event-related desynchronisation/synchronisation (ERD/ERS). ERD serves as an indicator of phasic alterations in the synchronicity of cell populations, presenting a reliable marker for heightened neuronal excitability within thalamocortical systems[167]. An experiment investigating the effect of kinematic and kinetic changes in hand grasping movements on ERD strength found that the strength of ERD could indicate the time differentiation of hand postures during the motor planning process or the changes in proprioception arising from hand movements[127]. Another research exploring deficits linked to the planning and execution of temporally cued movements, specifically examining neural oscillatory changes in the alpha and beta bands, revealed that the deceleration in motor reaction times observed in speech production and limb movement among older adults was attributable to desynchronisation of pre-motor alpha and beta band activities[78].

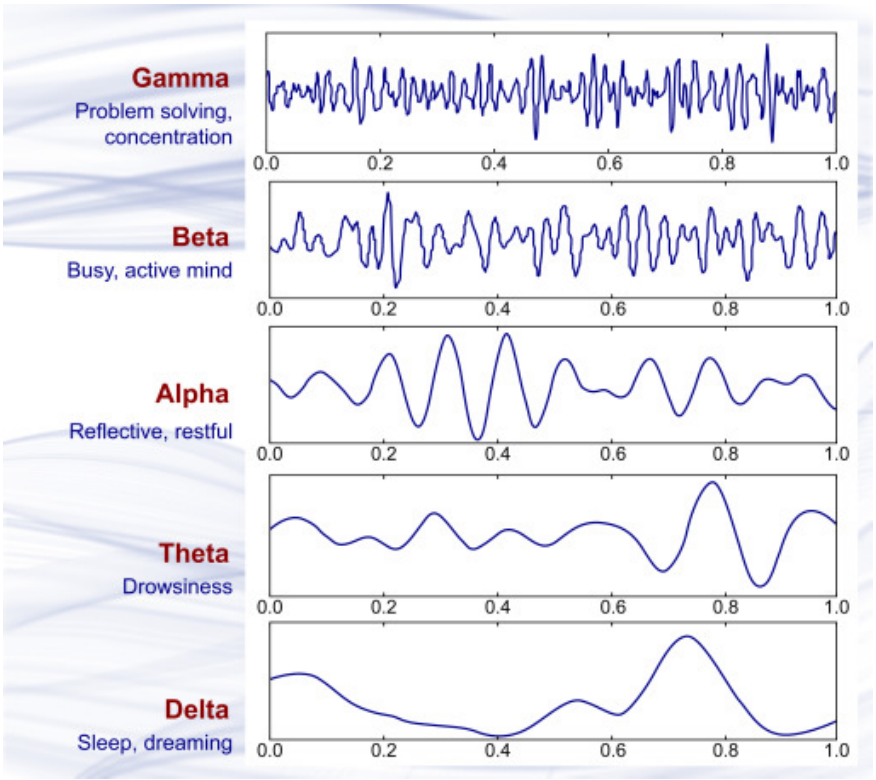

Figure 2.3: EEG rhythms[1]

2.3.3 EEG recording and artefacts

Richard Caton, a Liverpool physician, made the first attempt to record the electrical activity of the animal brain with the help of a reflecting galvanometer. He published his results in 1875[152]. With the advancement of technology, recording systems were developed with electrodes and needle-type registers. The multi-channel recording of EEG signals was made possible with the

help of these and EEG waves were plotted on plain paper or paper with grid. Later, analog to digital converters were introduced to digitise the signals for analysis in computer based systems[148]. Current EEG recording systems involve different sets of electrodes and operational amplifiers followed by filters. These electrodes are made up of conductive materials. The signals collected via the sensor electrodes are stored in a computer for later analysis. In intracranial EEG acquisition, needle electrodes are implanted under the scull. Scalp EEG acquisition systems usually have Ag-AgCl disks placed on the scalp as electrodes[148]. Electrode caps are often used for multichannel EEG acquisition. To preserve the quality of the recorded signal, the contact impedance between the electrode surface and scalp must be at minimum. Skin preparations are often carried out for this. A conductive gel or paste is used on the scalp to reduce the contact impedance between the electrode surface and scalp[178]. The type of electrodes which use conductive gel between the scalp and electrodes are termed wet electrodes. There is another category of electrodes which does not use any conductive materials at the junction between electrodes and scalp and is termed dry electrodes. Dry electrodes are easier to apply, however, they are more susceptible to movement artefacts[137]. The signal quality is at risk when using dry electrodes. Dry electrodes are suitable in experiments with longer duration since they provide better stability. On the other hand wet electrodes produce good quality signals for shorter duration[48].

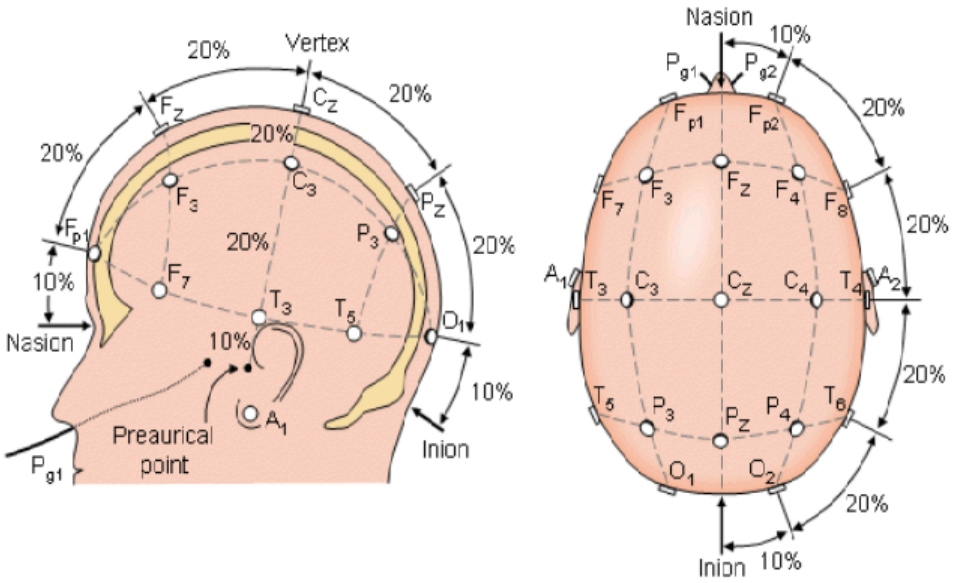

Figure 2.4: International 10-20 electrode positioning system[110]

The electrode placement on the scalp is standardised by the International Federation in Electroencephalography and Clinical Neurophysiology which has defined the 10-20 electrode placement system[71]. In this system, 21 electrodes are positioned on the scalp between the nasion

and inion and between the auricular (ear) positions as shown in Figure 2.4. Nasion is the point at the bridge of the nose and inion is the prominent bump on the back of the head representing the lowest point of the skull[21]. Each electrode is represented with a unique letter which points to the lobe where the electrode is located followed by a number. Electrodes on the left side of the head are odd numbered and those on the right side are even numbered. 10-20 represents the positioning of electrodes at standard intervals of 10 percent or 20 percent. To incorporate additional electrodes the international 10-10 system is introduced which is an extension of the 10-20 electrode placement system. Here the additional electrodes are placed halfway between the electrodes in a traditional 10-20 system[128]. This is illustrated in Figure 2.5. The mode of recording can be either differential or referential. In differential recording mode signals from two electrodes are fed into two inputs of the differential amplifier. On the other hand, in a referential system, one or two electrodes are kept as a reference electrode[148]. An inactive site which is maximally distant from the brain sources is normally used as the reference electrode[69].

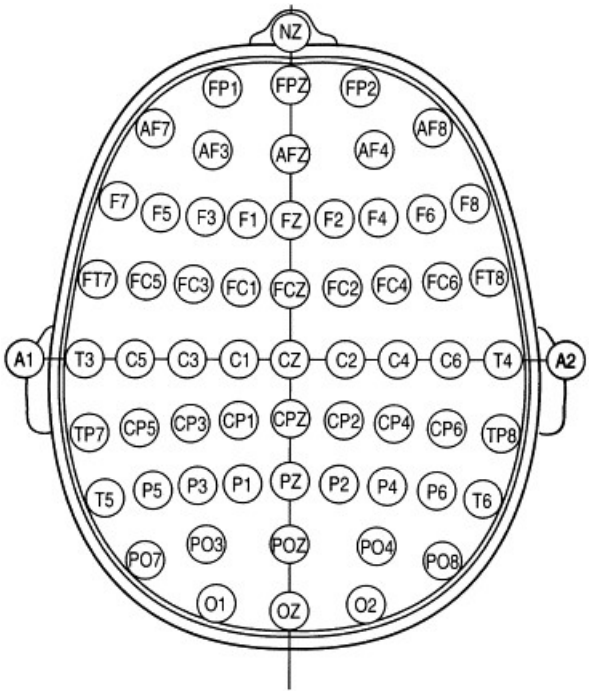

Figure 2.5: 10-10 electrode positioning system[128]

A non invasive EEG acquisition system with g.GAMMA cap and a biosignal amplifier is utilised in this study for the EEG signal acquisition. The electrode positions on the cap follow the international 10-10 system and the g.LADYbird active electrodes are used for signal acquisition. The right ear lob served as the reference electrode in this study.

There are person-related and system-related artefacts which corrupt the recorded EEG signal. Body movement related artefacts, EMG, ECG, EOG, sweating, etc., are classified as person-related artefacts. Power supply interference, impedance fluctuation, cable defects and interference from

electrical components come under the system artefacts[148]. These artefacts are often removed in the preprocessing stage to retain the quality of the signal. EEG has the potential to enhance our understanding of human mental states, imagination and cognitive processing. The most common application of EEG is in Brain Computer Interfaces (BCI) where real time EEG data is used for controlling mechanical and electronic devices[160]. Research was conducted on the EEG to help people with disabilities and motor activity impairment, such as directing electrical wheelchair movement[121][158], recognising movement attempt in stroke patients[161], Post-stroke motor rehabilitation[164][37], robotic rehabilitation[25][166][103] etc.

2.4 Electromyography (EMG)

Electromyography (EMG) is a sensing and diagnostic procedure that helps to explore muscle activity and the nerve cells that control them. The basic theory behind EMG is that when the contraction of muscles happens a burst of electrical activity is generated in the muscles which can be recorded from the overlying skin areas. Human muscles are capable of contraction and relaxation. Similar to nerve cells, muscle tissues are also capable of conducting electric potentials which are called muscle action potential. A noninvasive electrode placed on the skin or a needle electrode inserted in the muscle can detect a motor unit action potential (MUAP) which is the summation of muscle fibre action potentials from all the muscle fibres of a single motor unit[143]. When muscle fibres are at rest, the difference in concentrations of sodium (Na^+), potassium (K^+) and chloride (Cl^-) on either side of the muscle membrane gives rise to a voltage gradient (about -90mV). Under resting conditions, the concentration of Na^+ is lower inside the membrane compared to outside. Conversely, for K^+ the inside concentration is higher compared to the outside membrane[57]. When the muscle cells are excited by a stimulus, the permeability of the muscle membrane changes and an influx of Na^+ happens. This leads to the depolarisation of the membrane. This depolarisation is immediately restored by a backward exchange of ions[92]. Depolarisation of the membrane by a certain threshold will lead to muscle fibre action potential. An electric field will be created near each muscle fibre as a result of this depolarisation-repolarisation process. While initiating a movement the central nervous system activates muscles. Since a single motoneuron can stimulate multiple muscle fibres, the firing of a motoneuron results in the activation of many muscle fibres. The combination of electrical activities of all these muscle fibres results in the generation of a motor unit action potential or MUAP[57]. The sequence of Motor Unit Action Potential (MUAP) in response to neural stimulation constitutes the EMG signal[143].

A basic motor control mechanism schematic is shown in Figure 2.6. While initiating a movement signals are generated from the primary motor cortex which influences different neurons of the brain stem and spinal cord. A motor unit is composed of α-motoneuron and the muscle fibre that it innervates[114]. When the central nervous system excites the α-motoneuron,

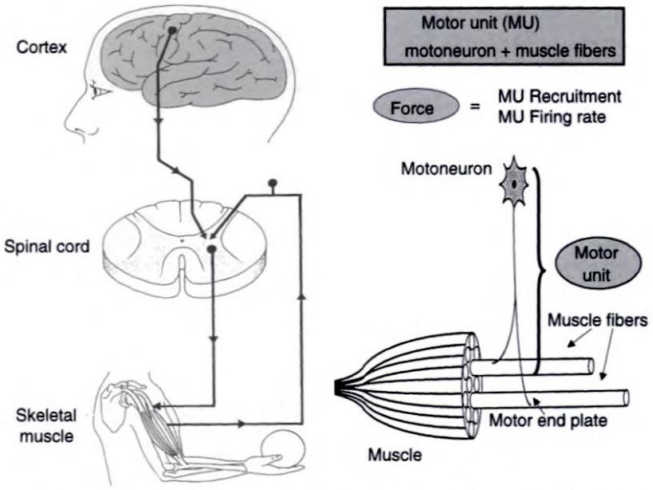

Figure 2.6: Schematic of basic motor control mechanism[114]

it causes the transmission of the excitation along the motor nerve[92]. The firing pattern of the motor unit is determined by the net current induced by various synaptic innervation sites. Depending on the size of the muscle the number of MUs per muscle in humans ranges from about 100 to 1000[114]. The peak-to-peak amplitude of EMG ranges between +5mV and -5mV with frequency ranges between 6 and 500Hz[92]. Surface EMG can be recorded by applying adhesive electrodes to the skin and connecting these to a biosignal amplifier. Different factors affect the quality of recorded EMG signal like the type of the detection surface, the electrode shape, the distance between the electrode detection surface, and the placement of the electrode in relation to the muscle's motor points. Physiological, anatomical, and biochemical factors like blood flow, fibre diameter, depth and location of active fibres also affect the EMG recording[143]. Technological advancements in EMG recording and processing methods enabled the use of EMGs in a wide variety of applications. EMG signals are extensively used in post-stroke rehabilitation by using EMG-driven computer games[156], developing control models for upper limb orthosis[181],[145], gesture classification[39][125], user intention detection[195], etc.

2.5 Fatigue

Fatigue is a common symptom experienced by individuals in both acute and chronic illnesses, as well as in daily life. Defining fatigue has been a challenge for scientists, given the complex interaction of biological processes, psycho-social phenomena, and behavioural manifestations. Fatigue can be described as an ongoing sensation of exhaustion or weakness that can manifest itself as either physical, mental or a blend of both. Fatigue can impair a person's ability to think clearly, concentrate, and make decisions[51]. Fatigue can cause muscle weakness, decreased endurance, and slower reaction times, which can negatively affect physical performance[23].

Fatigue can significantly impact a person's ability to enjoy life and engage in normal activities, leading to a reduced quality of life[64].

2.5.1 Physical fatigue

Physical fatigue or muscle fatigue is a common phenomenon that occurs when a muscle is no longer able to maintain its contractile force or sustain its performance over time[49]. The symptoms of physical fatigue can manifest themselves in a variety of ways, including weakness, decreased coordination, and reduced physical performance. Physical fatigue can also cause mental fatigue, making it challenging to concentrate or think clearly. Muscle fatigue is the outcome of several physiological alterations in the active muscle and is usually mild or short-lived. Once the exercise is terminated, the discomfort typically subsides[77][49]. The intensity and duration of physical fatigue can vary depending on the type and intensity of the activity, muscle groups involved, an individual's fitness level, and their overall health status[186].

Muscle fatigue can be classified as temporary or chronic. Temporary muscle fatigue is often caused by strenuous physical activities which will lead to the accumulation of intermediary energy metabolism waste (e.g., lactate) in the intracellular space of working muscles or the depletion of energy-rich compounds (e.g., muscle glycogen store). Chronic muscle fatigue can result from various factors, including thinning of muscle tissues due to the presence of chronic inflammation in cardiovascular and respiratory disorders, trauma, critical illness, and certain medications[38]. Fatigue can have a significant impact on overt performance, causing the task to be performed more slowly or even unsuccessfully. Additionally, fatigue can alter the neuromuscular activity required to perform the task. The standard approach for assessing muscle fatigue involves temporarily halting the fatiguing activity and performing a brief maximum contraction to determine the reduction in maximum force capacity. Additionally, EMG can serve as a marker of muscle fatigue[193]. Muscle fatigue is a common symptom experienced by stroke survivors. The diminished ability to enhance central excitability in response to an increased cortical inhibition associated with the fatiguing contraction may contribute to central fatigue observed in affected limb[89]. This type of fatigue may also be related to a rise in self-reported fatigue experienced during the performance of daily activities. Fatigue experienced by stroke survivors in the early post-stroke phase may be caused by biological factors. In contrast, the causes of fatigue experienced in the later stages of stroke recovery may be more related to psychological and behavioural factors[131].

2.5.2 Cognitive fatigue

Mental or cognitive fatigue refers to a reduction in cognitive abilities that occurs over time during sustained cognitive demands. This can lead to difficulties in suppressing irrelevant information during selective attention, weakened cognitive control, decreased high-level information processing, as well as declining physical performance[187]. Cognitive fatigue can negatively

impact productivity, increase accident risks, and reduce the quality of life in both normal and clinical populations. Extensive research has been done in the areas of EEG and cognitive fatigue. The effectiveness of EEG energy parameters as indicators of attention and alertness levels are explored and found that EEG energy levels increase with an increase in cognitive load[154]. Mental fatigue can also be impacted by physical activities and physical activities speed up the fatigue process[193]. A study of EEG and ERP (Event Related Potential) correlates of cognitive fatigue during sustained mental work showed that time on task had a progressive influence on frontal midline theta and parietal alpha activity[177]. Event-related potentials (ERPs) refer to voltage changes in the ongoing EEG activity that are synchronised in time with sensory, motor, and cognitive events[43]. Cognitive impairment and depression exhibit a relatively high prevalence subsequent to Transient Ischemic Attack (TIA) as well as minor stroke, which undergoes a reduction over time. The frequency of cognitive impairment following TIA and minor stroke was found to be influenced by the measurement tool employed[122]. EEG indicators of fatigue during robot-assisted activities are contingent on whether the task is physically or cognitively demanding and whether it involves the proximal or distal regions of the upper limb[47].

2.6 EEG-EMG coherence

Temporal and spatial relations among the cortical activities and voluntary or involuntary movements can be understood with the help of simultaneous recording of electroencephalograms and electromyograms[155]. EEG signals reflect the collective activity of neurons in the brain and EMG measures the collective firing of a motor unit. Consequently, EEG-EMG coherence is deemed suitable for exploring the control of muscle activity by the cerebral cortex[106]. EEG-EMG coherence is a measure of functional connectivity between the cortex and muscles during continuous muscle contractions, which originates from the communication in corticospinal pathways between the primary motor cortex and muscles[106].

Coherence is a measure of the temporal correlation between two signals at various frequencies. The outcome is represented by a coherence spectrum ranging between 0 and 1 for each relevant frequency, where a value of 1 implies a complete temporal correlation, whereas 0 indicates no correlation[146]. For two time series signals $x(t)$ and $y(t)$, coherence is calculated by normalising the square of the cross spectral density between signals $x(t)$ and $y(t)$ by the product of their individual auto spectral densities. The mathematical expression for coherence *Cxy(f)* can be represented as

$$Cxy(f) = \frac{|Pxy(f)|^2}{Pxx(f)Pyy(f)} \tag{2.1}$$

where *Pxx(f)* and *Pyy(f)* are the power spectral densities of $x(t)$ and $y(t)$ respectively and *Pxy(f)* is the cross spectrum for $x(t)$ and $y(t)$ at a given frequency f [118].

The level of coherence between cortical and muscle activities is subject to variation depending on the extent of cortical engagement in distinct tasks. The coherence between EEG and EMG in the beta frequency band (13-30 Hz) has been reported to be significant during visuomotor tasks[86]. Significant gamma band coherence can be seen in dynamic movements and intense hand muscle contractions[22][13]. Active exercises with movement intention can modulate the coherence and mutual information between EEG and EMG[87]. Modulations of corticomuscular coupling occur as a result of visuomotor skill learning, immobilisation, and development. This suggests modifications in synchronisation between the cortex and peripheral neurons as part of the motor adaptation process[136][109][70]. Another study uses corticomuscular coupling as a way for classifying various grasps [34]. The results provide information about the synchronisation between brain and muscles during motor activities. The work suggests that CMC can be used as an effective tool for classifying different motor activities.

2.6.1 EEG-EMG coherence and fatigue

Fatigue is a complex construct that encompasses both physiological and psychological dimensions. The extent of cortical centres' involvement in inducing fatigue during voluntary motor tasks or regulating muscle fatigue remains largely uncertain[201]. EEG-EMG coherence can serve as a measure of the functional link between the cortex and muscles during fatigue. A study of EEG-EMG coherence showed that fatigue enhanced the functional synchronisation between the cortex and the muscles during an intermittent handgrip fatigue task[66]. Single trial wavelet coherence analysis on the effects of muscle fatigue on corticomuscular coupling provided information regarding dynamic adaptations of the brain and exhibited a reduction in corticomuscular coupling[140]. Fatigue impacts the connection strength and topology of the cortical-muscle network during isometric contraction at 30% maximal voluntary contraction, also dynamic forces in fatigue lead to a shift from the beta band to gamma band[191]. The development of muscle fatigue enhances the corticomuscular coupling during sustained submaximal isometric contraction. Corticomuscular coherence can also be modulated by sensory feedback[179].

The effects of acute muscle fatigue on corticomuscular coupling remain an area of significant controversy within the research literature. While some investigations have reported an increase in corticomuscular coupling with fatigue, others have demonstrated a decrease in this phenomenon. It is worth noting that the variability in the muscles studied across different investigations might also influence corticomuscular coupling. Despite an increase in EEG and EMG power as a result of fatigue, weakening of EEG-EMG coherence during sustained isometric elbow flexion at 30% of MVC was observed in the beta band[194]. An investigation on the influence of physical activities on mental fatigue found a reduction in beta band coherence[193]. Impaired functional coupling between the brain and muscle signals was observed in patients who experience cancer-related

fatigue compared to healthy participants[75]. Qian et al. [141] investigated the effects of force load and muscle fatigue on the EEG-EMG coherence in different frequency bands during side arm lateral raise tasks. They found that there is a significant reduction in gamma band coherence area under muscle fatigue. They proposed that this effect can be removed by applying magnetic stimulation.

2.6.2 EEG-EMG coherence and stroke

Despite the lack of a clear understanding of the physiological significance of corticomuscular coherence, there is already evidence suggesting that abnormal coupling between the cortex and muscles plays a role in the pathophysiology of movement disorders[151]. Zheng et al. investigated the feasibility of reflecting the motor function improvement after stroke with the measurement of CMC [188]. The study found that the beta-band CMC of the paretic limb increased after recovery compared to the unaffected side. Chen et al. [31] performed a study on stroke patients and found that the corticomuscular coupling gets affected in stroke patients compared to healthy controls. They suggested that the gamma band coupling is linked to somatosensory tasks and the beta band oscillations are associated with controlling and maintaining steady state force. During movement, individuals who have suffered from a stroke exhibit significantly lower levels of corticomuscular coherence compared to healthy controls in both the beta (20-30 Hz) and lower gamma (30-40 Hz) frequency bands[50]. A study on EEG-EMG coherence during wrist extension in patients who suffered ischaemic stroke showed a gradual increase of coherence over time. It even reached a greater level than that seen in healthy participants[93]. Brain regions in the contralesional hemisphere play a role in the activity of affected muscles after stroke thereby supporting functional recovery[147]. A case study during an elbow flexion task shows an increase in corticomuscular coupling accompanied by the motor function recovery of the paretic limb[200]. An investigation on temporal dynamics of corticomuscular interactions in post-stroke recovery found large corticomuscular coupling(CMC) amplitudes on the unaffected side in the acute period compared to the chronic period [183]. Moreover, CMC amplitudes were larger on the unaffected side compared to the affected side. Correlations have been observed between changes in corticomotor connectivity and motor improvement at various stages of stroke. However, when compared to clinical metrics, follow-up scores based on CMC have not demonstrated statistically significant correlations[113].

2.7 EEG Microstates

Electroencephalography (EEG) microstates are brief periods of stable EEG topography that reflect the momentary functional organisation of the brain[20]. The concept of EEG microstates was developed by Dietrich Lehmann and his team in the late 1970s to quantify the spatio-temporal dynamics of the brain[91]. They suggested that the multichannel EEG recorded over the brain

follows a stable map configuration for a short period of time. Within a defined period of consistent configuration, the electric field's strength undergoes fluctuations of increase and decrease, while the topography itself remains stable. This observation, initially articulated by Dietrich Lehmann and colleagues, posits that these intervals of stable electric field configurations reflect specific stages or components of information processing, essentially serving as the fundamental elements constituting the content of consciousness-referred to as "atoms of thoughts" and termed functional microstates[117]. Changes in the scalp electric field configuration imply changes in the distribution of underlying neural generators. This means that different microstate topographies at any time reflect the neural network activity predominating at that time[196]. EEG microstate analysis has been applied in clinical and cognitive research to explore altered brain activity patterns associated with various neurological and psychiatric disorders.

EEG data collected from different electrodes on the human scalp can be viewed as a series of maps of the momentary spatial distributions of electric potential[102]. The topography of the electric field and the potential map's configuration remain stable for a certain period before abruptly transitioning to a new configuration. The Global Field Power (GFP), calculated as the standard deviation of all momentary potential values across the map, provides a singular numerical representation for each moment in time from multiple simultaneously recorded electrode locations. At these specific time points of maximal global field power, the momentary maps tend to exhibit consistent landscapes over several successive maps[101]. Sharp transitions separate discrete segments of electrical stability maps. During a stable configuration period, although the strength of the field may fluctuate, the topography of the potential map remains unchanged[117]. The maps during periods of maximal global field power are selected for analysis, utilising the locations of maximal and minimal values of potentials (extrema dipole) as descriptors for the landscape (Figure 2.7). A series of "extrema dipole maps" are generated, one at each time of maximal global field power which is presented in Figure 2.8. Maps exhibiting the same dipole orientation are categorised under the same microstate. The stability of map topographies over time in the spontaneous EEG is demonstrated in Figure 2.9.

The process of microstate analysis can be divided into two primary stages. The first step involves the selection of a group of microstate topographies with the help of mathematical clustering, and the second step entails re-expressing the initial data as an alternating sequence of these microstate topographies[84]. Momentary spatial distribution maps at peak times of global field power (GFP) are used for microstate analysis [150]. Optimal signal to noise ratio and stable topography are obtained at the local maximum of GFP[198]. Global field power is used to measure the strength of the scalp potential. The global field power (GFP) can be calculated as

$$GFP(t) = \sqrt{\frac{\sum_i^k \left(V_i(t) - V_{mean}(t)\right)^2}{k}} \tag{2.2}$$

where $V_i(t)$ is the voltage at electrode i at time t, $V_{mean}(t)$ is the mean voltage across all

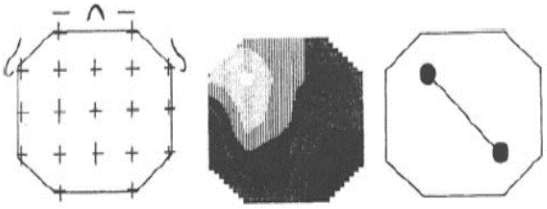

Figure 2.7: Representation of a momentary map of the brain electric field using the "extrema dipole." Left, 19-electrode array where the anterior row was at 40% nasion- inion, the posterior row at the inion and interelectrode spacing was about equidistant on the head. Center, Interpolated surface as equipotential areas white is more negative, black more positive. Right, Two extrema in the array outline connected by a line that visualises the orientation of the " extrema dipole." [101].

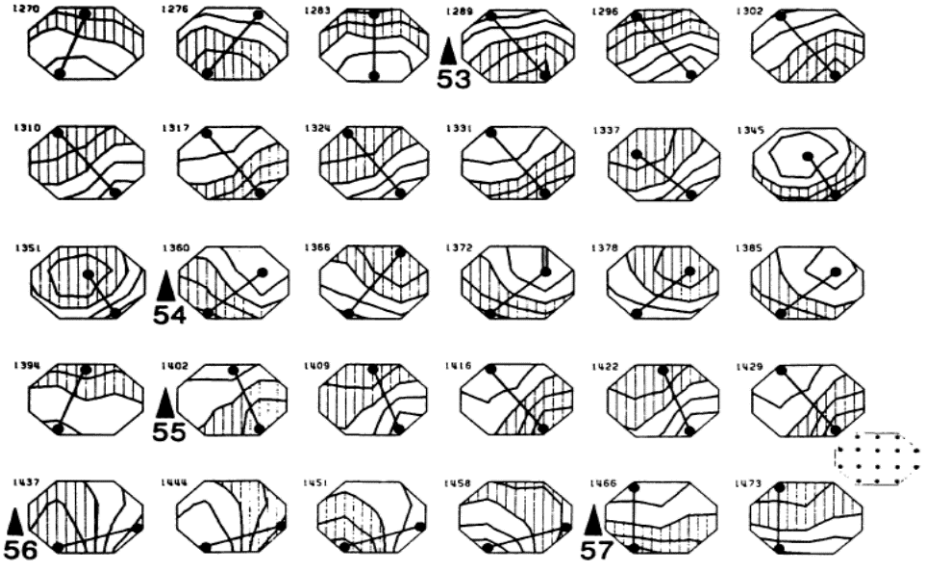

Figure 2.8: Sequence of EEG maps presenting the spatial distribution of the extreme potential values at maximal global field power. The number above each map gives the precise number of global field power maxima. The number at the bottom shows a segment of similar EEG maps. All the EEG maps between numbers 54 and 55 have the same orientation for dipole, hence belonging to the same microstate[101].

electrodes at time t and k is the number of electrodes[84]. A clustering algorithm is applied to these EEG signals at the GFP peaks to produce a small number of cluster maps. The selection of the number of maps is typically determined by a cross-validation criterion[1], which is a measure of fit[56]. The cross-validation criterion (CV), as introduced by Pascual-Marqui et al.[134], is

[1]This is different from the cross validation used in machine learning.

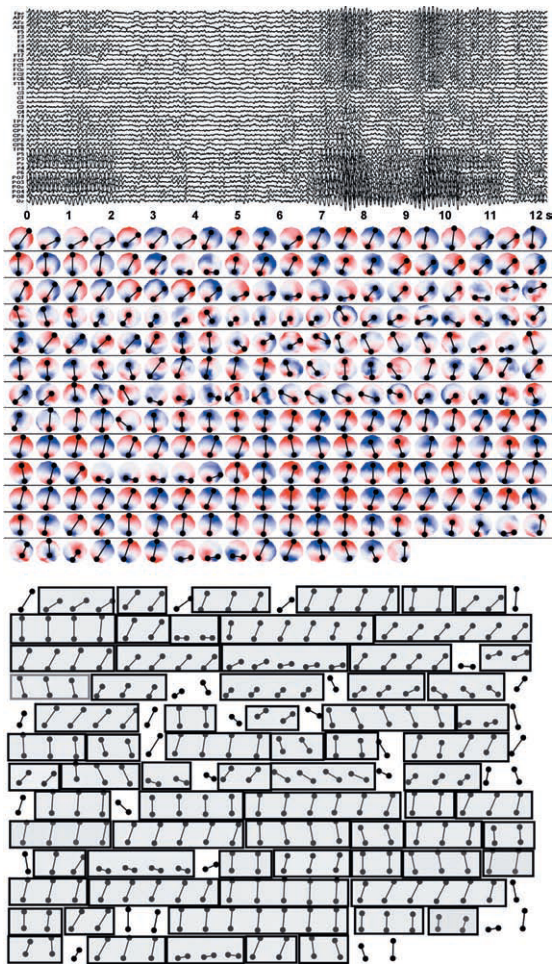

Figure 2.9: Demonstration of the stability of map topographies over time in the spontaneous EEG. Top: 42-channel spontaneous eyes-closed EEG of 12 s duration. Middle: Succession of maps over the 12 s. Only maps at GFP peaks are shown. Bottom: Only the positive and negative maxima positions are shown and connected. Periods of stable map topographies are surrounded by boxes and marked in gray[117].

associated with residual noise, aiming to achieve a minimized CV value.

$$CV = \hat{\sigma^2}.\left(\frac{C-1}{C-K-1}\right)^2, \tag{2.3}$$

where $\hat{\sigma^2}$ is an estimator of the variance of the residual noise calculated as:

$$\hat{\sigma^2} = \frac{\sum_n^N x_n^T x_n - \left(a_{l_n}^T x_n\right)^2}{N(C-1)} \tag{2.4}$$

Here C is the number of EEG channels, N is the number of time samples, K is the number of clusters (microstate classes), x_n is the n'th time sample of the recorded EEG, a_k is the prototypical map for the k'th microstate cluster, l_n is the microstate label of the n'th EEG sample.

After determining the cluster maps, they are fitted to the individual participant's EEG data to extract the different temporal parameters associated with each of them. Temporal parameters of microstates that are commonly calculated are:

- Duration: the average duration that a given microstate remains stable
- Occurrence: the frequency of occurrence for each microstate independent of its duration
- Coverage: the fraction of total recording time for which a given microstate is dominant
- Global Explained Variance: the amount of EEG data variance captured by the set of microstate maps[116]

Microstate analysis results can be affected by different data acquisition strategies, preprocessing methods, and smoothing parameters used. However, a study on the test-retest reliability on microstate features revealed that the results remain highly stable, independent of the strategies used to determine the cluster maps and the number of recording electrodes[84]. Remarkably, most studies investigating resting-state EEG have identified the same four prototypical microstates that account for the majority of the global topographic variance[85]. These microstate maps are labelled as A, B, C and D and are presented in Figure 2.10.

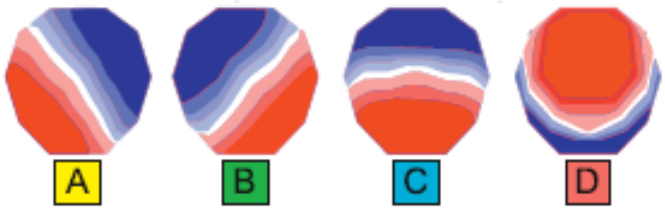

Figure 2.10: Four microstate maps that commonly occur in literature[85]

2.7.1 EEG microstates and fatigue

The analysis of EEG microstates is highly relevant for investigating various diseases and changes in behavioural states in humans. However, limited research has been conducted on the effects of fatigue on microstates. An increase in the amplitude of microstate intensity is observed in individuals when moving from alert to fatigued state[173]. The effects of mental fatigue induced by continuous simulated flight multitasking on EEG microstate parameters are explored in [104]. The study suggests that EEG microstates can detect the global brain network activation related to mental fatigue. A decline in the mean duration, time coverage and global explained variance of resting state microstates was observed in healthy individuals who participated in an extreme mountain ultramarathon[163]. In a recent study examining the impact of acute motor

fatigue on large-scale brain functional networks, it was found that exhaustive exercises could modulate resting state microstates[199]. Resting state microstate duration is altered by acute exercise, and this effect lasts for a minimum of one hour after exercise[162]. This suggests that microstate parameters could be regarded as an electrocortical indicator of exercise-related brain modification.

2.7.2 EEG microstates and stroke

EEG microstates have shown significant potential for investigating neurological disorders such as stroke. In stroke patients, the analysis of EEG microstates can provide important insights into the extent and location of the brain damage and the changes that occur during the recovery process[63]. A significant correlation between microstate parameters and clinical scales is observed in stroke patients which suggests that microstate analysis of resting state EEG has the potential to assist clinical and assessment applications[189]. Compared to healthy individuals stroke patients exhibit significant changes in microstate parameters and each microstate class was associated with a specific functional connectivity pattern[63]. EEG microstates analysis has the potential to track brain patterns during BCI-aided stroke rehabilitation and the frequency of occurrence of particular maps can serve as a reliable indicator of the proper execution of the rehabilitation tasks[14]. An investigation on the ability of resting state EEG microstates to predict recovery in acute stroke revealed alterations in microstate dynamics compared to controls[197]. Also, the study demonstrated that preserved microstate duration in post-stroke acute phase correlated with a better effective recovery. The dynamic pattern of scalp potentials reflects the momentary state of global neural activity and could be indicative of alterations in consciousness over time[60].

2.8 Rehabilitation Robotics

Repetitive, intensive, and goal-oriented rehabilitation can enhance motor function and cortical reorganisation in stroke patients with both acute and chronic impairments. However, this recovery process is generally slow and demanding, often necessitating considerable interaction between one or more therapists and a single patient. The primary motivation for the development of rehabilitation robotic devices is to automate interventions that are typically monotonous and physically strenuous[83]. Robot-assisted therapy is increasingly becoming a part of rehabilitative care following stroke. The main advantage of robot-assisted therapy is that quantitative feedback on the performance of the patients can easily be implemented. Also, robot-assisted therapy allows patients to use robotic systems at locations outside the rehabilitation hospital under the supervision and/or tele-control of a therapist or physician [33].

Various research teams have created numerous robotic systems with the objective of improving the rehabilitation of the upper limb. Charles et al. developed virtual reality (VR) simulations of

rehabilitation tasks for the upper arm using a Leap camera [29]. The GENTLE/S project utilised haptic and virtual reality technologies for neuro rehabilitation[108]. This framework is well-suited for offering better rehabilitation therapy as it can be adapted to provide different levels of patient engagement. The GENTLE/A rehabilitation system can offer adaptive robotic assistance in upper limb rehabilitation with the help of haptic master robot[30]. A study which evaluated the efficacy of robotic upper limb treatment found significant improvement in upper limb motor function in participants with subacute stroke[7]. The Supervised Care and Rehabilitation Involving Personal Tele-robotics (SCRIPT) project developed a hand/wrist rehabilitation device for home-based therapy after stroke. The SCRIPT system provided two different interfaces for patients and therapists and also enables therapists to remotely and indirectly monitor the progress of the patient's recovery[3].

EMG measurements from the upper limb muscles are reliable fatigue indicators for adaptive robotic interaction in rehabilitation training[171]. The collection of kinematic data through multiple sensors during a robotic intervention can provide insight into the process of motor learning. A study which utilised robot-assisted measurements to quantitatively evaluate the progress of recovery helped to attain a better understanding of the rate of improvement in patients[36]. This study has the potential to effectively plan and adjust rehabilitation strategies to enhance the patient's motor outcome. Incorporating robotic and device-based therapy into rehabilitation plays a significant role in ensuring an adequate number of movement repetitions with personalised feedback mechanisms. Robot-assisted therapy helps to increase the amount and intensity of upper limb practice performed by stroke survivors in routine clinical practice[52]The patient-therapist interaction, which includes both expertise and encouragement of active engagement, is a crucial factor in ensuring compliance and successful rehabilitation. The integration of robot-based therapy in neurorehabilitation helps therapists and physicians to understand the underlying principles and mechanisms of motor learning to develop effective rehabilitation strategies that can be adapted to each patient's individual needs[149].

2.9 Nine Hole Peg Test

The Nine Hole Peg Test (NHPT) is a standardised assessment tool used to evaluate the fine motor function and dexterity in the hands and fingers[112]. The test consists of a board with nine holes and nine pegs that must be placed in the holes and then removed as quickly as possible with one hand. Numerous studies in the existing literature have demonstrated that the Nine Hole Peg Test (NHPT) is a dependable and valid tool for assessing finger dexterity[130][159][112]. Moreover, the test has been found to be effective in evaluating hand dexterity across different populations with various medical conditions[65][32][79][24]. The NHPT is often used in clinical settings to assess a person's fine motor function over time, such as after an injury or illness, or to evaluate the effectiveness of rehabilitation interventions.

This study adapted the NHPT from Wade's Nine-Hole Peg Test[185], which assesses the fine motor skills of a stroke patient. The equipment used for this test includes nine wooden dowels, a wood base with nine holes and a tray which holds pegs. Typically, the patient sits in front of the apparatus and is asked to place each of the pegs, in turn, into each of the nine holes on the board. An observer records the times from start to end but can stop at 50 seconds and record the number of pegs placed. This test is sometimes employed by measuring the duration it takes for a patient to insert and extract the pegs. Its accuracy and consistency have been evaluated and confirmed. Typically, individuals without any impairments finish the assessment within 18 seconds.

A study of the haptic peg-in-hole test using Phantom Desktop 1.5 presented the concept that a clinically validated test such as NHPT can be replicated using the haptic simulation[4]. Bowler et al. designed a study to explore the efficacy of NHPT in three different methods: Real, Embedded and Virtual [17]. They found that an embedded reality approach, where a physical rig and a haptic device are present, may introduce new cognitive demands while providing more extensive performance metrics. Lisa et al. designed a multimodal system which explored the use of haptic technology for performing the Nine Hole Peg Test in visually impaired people[16]. This study compared the NHPT performance of sighted and non sighted people and found that the virtual haptic interface can aid non-sighted users to achieve the standard Wade's peg-in-hole time of healthy participants. Another study of the feasibility of using the virtual peg insertion test with MS patients emphasises the potential of this test to evaluate upper limb motor function[95]. Studies investigating the use of haptic devices for administering the Nine Hole Peg Test have demonstrated their potential in facilitating this assessment, yet none have investigated the neural correlates associated with it. Acquiring the physiological data along with the kinematic features provided by robotic devices will aid in giving more insight to optimise rehabilitation strategies.

2.10 Chapter summary

Stroke rehabilitation aims to restore independence and improve the overall quality of life in stroke patients. Repetitive training tasks in rehabilitation help in promoting neuroplasticity, which is the brain's ability to reorganise and form new neural connections. Through repetitive practice, the brain can strengthen existing connections, create new pathways, and facilitate the recovery of function. Robot-assisted therapy has emerged as a promising intervention capable of enhancing the quantity of practice undertaken by individuals recovering from a stroke. Assessment is often useful in therapy to guide and measure progress. Studies that utilised haptic technologies for evaluating the outcomes of clinical assessments have as yet never explored the neurophysiological correlates behind such assessments. The EEG collected from different parts of the brain provides information related to neurological disorders. EMG signals collected from the muscles can be used to understand the current physical state and the effort exerted by the participant during

movements. Exploring the neurophysiological correlates related to clinical assessment tests will have the potential to create better rehabilitation strategies. To the best of the author's knowledge, none of the past studies explored the neurophysiological correlates of the Nine Hole Peg Test. Hence this research aims to explore the brain and muscle activations while performing robot-mediated NHPT under fatigue conditions.

CHAPTER 3

EXPERIMENT DESIGN

An experiment was designed to check how EEG-EMG coherence and EEG microstates vary with physical fatigue while performing the NHPT using a haptic device. The experiment looked at fatigue in the upper limb muscles of eight healthy participants. The study was designed in such a way that EEG and EMG signals of participants are collected while they perform NHPT using the haptic device Geomagic Touch. The ethics approval was obtained from the University of Hertfordshire under approval reference: ECS/PGR/UH/04035.

3.1 Experiment Set up

The experiment setup included an EEG-EMG signal acquisition device (g.USBamp), EMG electrodes, g.GAMMAcap, the haptic device Geomagic Touch which recreated the NHPT in a virtual environment and a dynamometer. Figure 3.1 illustrates a participant performing the experiment.

Figure 3.1: A participant performing experiment

NHPT was performed using the stylus of the Touch device. The physical rig was kept in front of the participant, which was exactly mapped to a virtual rig on the LCD screen. There were nine pegs and a peg board on the screen. A peg was attached to the end of the stylus with the help of a rubber end cap. The stylus of the peg was shown on the screen as a small blue cone. Participants can feel the objects on the screen by touching them using the blue cone. The participant has to pick the pegs on the screen one by one and insert them in one of the holes. Because of the haptic feedback, participants can feel the virtual pegs. Participants could pick the peg by pressing the button on the stylus when the cursor is touching the peg. Once the peg is picked, the rendering of the cursor changes to a white peg. The peg can be released to the hole by releasing the button. The time at which each peg was picked and released was recorded as peg status. The haptic Virtual reality environment for the experiment is presented in Figure 3.2. This was developed by the author using OpenHaptics API. The virtual reality environment was generated using a C++ code executed on a Windows 10 (64-bit) system with Visual Studio 2017.

Kinematic data from Geomagic Touch and, EEG and EMG data from the participant were logged during the experiment. The position, orientation, velocity, force, current time and status of pegs that show which peg is picked were recorded in the servo loop of Geomagic Touch. These data were logged at a frequency of 1KHz and were saved as text files. EEG and EMG data were recorded at a frequency of 1200Hz and were saved as .mat files in the computer. These data were time stamped. System clock timings were also logged with the help of the MATLAB Simulink model. The author developed the MATLAB Simulink model for EEG and EMG data collection, as well as the programs for kinematic data collection. Kinematic data collection algorithms were

developed using C++ in Visual Studio 2017.

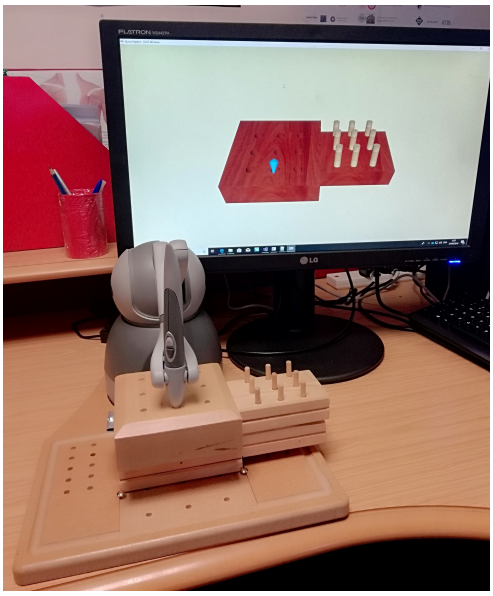

Figure 3.2: Haptic Virtual reality environment showing Geomagic Touch, NHPT physical rig and the virtual rig on the screen. The blue cone on the screen represents the stylus of Geomagic Touch.

3.1.1 EEG-EMG data acquisition

EEG and EMG signals from each participant were collected with the help of g.USBamp. It is a high-end biosignal amplifier which helps in the acquisition of any electrophysiological signal. The amplifier has 4 potential separated groups with 4 input channels each. This allows to simultaneously record EEG, EMG, Electrooculogram and electrocardiogram without interference. The amplifier can be connected directly to a PC or notebook with a USB connector without any additional data acquisition device needed. The 4 groups of a single g.USBamp was interconnected to record 16 EEG channels with the same ground and reference potentials. A second g.USBamp was used to record EMG signals from Flexor Carpi Radialis (FCR), Extensor Carpi Radialis (ECR) and Extensor Digitorum (ED). An electrode cable with a clip lead was attached to sterile disposable electrodes to measure EMG signals from the three upper limb muscles of the participants. A g.USBamp with EMG electrodes is shown in Figure 3.3 and EMG electrode positions are shown in Figure 3.4.

Figure 3.3: USBamp with sensor electrodes

Figure 3.4: EMG electrode positions

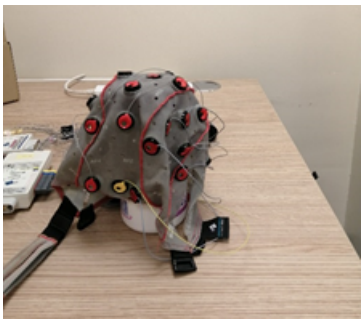

Figure 3.5: g.GAMMAcap

To collect EEG signals from the brain a g.GAMMAcap (Figure 3.5) was placed on the head of the participant. In this experiment, the EEG signals were collected from the electrodes FP1, FP2, F3, Fz, F4, FC3, FCz, FC4, C5, C3, C1, Cz, C2, C4, C6, and CP3. All electrodes were referenced to the right earlobe, and FPz was used as ground. Active electrodes were used for collecting EEG data and the only passive electrode was FPz, that is, ground. EEG electrode positions are shown in Figure 3.9 which is based on the international 10-10 system. EEG electrodes were connected to a biosignal amplifier with the help of g.GAMMAbox which is an active electrode driver box. The Simulink model for EEG-EMG data acquisition is shown in Figure B.1. EEG and EMG signals were recorded with a sampling rate of 1200Hz. The g.USBamp Simulink block helps to set the data acquisition parameters like the master/slave configuration for biosignal amplifier, sampling frequency, and notch filter. The collected EEG and EMG signals were saved as MATLAB (.mat) data files for later processing. Figure 3.6 presents the block diagram for data acquisition.

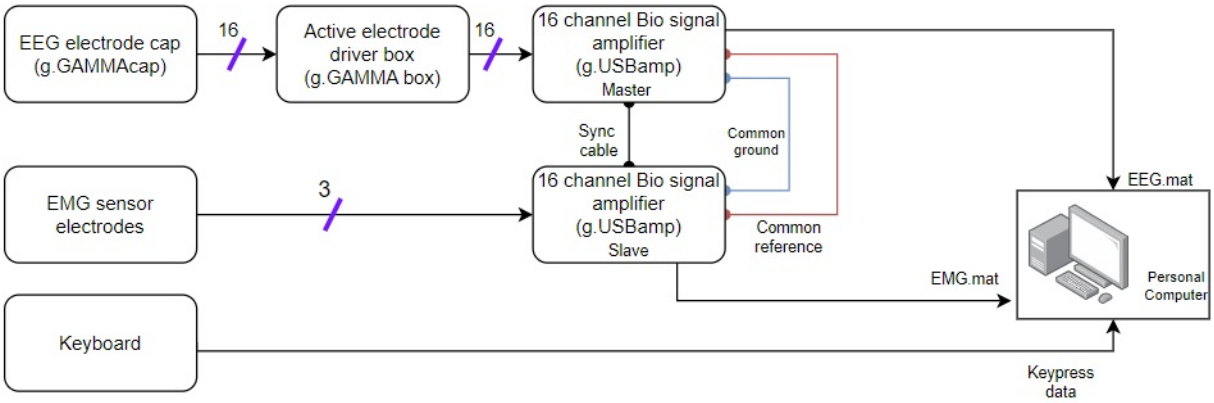

Figure 3.6: Blockdiagram for the EEG-EMG data acquisition. EEG data from 16 scalp electrodes and EMG from 3 upper limb muscles are collected and saved as .mat files on the personal computer. 'Key press' data is collected to differentiate between different stages of experiment.

Anterior and posterior muscles of the forearm are shown in Figure 3.7 and Figure 3.8. In this experiment, EMG signals were recorded from flexor carpi radialis, extensor carpi radialis and extensor digitorum. These muscles were selected because the study assesses fine movements of fingers and wrist.

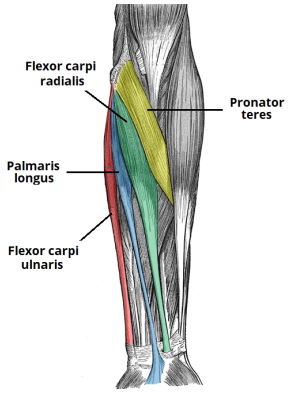

Figure 3.7: Muscles of anterior forearm[123]

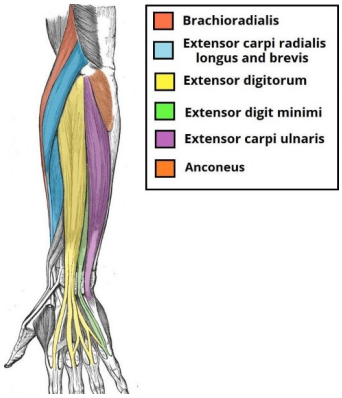

Figure 3.8: Muscles of posterior forearm[124]

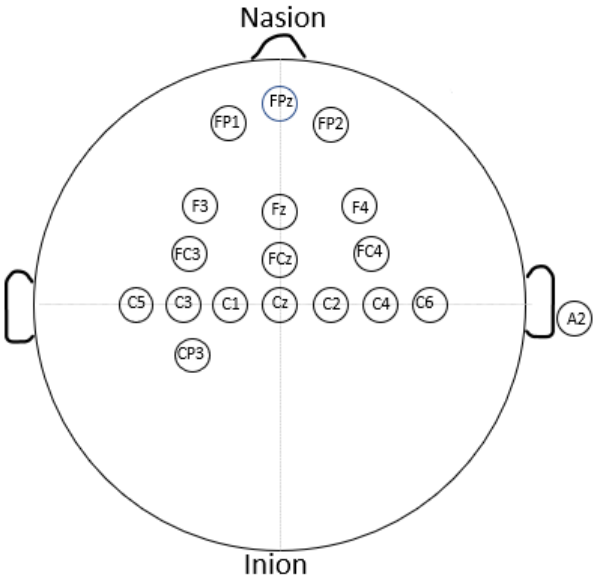

Figure 3.9: EEG electrode positions

3.1.2 NHPT using Geomagic Touch

Geomagic Touch developed by 3D Systems was used to recreate NHPT in a haptic virtual environment. It consists of a stylus, which is connected to a robotic arm, and a base that provides stability. The Geomagic Touch device has six degrees of motion provided by six axis points. Geomagic Touch enables the user to feel virtual objects by giving force feedback[176].

A C++ code running on a Windows 10 (64 bit) machine using Visual Studio 2017 was used to configure the virtual reality environment and the Geomagic Touch. Kinematic data during NHPT trials were logged to the computer. The Virtual Reality (VR) environment was developed by the author with the help of OpenHaptics from 3D systems. Geomagic Touch with physical rig for NHPT is shown in Figure 3.10. The virtual environment was set up such that the NHPT rig on the screen is exactly mapped to the physical rig in front of the participant. The original NHPT apparatus consists of a board with nine evenly spaced, holes arranged in a 3x3 grid and nine pegs. The time taken to complete the task was recorded. Faster times suggest better fine motor skills. In addition to recording the time taken for completing an NHPT, recreating the NHPT in a haptic environment helps to record information regarding the subject's movement, such as speed, position, forces exerted, and orientation of the end effector. Earlier work from our group involving haptic instruments for simulating the NHPT indicated the possibility of new cognitive demands by the addition of haptic and virtual reality[4][18].

Figure 3.10: Geomagic Touch with Rig

3.1.2.1 Clinically Approved Nine-Hole-Peg-Test

This study adapted the Nine-Hole-Peg-Test (NHPT) from Wade's widely used concept[185], which assesses the fine motor skills of a stroke patient. The equipment used for this test includes 9 wooden dowels, a wood base with 9 holes and a tray which holds pegs. Typically, the patient sits in front of the apparatus and is asked to place each of the pegs, in turn, into each of the nine holes on the board. An observer records the times from start to end but can stop at 50 seconds and record the number of pegs placed. This test is sometimes employed by measuring the duration it takes for a patient to insert and extract the pegs. Its accuracy and consistency have been evaluated and confirmed. Typically, individuals without any impairments finish the assessment within 18 seconds.

3.2 Experiment Protocol

Ten healthy right-handed participants with no previous injuries to the upper limb or brain were recruited for the study. Participants were advised to wear a loose garment for the ease of fixing the electrodes on the upper limb. The participant was asked to fill out a questionnaire at the beginning of the experiment. Each participant's weight, Body Mass Index (BMI), Visceral fat classification, skeletal muscle percentage, and body fat percentage were measured before the experiment using Omron digital weight scale. The Maximum Voluntary Contraction (MVC) of each participant was recorded with the help of a hand grip dynamometer (Takei Grip Strength Dynamometer). Participants were asked to perform MVC 4 times. Each MVC was performed by having the subject increase their force from resting to their maximal level, with the maximal force held for 3 s. The total duration of the experiment, including setup time, for one participant, was 45-60 minutes.

At the beginning of the experiment, participants were allowed to have a practice run to get familiarised with the haptic device.

Two sets of four-minute EEG recordings were taken, one at the beginning and one at the end of the experiment, with each set comprising two minutes of eyes closed and two minutes of eyes open. Simultaneously, EMG data from upper limb muscles were consistently collected throughout the entire experiment, ensuring a comprehensive dataset for analysis. The participants were instructed to stay focused and try to minimise eye blinks, swallowing or any other motions that alter EEG recordings. Then participants were asked to perform two trials of NHPT followed by a fatiguing exercise for the forearm. Once the participants get fatigued, they were asked to do the next two trials of NHPT. The experiment flow is given in Figure 3.11.

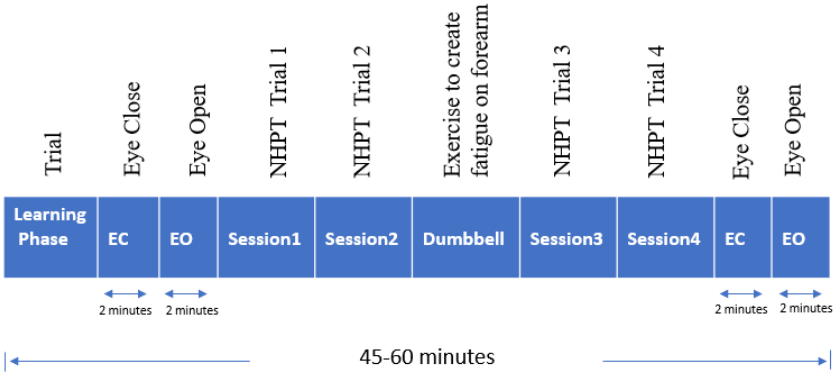

Figure 3.11: Experiment Flow

The fatigue exercise involved flexion and extension of the wrist using dumbbells. Participants were asked to select one dumbbell from the set of weights provided. The fatigue exercise involved the following:

- 12 repetitions of flexion and extension of the wrist using the selected weight while arm in both supine and pronate position.
- A break of 30 seconds.
- 10 repetitions of flexion and extension of the wrist using the selected weight while arm in both supine and pronate position.
- A break of 30 seconds.
- 8 repetitions of flexion and extension of the wrist using the selected weight while arm in both supine and pronate position.
- A break of 30 seconds.

If participants were not fatigued by this they were asked to continue flexion and extension till they are fatigued. The exercise protocol is presented in Figure 3.12.

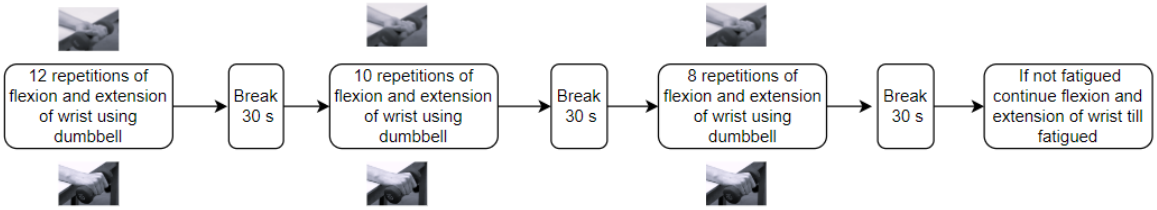

Figure 3.12: Exercise protocol to induce fatigue on wrist. Extension and flexion of wrist are done in both supine and pronate positions.

There was no break given between the end of the dumbbell exercise and the start of trial 3, however, 20 - 30 seconds elapsed between them during the experiment.

To assist the participant with various stages of the experiment, audio feedback was provided. A questionnaire was given as part of this experiment. Participants were asked to fill out some parts of the questionnaire at the beginning of the experiment. They were requested to update the fatigue status before NHPT rep1, after NHPT rep2, before NHPT rep3 and after NHPT rep4.

Kinematic data from Geomagic Touch and, EEG and EMG data from the participant were logged during the experiment. Data regarding the position, orientation, velocity, force, current time and status of pegs that shows which peg is picked were recorded in the servo loop of Geomagic Touch. These data were logged at a frequency of 1KHz and were saved as text files. EEG and EMG data were recorded at a frequency of 1200Hz and were saved as .mat files in the computer. These data were time stamped. System clock timings were also logged with the help of Simulink model. To differentiate between the stages of the experiment author used a 'key press 'which was also recorded with the help of Simulink.

CHAPTER 4

PRE AND POST FATIGUE EEG-EMG COHERENCE WHILE PERFORMING ROBOT-ASSISTED NINE HOLE PEG TEST

The previous chapter introduced the experiment setup for gathering EEG and EMG data. EEG signals from 16 electrode locations, the EMG from three upper limb muscles and the kinematic data from Geomagic Touch were collected. The EEG reflects the collective activity of neurons in different brain regions and EMG signals measure the collective firing of motor units. Therefore EEG-EMG coherence is considered capable of exploring the mechanism of the cerebral cortex's control of muscle activity[106]. It provides insight into the interaction between the cerebral cortex and the muscle tissue where the cerebral cortex sends commands to the muscle tissue and receives afferent feedback from muscle contraction. Thus, it helps to understand how the brain controls muscle movement and also the effects of muscle movement on neural activity in the brain; hence it can provide more insights towards understanding fatigue and its underlying mechanisms[106]. This chapter aims to explore how EEG-EMG coherence varies from a pre fatigue state to post fatigue state. While numerous studies have examined coherence under fatigue conditions, none have specifically analysed it during robot-assisted NHPT performance. In this experiment, each participant did four trials of NHPT, two before fatiguing exercise and two after fatiguing exercise. The EEG-EMG coherence was calculated for NHPT trial 1 which is the first trial and NHPT trial 3 which is the trial just after fatiguing exercise, to allow for observing the differences in coherence between these two phases. For ease of reference, the NHPT trial will be referred to as trial throughout this chapter.

4.1 Research Question

How does physical fatigue alter the coherence between EEG and EMG for healthy participants while performing a robot-assisted NHPT?

4.2 Materials and Methods

The experiment was conducted with ten participants. Upon checking data quality, two participants' data were removed because of corrupted EEG data recordings. Participants' demographics are presented in Table 4.1. Participants were at least 18 years of age (Mean±SD: 29.8±5.4 years) with variable BMI (Mean±SD: 26±5.7). The BMI of the participants was recorded to check its effect on fatigue development on the participants, as literature has shown an association between obesity and self-reported fatigue[144]. Using the Simulink model shown in Figure B.1 recorded EEG and EMG data were saved onto a computer as .mat files. These data were collected for the whole experiment. A notch filter was used while configuring g.USBamp for signal acquisition to remove powerline interference at 50 Hz. The EEG and EMG data analysis was conducted offline in MATLAB R2019a environment. Data were pre-processed and also segmented into four NHPT trials so that coherence for each trial could be found.

Table 4.1: Participants' Demographics

Subject	Gender	Age	BMI
1	Male	25	22
2	Female	36	21
3	Male	27	25
4	Male	36	28
5	Female	31	32
6	Male	34	36
7	Male	28	25
8	Male	21	19

4.2.1 EEG data preparation

With the help of the g.tec acquisition system, EEG signals were recorded at a sampling rate of 1200Hz. This EEG data was continuous and needed to be segmented into different sections. 'Key press' data recorded with the help of MATLAB Simulink model was used to extract EEG data corresponding to eye close and eye open at the beginning and end. Similarly, the time at which each peg was picked and released was logged during the experiment with the help of Geomagic Touch API. With the help of this time stamp data, the EEG for each trial was extracted separately using the MATLAB algorithm.

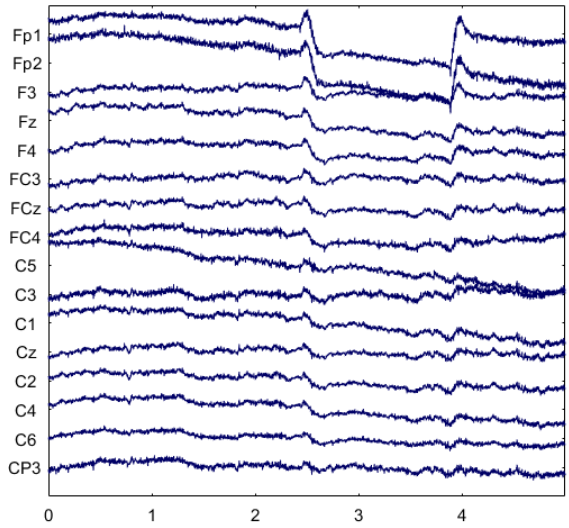

Figure 4.1: Raw EEG signal (Subject 1)

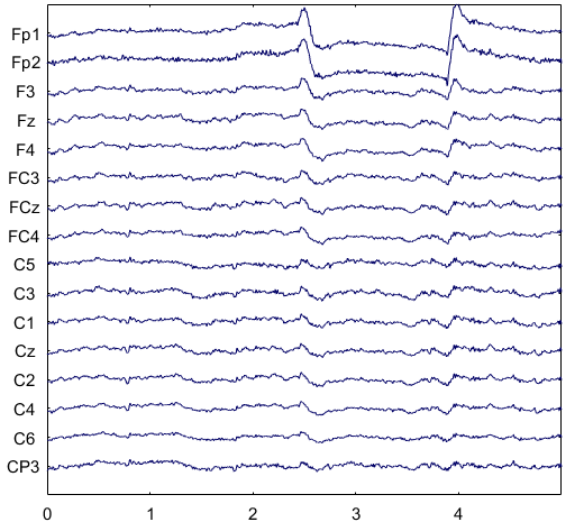

Figure 4.2: Filtered EEG signal: Basic FIR filter in EEG lab toolbox was employed for filtering the signal.

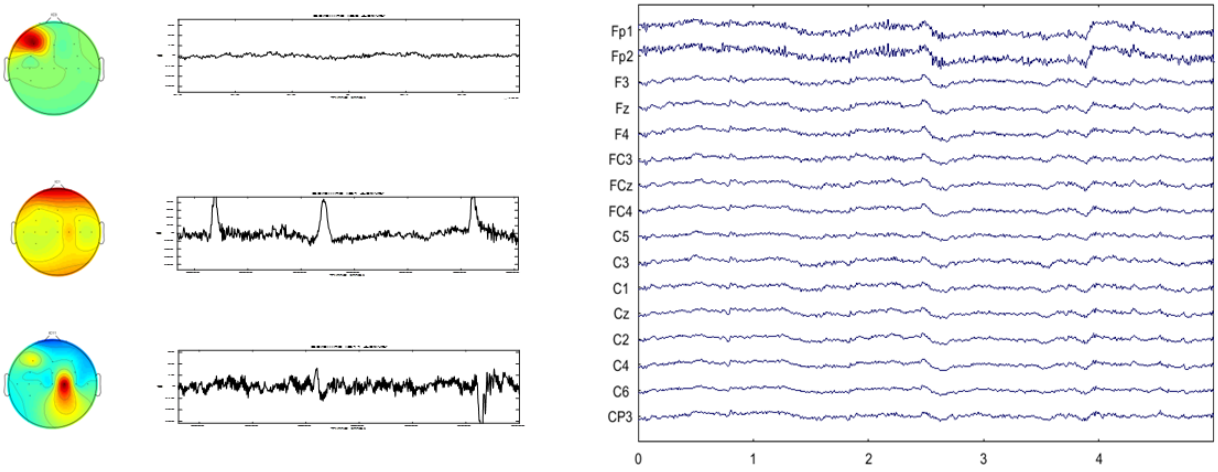

Figure 4.3: Independent components(IC) corresponding to muscle artefacts, eye blinks and line noise are shown on the left and EEG signal after removing ICs on the right (Subject 1). ICs were removed with the help of EEGlab toolbox.

The recorded raw EEG signal is shown in Figure 4.1. The raw EEG signals are often contaminated by different types of artefacts. These artefacts need to be removed before further processing. The segmented EEG signals were passed through a band pass filter(0.5-60 Hz) to remove high frequency noise and low frequency drifts. This filtered EEG is shown in Figure 4.2. Ocular artefacts are a major source of artefacts in EEG. Eye movements and blinks generate these artefacts. Independent Component Analysis (ICA) is a well known method used for removing

EEG artefacts[80]. ICA is widely used to remove eye, muscle and line noise artefacts. ICA was applied based on the assumption that the recorded EEG signal is a linear mixture of cerebral and artefactual sources. The ICA algorithm developed by EEGlab was used in this project to remove artefacts[45]. The ICA algorithm decomposes the source signal into independent components (ICs) based on the assumption that

- Source signals are statistically independent from each other and instantaneously mixed.
- The dimension of the observation signal must be greater than or equal to the source signal.
- Sources are non-Gaussian or only one source is Gaussian[76].

After extracting ICs from the original signal, the original signal can be reconstructed by discarding ICs corresponding to artefacts. With the help of EEGlab toolbox ICs were classified based on the label. Typical labels include brain, eye, muscle, heart, line noise, channel noise and other. This simplified the process of manually removing components corresponding to artefacts. This clean EEG data after removing artefact ICs were used for calculating the EEG-EMG coherence. Figure 4.3 shows ICA corrected EEG after removing 3 ICs from filtered EEG signal in Figure 4.2.

4.2.2 EMG data preparation

EMG signals from Flexor carpi radialis (FCR), Extensor digitorum (ED) and Extensor carpiradialis (ECR) of participants were collected during the experiment. Both EEG and EMG signals were collected at a sampling rate of 1200 Hz. While calculating EEG-EMG coherence both data must have the same sampling rate. So it will be easier to implement the algorithm for coherence if both signals are recorded with the same sampling frequency. Similar to EEG, EMG data also needs to be segmented and preprocessed. Raw EMG signals were band pass filtered in the frequency band 0.5-60 Hz. This band was selected for both EMG and EEG to help with analysing coherence corresponding to different frequency bands of EEG. Different categories of EEG bands are delta (0.5-4Hz), theta (4-7.5Hz), alpha (8-13Hz), beta (13-30Hz), and gamma (>30Hz)[148]. To compare muscle activities of different individuals, a good practice is to normalise EMG signals[62]. The maximum voluntary contraction (MVC) of each participant was measured at the beginning of the experiment with the help of a hand grip dynamometer. Participants were asked to execute MVC four times. Each MVC was performed by having the subject increase their force from resting to their maximal level, with the maximal force held for 3s. To normalise, filtered EMG data was divided by the RMS (root mean square) value of recorded MVC-EMG signals. With the help of peg status data, EMG signals for each trial were separated. Raw and filtered EMG signals are presented in Figure 4.4.

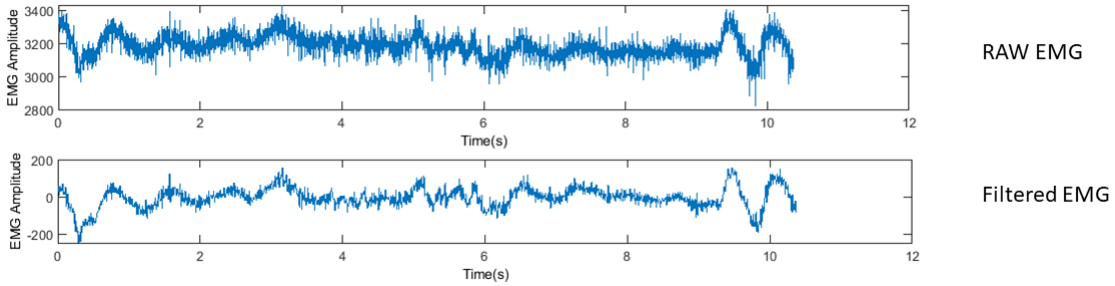

Figure 4.4: EMG collected from Subject 1. A Butterworth filter with fourth-order was utilized to filter the EMG data within the specified pass band of 0.5 to 60 Hz.

4.2.3 EEG-EMG Coherence

To measure the coupling between EEG and EMG signals, the magnitude squared coherence between the two signals was calculated using Welch's Periodogram method[120][31]. This gives the correlation between the two signals, at different frequencies. If X and Y denote EEG and EMG signals respectively, the magnitude squared coherence between them at a specific frequency f, *Cxy(f)* is calculated as

$$Cxy(f) = \frac{|Pxy(f)|^2}{Pxx(f)Pyy(f)} \tag{4.1}$$

where

$Pxx(f) = \frac{1}{N}\sum_{j=1}^{N} X_j(f)X_j^*(f)$

and

$Pyy(f) = \frac{1}{N}\sum_{j=1}^{N} Y_j(f)Y_j^*(f)$

are the power spectra for X and Y at the same frequency, respectively.

$Pxy(f) = \frac{1}{N}\sum_{j=1}^{N} X_j(f)Y_j^*(f)$ is the cross spectrum for EEG and EMG at a given frequency f. $X_j(f)$ and $Y_j(f)$ represents the fourier transforms of X and Y for a given segment number j=1,2,....N. $X_j^*(f)$ and $Y_j^*(f)$ are the complex conjugates of $X_j(f)$ and $Y_j(f)$ respectively[31].

While calculating coherence between EEG and EMG a window size of 1024 samples was selected which provided a frequency resolution of 1.17. This value of frequency resolution ensures that the coherence is calculated at increments of 1.17 Hz. The level of significance of the coherence value is determined based on the confidence level (CL) [87], which is given by equation

$$CL = 1 - (1-\alpha)^{\frac{1}{L-1}} \tag{4.2}$$

where α is the confidence interval of 95%, and L is the number of data segments used in the calculation of coherence. The number of data segments was calculated by dividing the length of the data by the window size.

The different steps involved in calculating the EEG-EMG coherence are presented in Figure 4.5. Since we were interested in corticomuscular coupling while performing upper limb movements, the EEG electrodes from the motor area were used for finding coherence. C1, C3 and CP3 were the EEG electrodes used for this analysis due to belonging to the contralateral sensory motor area of the brain, which is involved in activating specific muscles for movements[141][179]. The coherence between the selected EEG electrodes and the FCR, ECR and ED muscles was calculated. These muscles were selected as they contribute to wrist and finger movements.

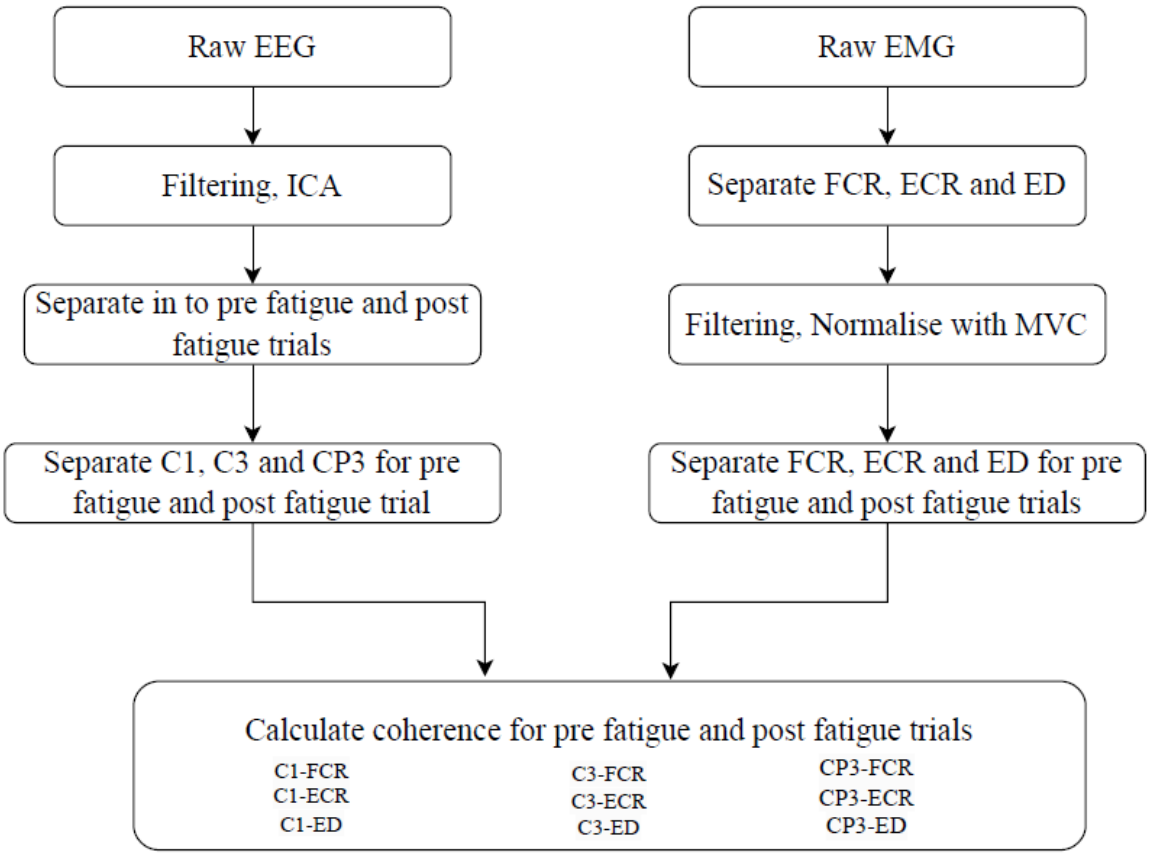

Figure 4.5: Steps involved in calculating coherence

Since the project aims to explore changes in corticomuscular coupling when a person performs NHPT in pre and post fatigue states, only the trials corresponding to these states were taken for further analysis. Thus, the analysis was performed for trial 1 and trial 3. Trial 1 was the first trial when the participant is not fatigued yet and can therefore be referred to as pre fatigue trial. Trial 3 was the trial just after the fatiguing exercise and can therefore be called the post-fatigue trial. A MATLAB algorithm was developed for offline calculation of the EEG-EMG coherence. The

EEG data from electrode C1 of Subject 5 was corrupted and this data was not used for analysis. The significant level of coherence for each trial for each subject was calculated using Equation 4.2 and is tabulated in Table 4.2.

Table 4.2: Significant coherence values for trial 1 and trial 3

Subject	Trial1	Trial3
1	0.0437	0.0387
2	0.0279	0.0200
3	0.0472	0.0392
4	0.0479	0.0560
5	0.0450	0.0540
6	0.0223	0.0327
7	0.0264	0.0550
8	0.0245	0.0397

4.3 Results

Coherence values and corresponding frequencies for trial 1 and trial 3 were calculated with the help of a MATLAB algorithm and were saved as Excel files for each participant. Figure 4.6 shows pre and post fatigue EEG-EMG coherence of a single participant. The coherence was calculated between the EEG electrodes C1, C3, CP3 and EMG electrodes FCR, ECR and ED. The pre fatigue coherence is plotted in pink and the post fatigue coherence is plotted in blue. The pink dotted line corresponds to a significant coherence level of pre fatigue trial and the blue dotted line corresponds to a significant coherence level of post fatigue trial. It can be seen that for this participant the post fatigue coherence is much higher compared to the pre fatigue coherence.

Performing NHPT with the help of a haptic device requires attention and focus. Since delta and theta frequencies of EEG correspond to deep sleep and drowsiness, respectively, the coherence in these bands was not analysed. Alpha rhythms which are in the frequency range 8Hz-13Hz are associated with relaxed wakefulness[148], whereas the experiment requires the participant to be alert. Corticomuscular coupling was found for the alpha band and it is noted that the coherence values observed between EEG and EMG were always well below the significant coherence values calculated with the help of Equation 4.2. Thus, this band was also excluded from further analysis. The pre fatigue and post fatigue coherence values corresponding to the beta band and gamma band for each participant were separated and analysis was performed on them separately.

4.3.1 Beta Band Coherence

Beta rhythms of EEG are associated with focused attention[100]. These come in the range 13-30Hz. The coherence values within this frequency range for each participant were separated for both the pre fatigue and post fatigue trials and subsequently subjected to further analysis.

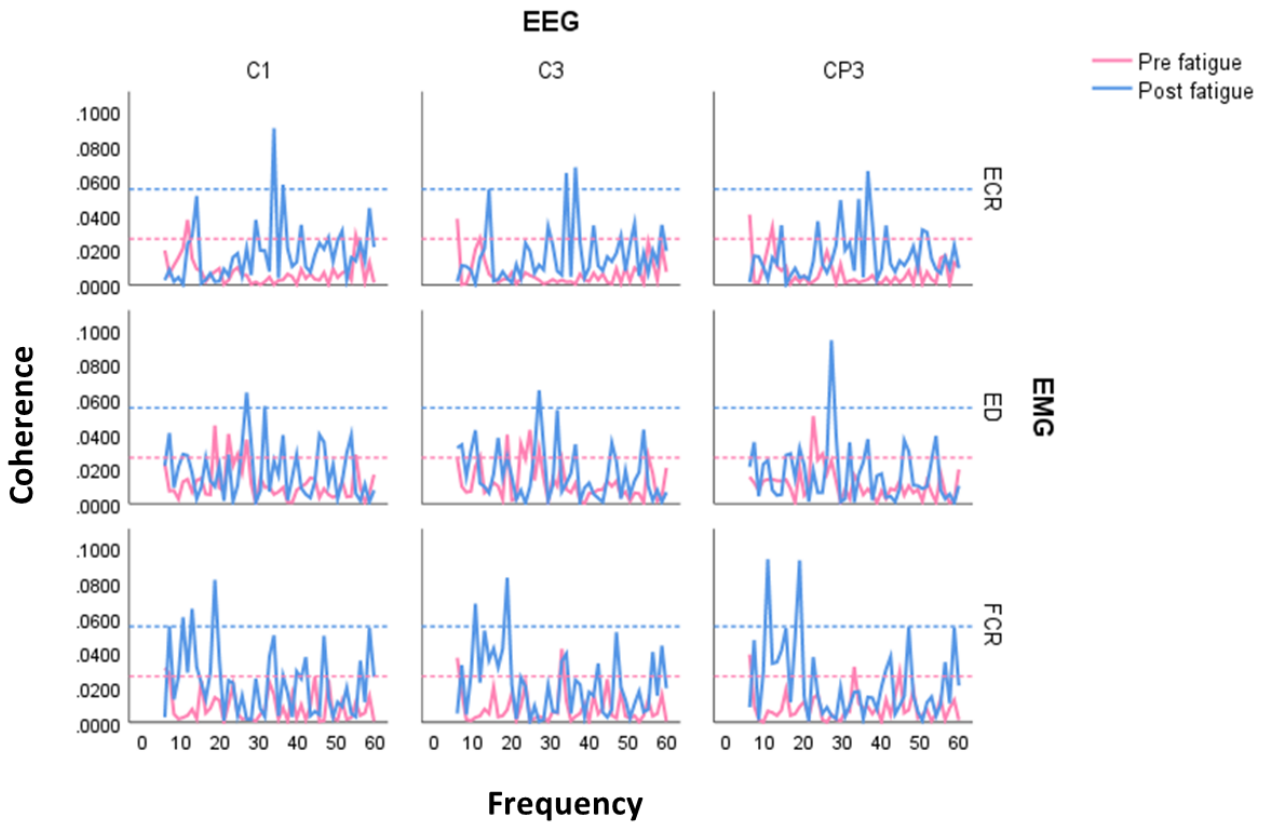

Figure 4.6: Pre and post fatigue coherence for a single participant (Subject 7). Pre fatigue coherence is plotted in pink colour and post fatigue coherence is plotted in blue colour. Significant level of coherence is plotted in dashed lines.

Box plot for coherence in beta band between C1 and the muscles is presented in Figure 4.7. Pre fatigue trial is shown with pink and post fatigue trial is shown with blue colour. The median value of coherence between C1 and muscles ECR and FCR increased with fatigue whereas beta band coherence between C1 and ED decreased with fatigue. Pre-fatigue coherence levels for the C1-ECR and C1-FCR had similar median values. The post-fatigue coherence of the C1-ECR and C1-FCR exhibits a similar pattern.

A box plot depicting coherence values within the beta frequency range between C3 and the muscles is presented in Figure 4.8. Here the coherence increased with fatigue for all the muscles which means the coupling between muscles and C3 became stronger as a result of fatigue. Similar to the coupling between C1 and muscles, here also the median values of the pre fatigue coherence values for C3-ECR and C3-FCR were close to each other. The median of pre fatigue coherence values for C3-ED was slightly higher but still closer to other muscles' coupling with C3. Post fatigue coherence levels for C3-ECR, C3-FCR and C3-ED had similar median values.

A box plot for the coherence in beta band between CP3 and the muscles is presented in Figure 4.9. Similar to C1 here also coupling between CP3 and ED decreased with fatigue where

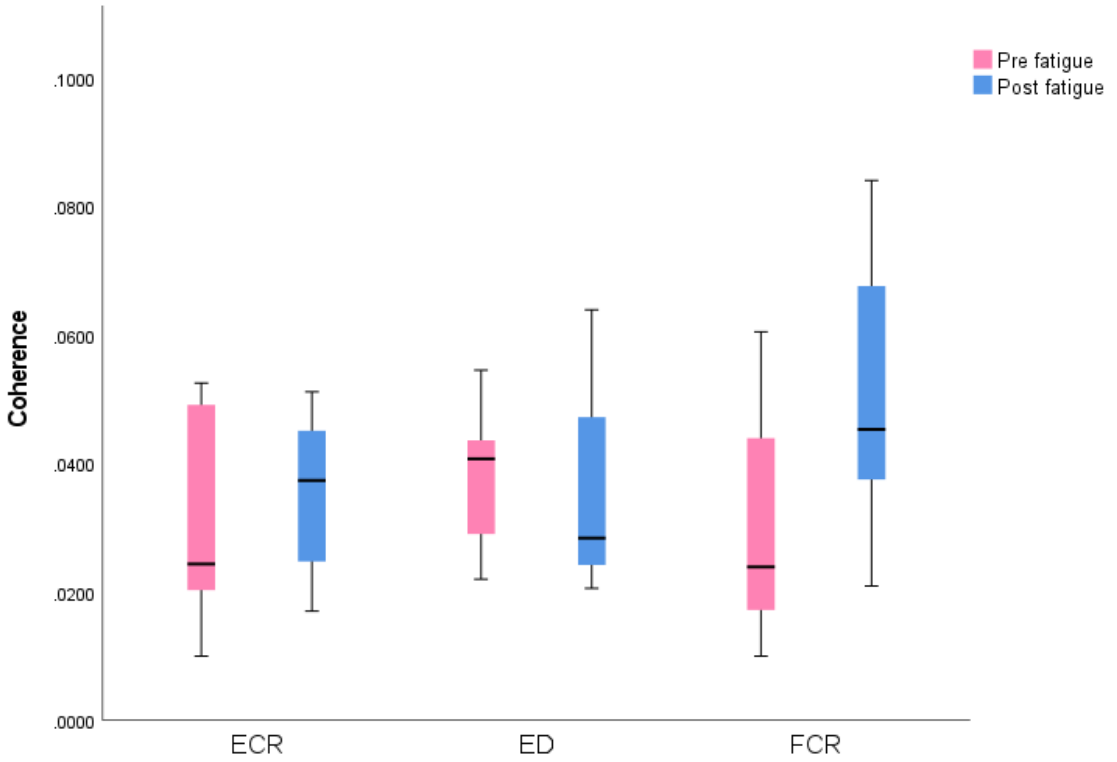

Figure 4.7: Boxplot showing pre and post fatigue coherence between EEG electrode C1 and muscles ECR, ED and FCR in beta band for all the participants. Pre fatigue coherence is presented in pink colour and post fatigue coherence is in blue colour.

as the other two muscles' became strongly coupled with CP3 after fatigue.

The maximum coherence values calculated for each participant in the beta band for pre fatigue and post fatigue trials are presented in Table 4.3. For trial 1 and trial 3 maximum coherence was calculated between the EEG electrodes C1, C3, CP3 and the muscles FCR, ECR and ED. The coherence values which are above the confidence level are shown in bold in the table. The calculation of coherence between C1 and the muscles for subject 5 was excluded due to insufficient quality of the recorded C1 values. The mean, standard deviation and median of coherence values across the subjects for each EEG-EMG pair for pre fatigue and post fatigue trials were also calculated. The average beta band coherence values for C1-FCR and C1-ECR increased with fatigue, whereas fatigue caused a decrease in the average coherence value for C1-ED. Increased coherence was observed between C3 and the muscles as a result of fatigue. Also, the mean value of post fatigue coherence between C3 and FCR was higher than the coherence between C3 and other muscles. The mean coherence values of CP3 with all the muscles increased as a result of fatigue. Figure 4.10 shows the change in pre and post fatigue coherence for all the subjects in the beta band. Trial 1 corresponds to the pre fatigue state and trial 3 corresponds to the post fatigue state.

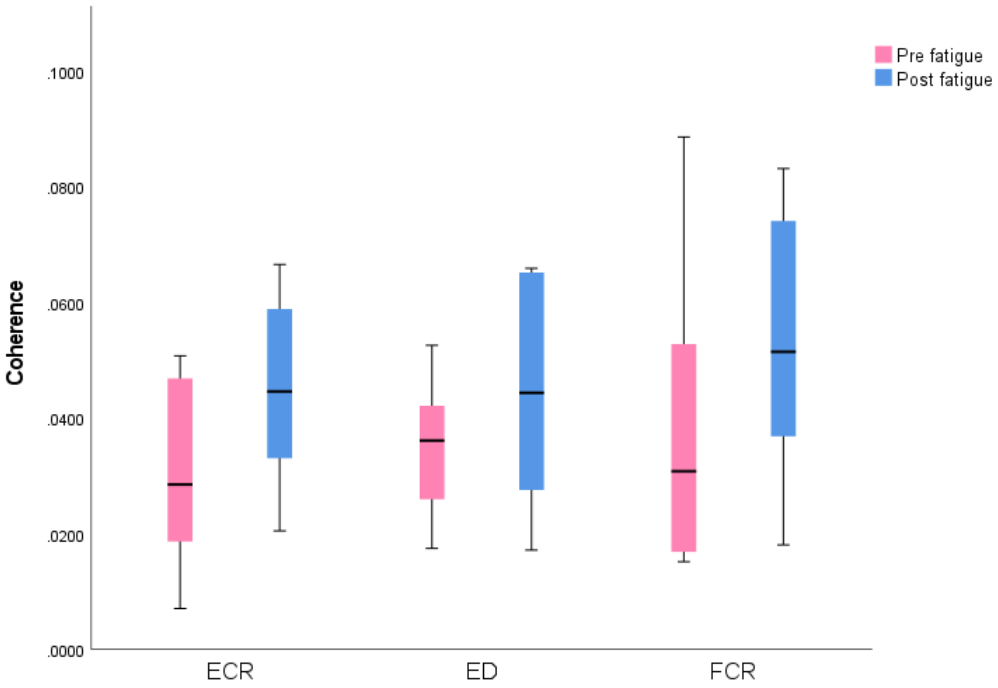

Figure 4.8: Boxplot showing pre and post fatigue coherence between EEG electrode C3 and muscles ECR, ED and FCR in beta band for all the participants. Pre fatigue coherence is presented in pink colour and post fatigue coherence is in blue colour.

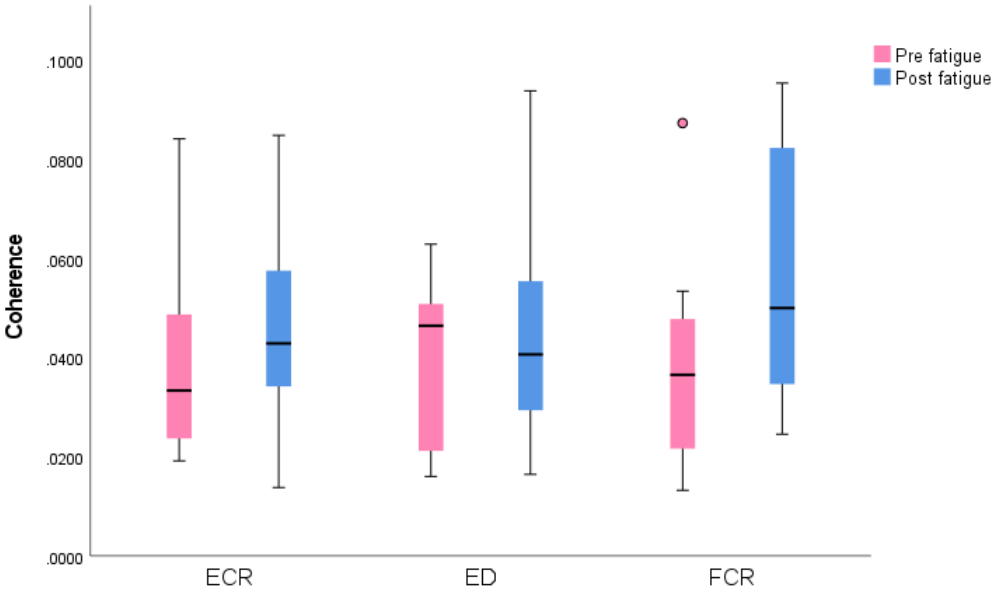

Figure 4.9: Boxplot showing pre and post fatigue coherence between EEG electrode CP3 and muscles ECR, ED and FCR in beta band for all the participants. Pre fatigue coherence is presented in pink colour and post fatigue coherence is in blue colour. 'o' presents the outlier in data.

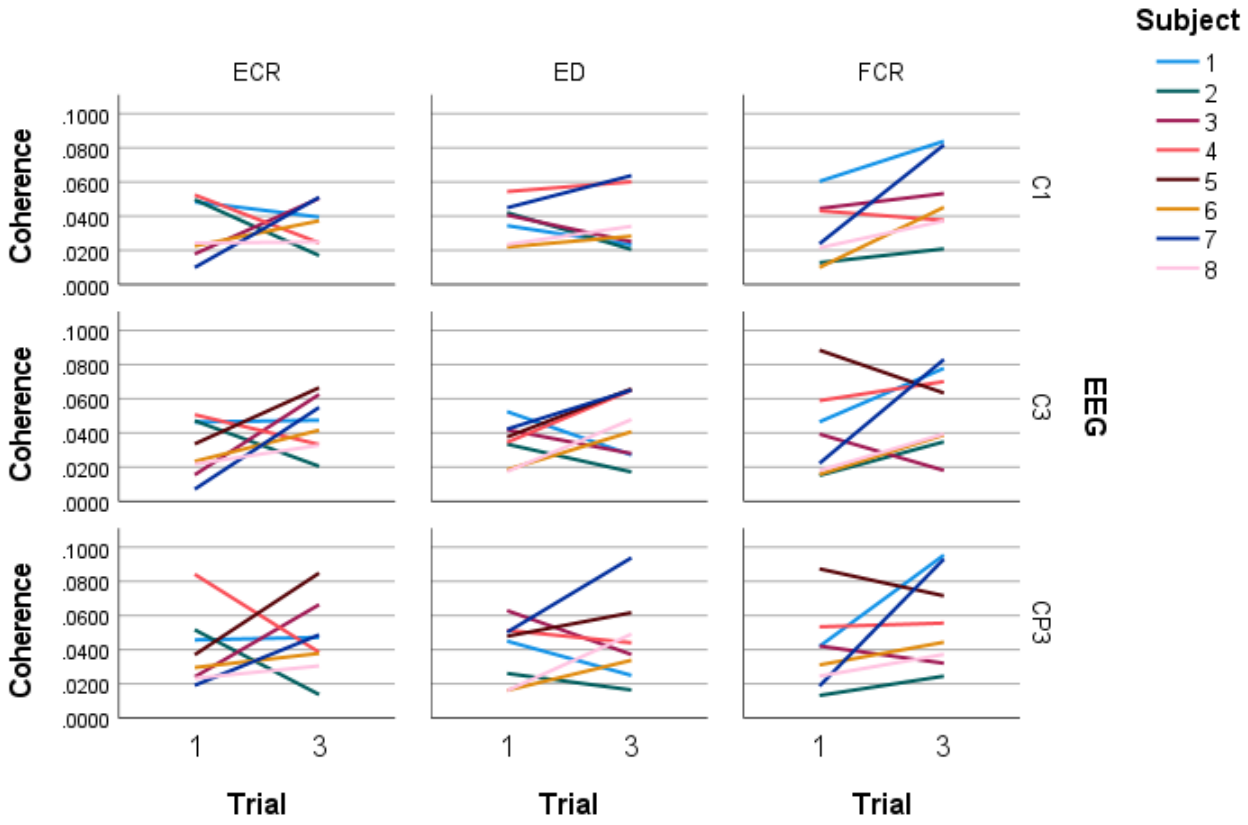

Figure 4.10: Beta band pre and post fatigue coherence between EEG from C1, C3, CP3 and EMG from ECR, FCR and ED. Coherence values for each participants are displayed using distinct colors.

Table 4.3: Betaband Maximum coherence. (The coherence values which are above the confidence level are shown in bold. The coloured cells indicate an increase in coherence values)

EEG-->	C1						C3						CP3					
Subjects	Trial1			Trial3			Trial1			Trial3			Trial1			Trial3		
	FCR	ECR	ED	FCR	ECR	ED	FCR	ECR	ED	FCR	ECR	ED	FCR	ECR	ED	FCR	ECR	ED
1	**0.0604**	**0.0484**	0.0345	**0.0839**	**0.0395**	0.0233	**0.0465**	**0.0464**	**0.0525**	**0.0779**	**0.0475**	0.0271	0.0420	**0.0458**	**0.0451**	**0.0955**	**0.0472**	0.0250
2	0.0128	**0.0497**	**0.0421**	**0.0209**	0.0170	**0.0205**	0.0152	**0.0472**	**0.0334**	**0.0348**	**0.0205**	0.0172	0.0132	**0.0517**	0.0261	**0.0245**	0.0138	0.0165
3	0.0445	0.0179	0.0407	**0.0533**	**0.0505**	0.0251	0.0393	0.0155	0.0419	0.0181	**0.0626**	0.0280	0.0422	0.0241	**0.0629**	0.0321	**0.0664**	0.0372
4	0.0432	**0.0524**	**0.0544**	0.0376	0.0244	**0.0602**	**0.0589**	**0.0507**	0.0345	**0.0701**	0.0332	**0.0650**	**0.0534**	**0.0842**	**0.0514**	0.0556	0.0386	0.0441
5	Not Used						**0.0885**	0.0336	0.0376	**0.0634**	**0.0665**	**0.0658**	**0.0874**	0.0371	**0.0479**	**0.0716**	**0.0849**	**0.0617**
6	0.0100	**0.0226**	0.0219	**0.0452**	**0.0373**	0.0283	0.0157	**0.0234**	0.0184	**0.0388**	**0.0416**	**0.0407**	**0.0311**	**0.0296**	0.0162	**0.0444**	**0.0379**	**0.0338**
7	**0.0239**	0.0100	**0.0449**	**0.0817**	0.0511	**0.0638**	0.0222	0.0071	**0.0423**	**0.0831**	**0.0550**	**0.0651**	0.0187	0.0192	**0.0503**	**0.0931**	0.0487	**0.0939**
8	0.0215	0.0243	0.0234	0.0373	0.0250	0.0341	0.0180	0.0218	0.0175	0.0394	0.0328	**0.0479**	**0.0245**	0.0233	0.0160	0.0372	0.0306	**0.0492**
Mean	0.0309	0.0322	0.0374	0.0514	0.0350	0.0365	0.0381	0.0307	0.0348	0.0532	0.0450	0.0446	0.0391	0.0394	0.0395	0.0568	0.0460	0.0452
SD	0.0188	0.0175	0.0117	0.0236	0.0133	0.0180	0.0260	0.0163	0.0119	0.0235	0.0159	0.0195	0.0236	0.0214	0.0176	0.0273	0.0218	0.0242
Median	0.0239	0.0243	0.0407	0.0452	0.0373	0.0283	0.0308	0.0285	0.0361	0.0514	0.0446	0.0443	0.0365	0.0333	0.0465	0.0500	0.0429	0.0406

A paired sample t-test was conducted with the help of SPSS, to compare the EEG - EMG coherence in pre and post fatigue conditions in the beta band. The output of the t-test showed that there is a significant increase in coherence between C1 and FCR in the beta band with a p-value of 0.041. The output of paired sample t-test performed on coherence between C1 and muscles is presented in Table 4.4. None of the other EEG-EMG pairs showed any significant changes. The t-test results for other EEG-EMG pairs are added in Appendix B.

Table 4.4: Paired sample t-test performed on pre and post fatigue EEG EMG coherence pairs in beta band. Trial 1 corresponds to pre fatigue coherence and trial 3 corresponds to post fatigue trial. There was a significant difference in pre and post fatigue C1-FCR coherence with p-value 0.041.

Paired Samples Test									
		Paired Differences					t	df	Sig. (2-tailed)
		Mean	Std. Deviation	Std. Error Mean	95% Confidence Interval of the Difference				
					Lower	Upper			
Pair 1	C1-FCR_trial1 - C1-FCR_trial3	-0.020514	0.020858	0.007884	-0.039805	-0.001224	-2.602	6	0.041
Pair 2	C1-ECR_trial1 - C1-ECR_trial3	-0.002786	0.028422	0.010742	-0.029071	0.023500	-0.259	6	0.804
Pair 3	C1-ED_trial1 - C1-ED_trial3	0.000943	0.015141	0.005723	-0.013060	0.014946	0.165	6	0.875

4.3.2 Gamma Band Coherence

Gamma waves are the fast oscillations of the brain which occur at frequencies of more than 30Hz. These waves are related to cognitive functioning, learning and information processing[1]. From the calculated coherence values of all the participants, the maximum coherence value corresponding to gamma frequencies for each participant was separated and tabulated in Table 4.5. The coherence was calculated between EEG electrodes C1, C3, and CP3 and the muscles FCR, ECR and ED for pre fatigue and post fatigue conditions. The coherence values which are above the confidence level are shown in bold in the table. The mean, standard deviation and median of coherence values across the subjects for each EEG-EMG pair for pre fatigue and post fatigue trials were also computed.

The mean value of coherence in the gamma band for C1-FCR and C1-ED increased after fatigue. Contrarily, fatigue caused a reduction in coherence between C1 and ECR. A similar pattern can be observed for C3 and CP3. Coupling between C3, CP3 and the muscles FCR and ED improved after fatigue, whereas there was a reduction in coupling with ED. A stronger coupling can be observed between FCR and the brain signals after fatigue, where it reached 0.8 for one participant.

Box plots for the coherence in gamma band for each of the EEG electrodes are shown in Figure 4.11, Figure 4.12, and Figure 4.13. The pre fatigue trial is shown with pink and the post fatigue trial is shown with blue colour. The outliers present in the coherence values make it

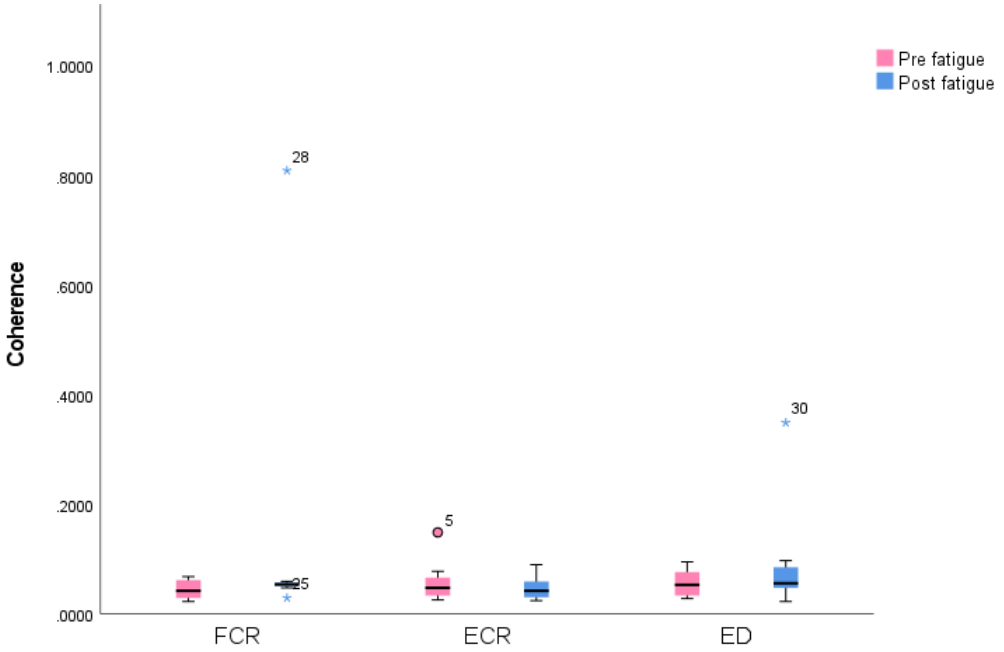

Figure 4.11: Boxplot showing pre and post fatigue coherence between EEG electrode C1 and muscles ECR, ED and FCR in Gamma band for all the participants. Pre fatigue coherence is presented in pink colour and post fatigue coherence is in blue colour. The outliers in the data are represented by 'o' and '*' and corresponding case number is shown next to it.

harder to understand the box plot. A paired sample t-test performed to compare the pre and post fatigue EEG-EMG coherence in gamma band cannot find any significant differences.

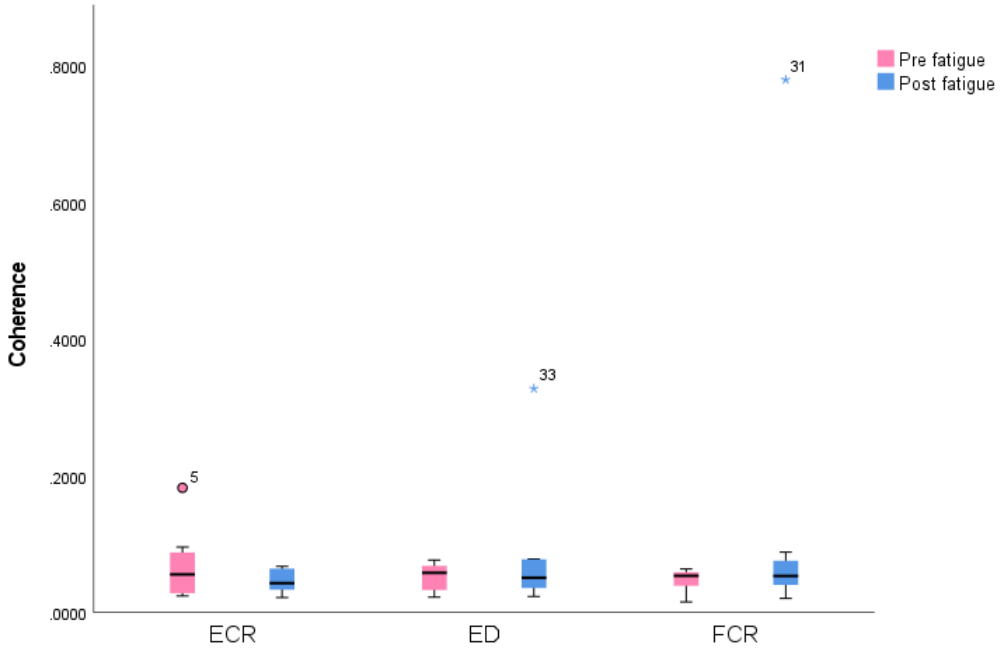

Figure 4.12: Boxplot showing pre and post fatigue coherence between EEG electrode C3 and muscles ECR, ED and FCR in Gamma band for all the participants. Pre fatigue coherence is presented in pink colour and post fatigue coherence is in blue colour. The outliers in the data are represented by 'o' and '*' and corresponding case number is shown next to it.

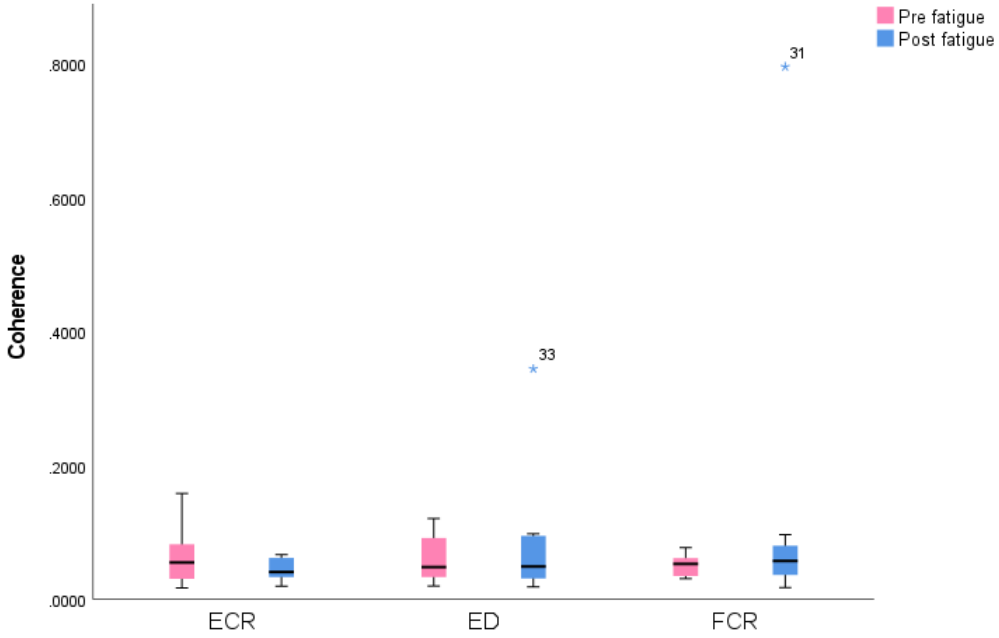

Figure 4.13: Boxplot showing pre and post fatigue coherence between EEG electrode CP3 and muscles ECR, ED and FCR in Gamma band for all the participants. Pre fatigue coherence is presented in pink colour and post fatigue coherence is in blue colour. The '*' mark represents the outliers present in the data and corresponding case number is shown next to it.

Table 4.5: Gamma band maximum coherence. (The coherence values which are above the confidence level are shown in bold. The coloured cells indicate an increase in coherence values)

EEG-->	C1						C3						CP3					
Subjects	Trial1			Trial3			Trial1			Trial3			Trial1			Trial3		
	FCR	ECR	ED	FCR	ECR	ED	FCR	ECR	ED	FCR	ECR	ED	FCR	ECR	ED	FCR	ECR	ED
1	0.0424	**0.0546**	**0.0950**	**0.0595**	**0.0440**	**0.0474**	**0.0588**	**0.0574**	**0.0760**	**0.0485**	**0.0459**	**0.0454**	**0.0546**	**0.0511**	**0.0759**	**0.0635**	**0.0412**	**0.0442**
2	**0.0683**	**0.1488**	**0.0372**	**0.0295**	**0.0243**	**0.0732**	**0.0596**	**0.1824**	**0.0388**	**0.0206**	**0.0220**	**0.0784**	**0.0637**	**0.1579**	**0.0438**	0.0175	0.0194	**0.0916**
3	**0.0658**	**0.0779**	**0.0852**	**0.8081**	0.0354	**0.3487**	**0.0549**	**0.0957**	**0.0768**	**0.7794**	0.0334	**0.3275**	**0.0508**	**0.1037**	**0.1072**	**0.7950**	0.0382	**0.3440**
4	**0.0576**	0.0477	**0.0680**	0.0544	**0.0745**	**0.0972**	**0.0524**	**0.0798**	**0.0599**	0.0549	**0.0676**	**0.0774**	**0.0772**	**0.0603**	**0.1206**	0.0467	**0.0666**	**0.0977**
5	Not Used						**0.0638**	**0.0540**	**0.0607**	**0.0883**	**0.0607**	0.0235	**0.0590**	**0.0588**	**0.0462**	**0.0966**	**0.0578**	0.0185
6	**0.0227**	**0.0393**	**0.0534**	**0.0478**	**0.0424**	0.0228	0.0155	**0.0323**	**0.0563**	0.0323	**0.0399**	0.0260	**0.0307**	**0.0289**	**0.0499**	0.0256	0.0282	0.0231
7	0.0263	**0.0285**	**0.0281**	0.0542	**0.0900**	**0.0560**	**0.0422**	0.0245	**0.0273**	0.0517	**0.0676**	0.0538	**0.0319**	0.0168	0.0197	0.0547	**0.0654**	0.0389
8	**0.0323**	**0.0257**	**0.0299**	**0.0539**	0.0254	**0.0476**	**0.0362**	0.0241	0.0224	**0.0635**	0.0334	**0.0478**	**0.0375**	**0.0323**	0.0226	**0.0597**	**0.0402**	**0.0534**
Mean	0.0451	0.0603	0.0567	0.1582	0.0480	0.0990	0.0479	0.0688	0.0523	0.1424	0.0463	0.0850	0.0507	0.0637	0.0607	0.1449	0.0446	0.0889
SD	0.0189	0.0428	0.0269	0.2868	0.0250	0.1125	0.0160	0.0526	0.0207	0.2582	0.0172	0.1001	0.0164	0.0464	0.0373	0.2638	0.0172	0.1071
Median	0.0424	0.0477	0.0534	0.0542	0.0424	0.0560	0.0536	0.0557	0.0581	0.0533	0.0429	0.0508	0.0527	0.0550	0.0481	0.0572	0.0407	0.0488

4.3.3 Subjective measures of fatigue and performance time

During the experiment, the forearm fatigue status of each participant was recorded. Participants were asked to update their fatigue status on a scale of 1 (indicating not fatigued), to 10 (indicating extremely fatigued), before trial 1, after trial 2, before trial 3 and after trial 4. The participants were asked to perform three sets of wrist flexion and extension as explained in section 3.2. It was expected that the participant would become fatigued by the third set of exercises. However, none of the participants reported fatigue after the three sets. Thus, they were asked to do extra repetitions of flexion and extension until they felt fatigued. The fatigue score of each participant is shown in Table 4.6. This table indicates that all participants reported fatigue before trial 3.

Table 4.6: Self-reported Fatigue status of each participant. The fatigue score is collected on a scale of 1-10 where 1 indicating not fatigued and 10 indicating extremely fatigued.

Subject	Before Trial1	After Trial2	Before Trial3	After Trial 4
1	1	2	8	7
2	1	1	8	8
3	1	2	8	9
4	1	1	8	6
5	1	2	8	8
6	1	4	9	9
7	1	2	8	7
8	1	3	8	4

Table 4.7 shows the time taken for each trial which is recorded with the help of Geomagic Touch API. A paired sample t-test was done between trial 1 and trial 3 and it was found that the time taken for post fatigue trial is not statistically different from the time taken for pre-fatigue trial (p-value 0.366).

Table 4.7: Time taken for different trials of NHPT in seconds

Subject	Trial 1	Trial 2	Trial 3	Trial 4
1	67	58	78	67
2	90	118	127	102
3	54	31	65	37
4	53	49	46	37
5	56	57	47	46
6	114	86	79	69
7	96	62	47	55
8	104	69	64	56
Mean (SD)	79.25 (24.59)	66.25 (26.15)	69.125 (26.95)	58.625 (21.29)

4.3.4 Kinematic Data analysis

Kinematic data, including stylus position, orientation, velocity, force, current time, and peg status indicating the selected peg, were recorded in the servo loop of Geomagic Touch. These data, logged at a frequency of 1KHz, were saved as text files. Peak velocities in both pre-fatigue and post-fatigue trials were determined and compared with coherence values. The trajectory of each peg transfer in these trials was also analyzed, and the Root Mean Square Error (RMSE) for each peg transfer was computed. Correlation analyses were conducted between maximum coherence and maximum RMSE, as well as between maximum coherence and peak velocity in both beta band and gamma band. Notably, a significant negative correlation was identified between pre-fatigue C1-FCR coherence in the beta band and RMSE (p-value 0.021). Furthermore, significant negative correlations were observed between RMSE and pre-fatigue C1-ED coherence (p-value 0.017) and pre-fatigue C3-ED coherence in the gamma band (p-value 0.016). The correlation analysis was performed using IBM SPSS and the results are presented in Table 4.8 and Table 4.9. A 3D plot presenting the trajectory of a single peg transfer is shown in Figure 4.14.

Table 4.8: Correlation Analysis of EEG-EMG Coherence in beta band with Motor Performance Metrics. The figure illustrates the relationship between EEG-EMG coherence and two key motor performance metrics: Root Mean Square Error (RMSE) and Velocity. * indicates significant correlation with p<0.05

		TRIAL1									TRIAL 3								
		C1-FCR	C1-ECR	C1-ED	C3-FCR	C3-ECR	C3-ED	CP3-FCR	CP3-ECR	CP3-ED	C1-FCR	C1-ECR	C1-ED	C3-FCR	C3-ECR	C3-ED	CP3-FCR	CP3-ECR	CP3-ED
Velocity	Pearson correlation	0.291	-0.442	0.128	-0.221	-0.412	0.23	-0.177	-0.221	0.449	0.398	0.37	0.332	0.264	0.199	-0.044	0.286	0.099	0.276
	p value	0.527	0.32	0.784	0.599	0.311	0.584	0.675	0.6	0.264	0.376	0.414	0.467	0.527	0.637	0.918	0.492	0.815	0.508
RMSE	Pearson correlation	-.831*	-0.046	-0.225	-0.649	-0.071	-0.581	-0.643	-0.168	-0.688	-0.315	-0.262	-0.076	-0.31	-0.5	-0.341	-0.387	-0.629	0.034
	p value	0.021	0.922	0.628	0.081	0.867	0.131	0.085	0.69	0.059	0.491	0.57	0.871	0.455	0.208	0.409	0.344	0.095	0.937

Table 4.9: Correlation Analysis of EEG-EMG Coherence in gamma band with Motor Performance Metrics. The figure illustrates the relationship between EEG-EMG coherence and two key motor performance metrics: Root Mean Square Error (RMSE) and Velocity. * indicates significant correlation with p<0.05

		TRIAL1									TRIAL 3								
		C1-FCR	C1-ECR	C1-ED	C3-FCR	C3-ECR	C3-ED	CP3-FCR	CP3-ECR	CP3-ED	C1-FCR	C1-ECR	C1-ED	C3-FCR	C3-ECR	C3-ED	CP3-FCR	CP3-ECR	CP3-ED
Velocity	Pearson correlation	0.195	-0.025	0.542	-0.195	0.029	0.492	-0.195	0.081	0.525	0.356	0.43	0.461	0.369	0.218	0.481	0.378	0.356	0.462
	p value	0.675	0.958	0.209	0.644	0.945	0.216	0.643	0.85	0.181	0.434	0.335	0.298	0.368	0.603	0.228	0.356	0.387	0.25
RMSE	Pearson correlation	0.006	0.414	-.845*	-0.224	0.362	-.805*	-0.204	0.336	-0.634	-0.087	-0.278	-0.051	-0.026	-0.511	0.11	-0.034	-0.366	0.11
	p value	0.989	0.356	0.017	0.594	0.378	0.016	0.629	0.415	0.092	0.852	0.546	0.914	0.951	0.195	0.796	0.937	0.373	0.795

4.4 Discussion

Alterations in corticomuscular coupling when a person was performing a haptic Nine Hole Peg Test before and after fatigue conditions were explored in this chapter. NHPT is a standardised test

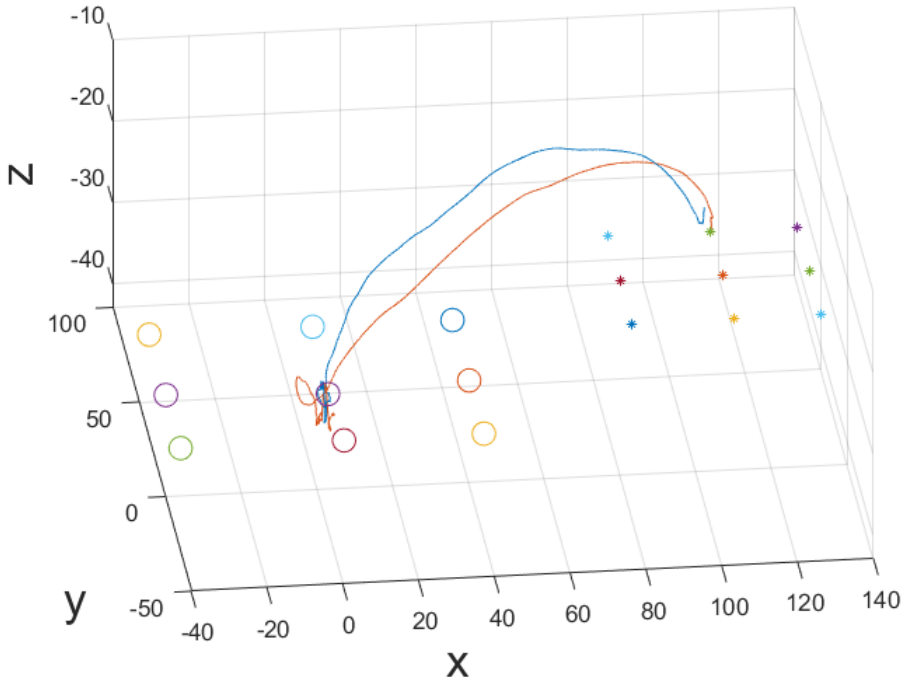

Figure 4.14: Trajectory plot for a single peg transfer for Subject 1. Trajectory plotted in blue corresponds to trajectory of peg transfer in pre fatigue trial and in orange corresponds to trajectory of peg transfer in post fatigue trial. '*' represents the positions of pegs and 'o' presents the positions of holes.

to measure fine motor dexterity whose outcome is just the time taken for completion of the test. Our analysis detailed in the chapter provides more insights into the background physiological changes in a person while carrying out NHPT. The study mainly focused on the coupling between the signals from the forearm muscles and the motor cortex. The EEG-EMG coherence is commonly used to measure the coupling strength between the brain and muscles.

The EEG-EMG coherence values during a pre-fatigue stage (trial 1) and a post-fatigue stage (trial 3) are compared here. The EEG-EMG coherence was calculated for these two trials and the beta band and gamma band coherence values were separately observed and assessed. The analysis showed an increase in corticomuscular coupling with fatigue in both bands. The increased EEG-EMG coherence suggests that the functional coupling between the brain and muscles becomes stronger with fatigue in healthy participants. This is in agreement with previous studies of corticomuscular coupling[170][86][190]. The increase in EEG-EMG coherence indicates that as a person is fatigued a larger number of neurons will fire, which will recruit more motor units to cope with fatigue. A study exploring the short-term impacts of muscular fatigue on the organization of the sensorimotor area[170] proposed an increase in cortico-muscular coherence indicating an elevated level of coordination between the synchronized firing of motor cortical neuronal pools and muscle motor units. The fatiguing activity involved a voluntary maximum

isometric contraction of Extensor Communis Digitorum (ECD), held for a minimum of 2 minutes. Coherence was computed during a non-fatiguing motor task involving isometric contraction of 20-35% of MVC force (sub-maximal voluntary contraction). The coherence in the aforementioned study was found between EEG electrodes C3, C4 and ECD. However in the current research coherence was calculated between C1, C3, CP3 and muscles FCR, ECR and ED. Additionally, this study's experiment delved into coherence during human-robot interaction.

Studies already showed that the beta band coherence is dominant during the weak-to-moderate contraction and that the EEG-EMG coherence shifts to the gamma band during very strong contraction[119]. The degree of association between the brain and muscles during arm movement increased during active movements with intention[87].

When a person is performing NHPT after fatigue, they need to take more effort physically and mentally to continue the task. The beta and gamma bands relate to the alert states of the human brain. Here we are working with motor areas of the brain where beta activity is known to be generated, and gamma activity is involved in cognitive motor tasks[170]. The dominance of both beta band and gamma band coherence indicates their potential importance in regulating motor tasks in the presence of fatigue.

The FCR and ECR muscles became strongly coupled with the brain regions C1, C3 and CP3 in the beta band after fatigue. This increase in coherence values with fatigue could indicate heightened neural synchronisation in these muscle groups, potentially related to increased motor unit recruitment. A paired sample test performed to compare the pre and post fatigue coherences found a significant increase in coherence between C1 and FCR in the beta band. Furthermore, FCR is showing a stronger coupling with EEG than other muscles. This could be because of the specific neural pathways associated with this muscle. The coupling between ED and EEG signals from C3 and CP3 became stronger after fatigue. However, the reduced coupling between C1 and ED muscle after fatigue could indicate reduced neural synchronisation, possibly due to a reduction in the number of active motor units or changes in the neural pathways responsible for coordinating the movement. This suggests that the cortical control of muscular activity for ED might shift from the C1 region to the C3 and CP3 regions after fatigue.

The analysis of gamma band coherence indicates a clear increase in coherence. There are studies which suggest that visual stimuli can increase the gamma activity[81]. In the given experiment the subjects needed to perform the NHPT in a virtual environment which required attention, learning and processing. When a person who is already fatigued is asked to perform a task which needs some cognitive work that may trigger EEG activity in the gamma band which will in turn recruit more motor neurons which in turn excite more muscle fibres. The coupling of FCR and ED with the EEG signals under consideration increased with fatigue in the gamma band. Also, much higher coherence values are observed between the FCR and EEG electrodes. The higher coherence values between FCR and EEG electrodes might imply increased neural synchronisation in the cortical regions responsible for generating the movements. Additionally,

the observed changes may reflect compensatory mechanisms in response to the development of fatigue. The post fatigue coherence value for FCR with EEG electrodes for Participant 3 is well above the rest of the values. Table 4.6, indicating that this participant reported an increase in fatigue score after trial 4 which highlights that the recovery time for this participant from fatigue was longer compared to the other participants. This leads to the conclusion that the fatigue on the forearm might have caused a substantial increase in the high frequency contractions of FCR.

ECR exhibited an increase in post fatigue coherence in the beta band while a decline in post fatigue coherence was observed in the gamma band. This decrease in coherence in the gamma band between ECR and EEG signals after fatigue might indicate alterations in the neural pathways responsible for coordinating movement in the high frequency range. This could be due to a reduction in the number of active motor units or changes in the neural processing of muscle activation during fatigue.

When attention is divided between a motor task and another simultaneously performed task, the level of significant beta range synchronisation decreases below the confidence level[94]. This might be the reason why the occurrence of coherence values above the confidence level is more prominent in the gamma band compared to the beta band. Previous studies already found that the EEG power increases with fatigue[2]. We argue that even though the focus is on physical fatigue, the individual is also experiencing mental fatigue as the virtual environment is imposing cognitive demands on the participants. The corticomuscular coupling might be affected by the cognitive load as well.

Except for three participants, all the other participants completed trial 3 in less time compared to trial 1. However, the interesting fact was that all these participants reported fatigue on their wrists after the dumbbell exercise. The reason for the reduction in completion time may be that familiarisation with the haptic NHPT might have helped the participants complete the task in a lesser time.

A correlation analysis between motor parameters and the coherence values suggest a strong negative correlation between certain coherence values and RMSE during trial 1. However, it is important to note that the low number of samples used in this study poses a challenge in achieving statistical significance. Despite the limitations, the observed negative correlation offers valuable insights into potential associations between coherence and motor performance, warranting further exploration with larger sample sizes for conclusive results.

The complex interplay between fatigue and coherence values suggests that this measure may be a valuable tool for assessing the neural correlates of muscle fatigue and motor function. It is important to note that these findings are frequency-specific and may differ across different cortical regions involved in motor control and performance. These findings highlight the importance of considering the frequency-specificity of coherence measures and the role of different cortical regions in motor control and performance. Further research is necessary to fully understand the implications of these changes for fatigue-related impairments in motor function.

4.5 Chapter summary

This chapter discussed the changes in corticomuscular coupling while performing the Nine Hole Peg Test using a haptic device under fatigue. It was found that the EEG-EMG coherence increased with fatigue. It was also found that when the person is performing NHPT, EEG-EMG coherence is mainly found in gamma band and beta band, both in pre fatigue and post fatigue conditions. Coherence changes specifically to the beta band and gamma band are also seen. The analysis showed that the coherence increases in both of these bands. However, the results were not able to be supported statistically because of the small number of participants.

The experiment was conducted on healthy participants. However, we argue that our approach could be valuable in real application scenarios for example with stroke patients with reduced physical and cognitive strengths due to the neurological condition. Our approach provided an observation of fatigue and its neural correlates during the performance of a task specific to the assessment of fine motor dexterity. However, the performance of the NHPT task mainly improved with repetition and did not suffer from fatigue. We argue that this could be very different in stroke patients where additional physical and neural capacity may be restricted due to their condition. Also, our approach had a limited cognitive load, due to the use of a virtual environment, but we did not gather subjective feedback on the state of mental fatigue, which limits our conclusion regarding the extent of cognitive fatigue during experiment phases. Future studies would benefit from separate physical and cognitive fatiguing elements, thus allowing the separate observation of such impacts on neural correlates presented by parameters such as coherence.

CHAPTER 5

IMPACT OF FATIGUE ON MICROSTATE PARAMETERS DURING EXECUTION OF A HAPTIC NINE HOLE PEG TEST AND PHYSICAL EXERCISE

Chapter 4 explained the changes in EEG-EMG coherence while performing NHPT under fatigue conditions. This chapter will look into the effect of fatigue on brain activity at millisecond levels which are better captured by the microstates. The literature has already established that the brain electrocortical activity increases after fatiguing physical exercise[40]. It will be interesting to investigate the changes in EEG microstates when a person performs a fatiguing exercise. The majority of microstate studies have been conducted on EEG data obtained during resting state conditions. Here an attempt is made to conduct microstate analysis on resting state EEG data as well as on the EEG measured while performing a task with fine motor control requirements and a physical exercise.

5.1 Research Question

Does fatigue impact EEG microstate parameters while interacting with a robotic rig and physical exercise?

5.2 Materials and Methods

The experiment setup and EEG acquisition are detailed in chapter 3. With the help of the g.tec acquisition system EEG signals were recorded at a sampling rate of 1200Hz. This EEG data was continuous and needed to be segmented into different sections. The recorded EEG data was stored as .mat files in the computer. 'Key press' data recorded with the help of MATLAB Simulink

model was used to extract EEG data corresponding to eye close and eye open at the beginning and end. Similarly, the time at which each peg was picked and released was logged during the experiment with the help of Geomagic Touch API. A MATLAB algorithm was employed which utilised this time stamp data to separate EEG for each trial of NHPT. Processing algorithms for EEG were developed using MATLAB R2019A. The calculation of microstates was performed with the help of the Microstate EEGlab toolbox.

5.2.1 EEG Microstates

The experiment was conducted on ten participants, but five participants' data were excluded because the EEG collected from some of the electrodes for these participants had high levels of noise which made it unsuitable for further processing. To conduct the microstate analysis, it is imperative to ensure that EEG data from all channels are available for each participant in the study. Hence only five participants' data were used for microstate analysis. Subject demographics are presented in Table 5.1. Participants were at least 18 years of age (Mean±SD: 31.8±5.02 years) with variable BMI (Mean±SD: 26.4±6.02). The BMI of the participants was recorded to check its effect on fatigue development on the participants.

Table 5.1: Demographics of participants

Subject	Gender	Age	BMI
1	Male	25	22
2	Female	36	21
3	Male	36	28
4	Male	34	36
5	Male	28	25

Microstates were found for the resting state data at the beginning and end of the experiment. Also, microstates were found for pre fatigue trial (NHPT trial 1), dumbbell exercise and post fatigue trial (NHPT trial 3). For ease of reference, the NHPT trial will be referred to as trial throughout this chapter. EEG microstate analysis was performed with the help of the Microstate EEGLAB toolbox in MATLAB R2019a[138]. The main part of the microstate analysis is to segment the EEG recordings into quasi-stable states using a clustering method. EEG microstates are called stable states since the brain's electric field configuration remains stable for a short period of time. Different clustering methods can be employed to find the EEG microstates. Modified K means clustering which has been widely employed in different studies was used in this project to find microstates[184][5]. In the modified K means clustering method, an initial set of K individual maps is randomly selected to serve as cluster templates. Subsequently, an iterative optimisation process is employed, wherein these template maps are refined to better align with the data. This iterative procedure involves repeatedly assigning all individual maps to their most similar template map and updating the template maps based on the first principal

component of the assigned individual maps until a convergence criterion is met[134]. The main advantage of using modified K means clustering is that it ignores the polarity of EEG topography, leaving the overall symmetry of the potential topography as the feature to be clustered[184]. The steps involved in the microstate analysis are shown in Figure 5.1.

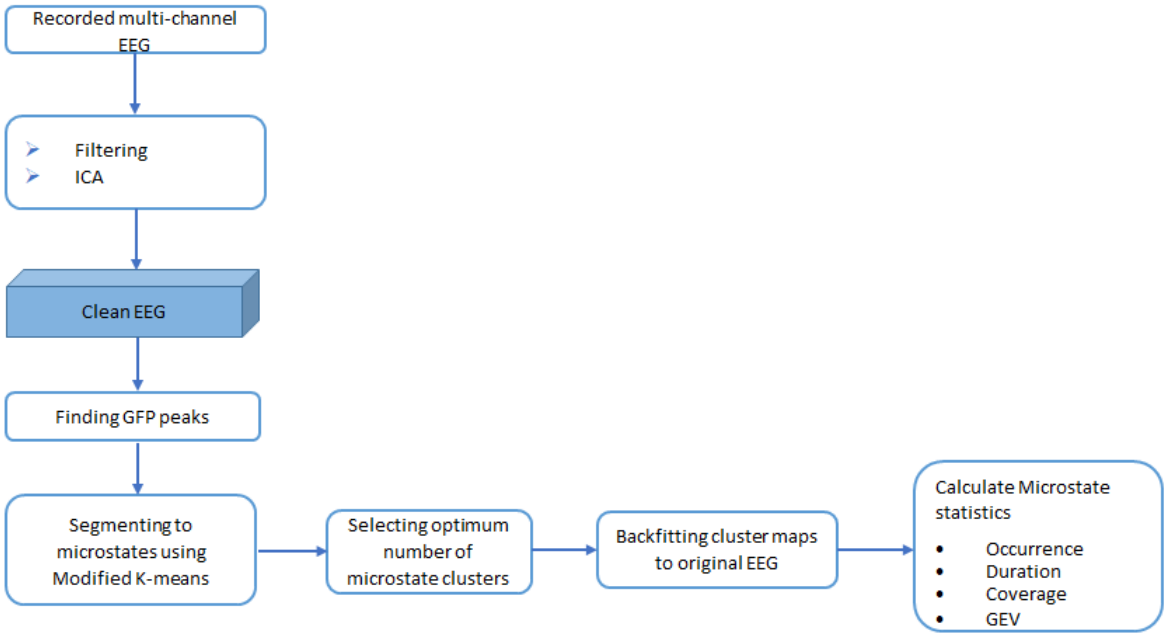

Figure 5.1: Flow diagram showing different steps in microstate analysis

Microstates were calculated for three phases of the experiment

- Resting state: EEG measured during eye close at the beginning and end were used for this analysis.
- NHPT trial: EEG data collected during the first peg transfer in trial 1 and trial 3 were used for this analysis.
- Dumbbell exercise: Here EEG data corresponding to the first set of repetitions and extra repetitions each participant made at the last during the exercise were used.

A two-step clustering was performed to find the microstate maps. Initially, clustering was performed on each participant's data, followed by a subsequent clustering process across all subjects included in the study[41]. First eye close data at the beginning and end was taken. Each data was segmented into 20 sets of 2s epochs. All 16 electrodes were used for finding EEG microstate topographies. For microstate analysis, topographies at maximal potential field strength are considered. The strength of the scalp potential can be quantified using global field power. The global field power (GFP) can be calculated as

$$GFP(t) = \sqrt{\frac{\sum_i^k \left(V_i(t) - V_{mean}(t)\right)^2}{k}} \tag{5.1}$$

where $V_i(t)$ is the voltage at electrode i at time t, $V_{mean}(t)$ is the mean voltage across all electrodes at time t and k is the number of electrodes[84].

The optimal signal to noise ratio and stable topography are obtained at the local maximum of GFP[198]. Hence in the first step global field power of all aggregated data sets were generated. For each EEG data segment, 1000 randomly selected GFP peaks were used for segmentation. EEG maps that correspond to GFP peaks were submitted to modified K-means clustering for generating microstate prototypes. While performing the clustering the polarity of the maps was ignored. Microstate prototypes were sorted by decreasing global explained variance. The number of random initialisation was set to 50 and the maximum number of iterations was set as 1000. A cross validation criterion was used as a measure of fit for selecting the best segmentation.

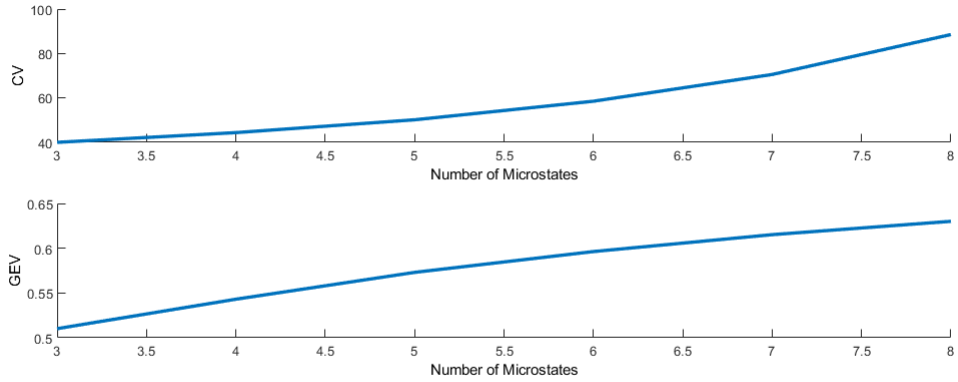

Figure 5.2: Measures of fit plotted for the different microstate segmentations. CV and GEV are used as measures of fit since they are polarity invariant. The optimal number of clusters reflects a trade-off between the goodness of fit and the complexity of clusters.

Most of the literature predefined the number of microstates as four which previously has been reported as able to explain more than 70% of the total topographic variance[84]. However, in this project, the number of microstates was selected based on the evaluation of prototype topographies and measures of fit. Since we are not considering the polarity of the EEG data, polarity invariant measures of fit Global explained variance (GEV) and cross-validation criterion (CV) were used for selecting the optimum number of microstate topographic clusters. Selecting the appropriate number of clusters involves a clear trade-off between achieving a good fit and managing the complexity introduced by a high number of microstates in the segmentation process. A low value of CV is desirable since it is a measure of residual noise. GEV becomes larger as the number of

clusters increases. Measures of fit plotted for the different microstate segmentations is presented in Figure 5.2. Here number of clusters was selected as three since it has the lowest CV value.

The microstate clusters obtained at the individual level were then again clustered to get the global microstate maps[11]. Three distinct microstates were observed for the resting state, NHPT trial and exercise EEG. These global microstate maps were backfitted to original EEG data to find microstate parameters[41]. After backfitting, microstate labels were smoothed temporally to remove small segments of unstable topography. For each microstate class, different microstate parameters were calculated from the backfitted EEG data. Microstate parameters were found for each participant before and after fatigue. The temporal parameters of microstates that were calculated in this project are the duration, occurrence, coverage and global explained variance. The duration of a microstate is the average time for which a given microstate remains stable whenever it appears. The coverage of a microstate is the fraction of the total recording time when the given microstate is dominant. The occurrence is the average number of times per second a microstate is dominant [85]. The global explained variance (GEV) quantifies the extent to which the clustering of microstates describes the given dataset[198].

5.3 Results

The EEG data were recorded continuously throughout the entire experiment, and the microstate analysis was performed for three specific conditions: one during rest, another during the performance of the NHPT task and a third during dumbbell exercise. For the analysis of resting state data, EEG during eye close at the beginning and end of the experiment was used. To find microstates while performing NHPT, EEG for the first peg transfer during trial 1 and trial 3 was used. Microstates for dumbbell exercise were found by analysing EEG data corresponding to the first set of repetitions and the extra repetitions each participant made during the exercise. Three distinct microstates were observed for each of these conditions. These microstates are presented in Figure 5.3.

5.3.1 Resting state microstates before and after fatigue

At the beginning and the end of the experiment, a two-minute resting state EEG was collected from the participants by keeping their eyes closed. This EEG was used to find any changes in microstate parameters because of fatigue. As detailed in section 5.2.1, the global microstate maps were backfitted to each 2s data segment used for clustering and microstate parameters were found by averaging. Three microstates, A, B and C, were observed for this data. The microstate parameters derived from the resting state data are presented in Table 5.2. It can be seen that the occurrence of microstate A increased for all subjects except subject 4. For microstates B and C, the occurrence increased for three subjects and decreased for two subjects. At the same time, the duration of microstate A increased for all subjects except subject 4. The duration of microstate B

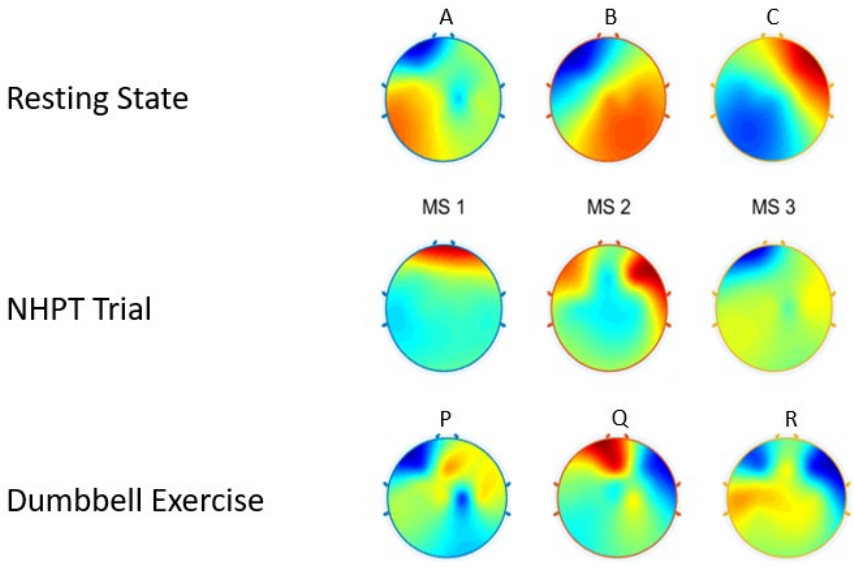

Figure 5.3: Microstates observed for resting state, NHPT trial and dumbbell exercise

increased for three subjects and decreased for one subject. The duration of microstate C decreased for all subjects. Figure 5.4 and Figure 5.5 show the changes in microstate occurrence and duration with fatigue.

Table 5.2: Pre and Post fatigue Resting state microstate parameters.

Subject	**Microstates**	**Occurrence**			**Duration(ms)**			**Coverage(%)**			**GEV**		
		Pre	Post	Change	Pre	Post	Change	Pre	Post	Change	Pre	Post	Change
1	A	4.32	4.57	↑	78.34	150.32	↑	34	64	↑	0.17	0.36	↑
	B	4.12	3.10	↓	77.74	57.16	↓	32	18	↓	0.15	0.07	↓
	C	4.35	2.85	↓	80.18	61.47	↓	35	18	↓	0.19	0.08	↓
2	A	2.00	2.42	↑	49.68	54.79	↑	10	13	↑	0.03	0.03	
	B	4.72	4.45	↓	101.05	140.23	↑	47	60	↑	0.18	0.21	↑
	C	4.77	3.55	↓	92.85	76.75	↓	43	27	↓	0.17	0.07	↓
3	A	0.57	1.30	↑	40.00	44.26	↑	3	6	↑	0.00	0.01	↑
	B	4.20	4.60	↑	123.88	106.72	↓	48	46	↓	0.17	0.13	↓
	C	4.25	4.47	↑	119.89	119.71	↓	49	48	↓	0.18	0.15	↓
4	A	1.15	0.62	↓	72.49	30.90	↓	11	3	↓	0.02	0.01	↓
	B	2.37	3.57	↑	116.21	116.41	↑	27	41	↑	0.07	0.14	↑
	C	2.45	3.67	↑	402.22	165.44	↓	62	55	↓	0.25	0.25	
5	A	0.95	2.30	↑	47.18	64.40	↑	6	15	↑	0.01	0.03	↑
	B	2.75	3.75	↑	60.34	74.45	↑	17	28	↑	0.03	0.08	↑
	C	3.62	4.30	↑	233.95	145.44	↓	77	56	↓	0.32	0.26	↓

↑ and ↓ indicates an increase and decrease of microstate parameters respectively

The coverage of microstate A increased for all subjects except subject 4. The coverage of microstate B increased for three subjects and decreased for two subjects. The coverage of microstate C decreased for all the subjects. Changes in coverage for resting state microstates are presented in Figure 5.6. The global explained variance of microstate A increased for all subjects except subject 4. GEV of microstate B increased for three subjects and decreased for two subjects. GEV of microstate C decreased for four subjects and remained unchanged for one subject. Figure 5.7 exhibits the changes to the global explained variance due to fatigue for resting state EEG.

A paired-sample t-test was employed to assess the impact of fatigue on microstate parameters. The analysis revealed a statistically significant decrease in both the coverage (p = 0.027) and Global Explained Variance (GEV) of microstate C (p = 0.046). The results of t-test performed on microstate C is presented in Table 5.3.

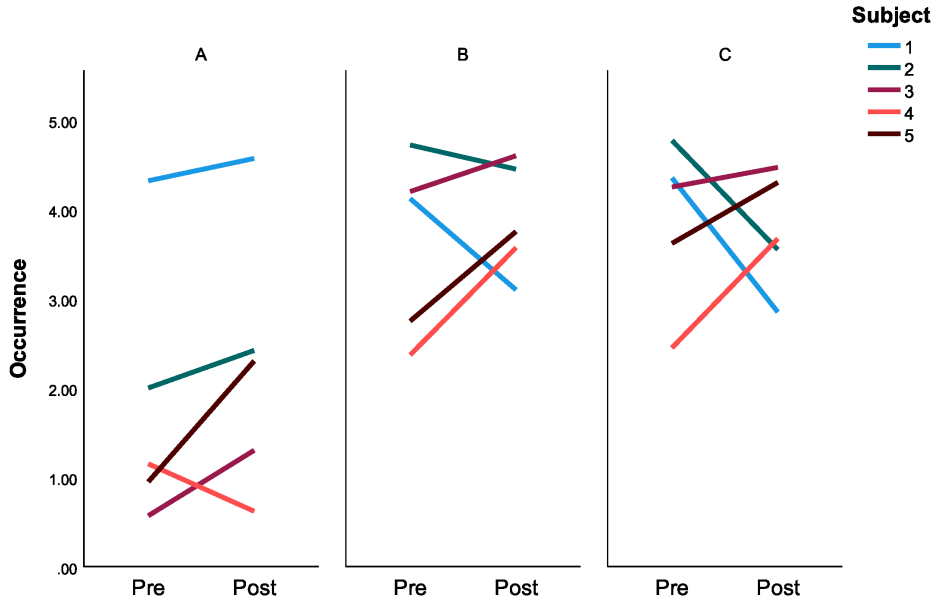

Figure 5.4: Microstate parameter: Changes in the occurrence of resting state microstates A, B, and C from pre fatigue to post fatigue

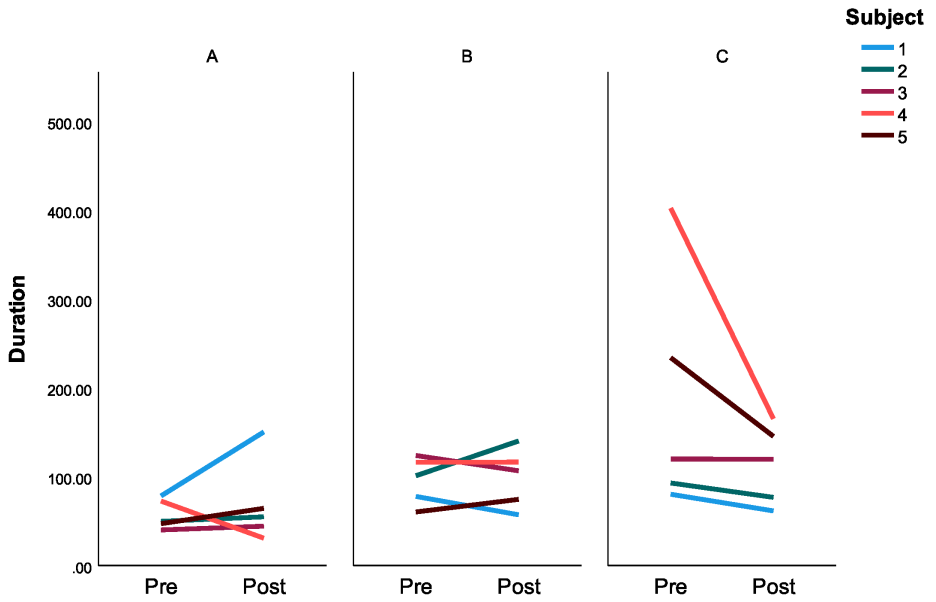

Figure 5.5: Microstate parameter: Changes in the duration of resting state microstates A, B, and C from pre fatigue to post fatigue

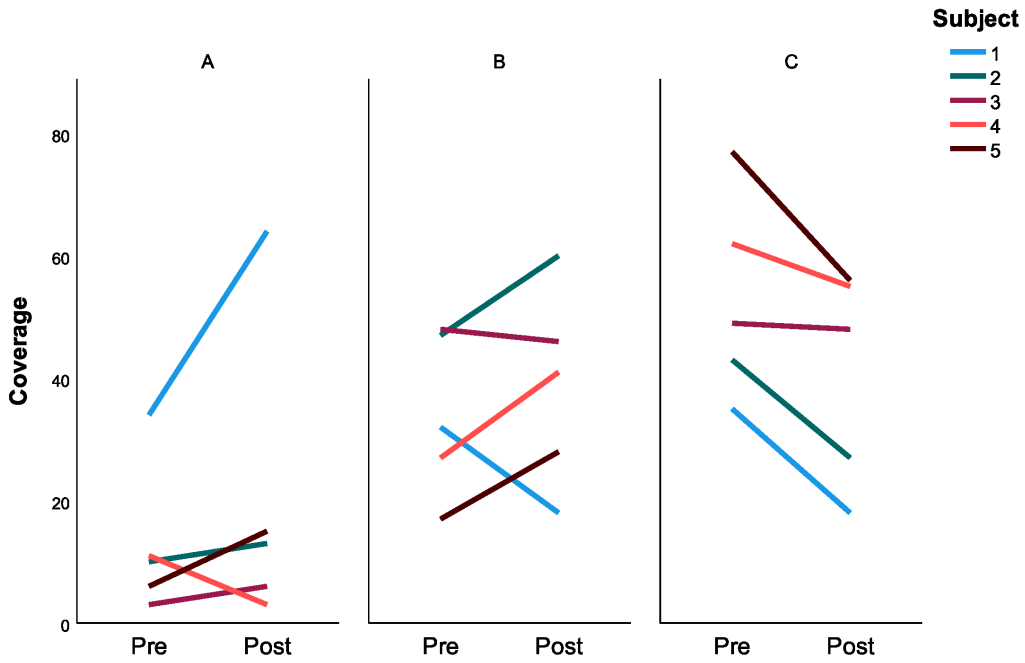

Figure 5.6: Microstate parameter: Changes in the Coverage of resting state microstates A, B, and C from pre fatigue to post fatigue

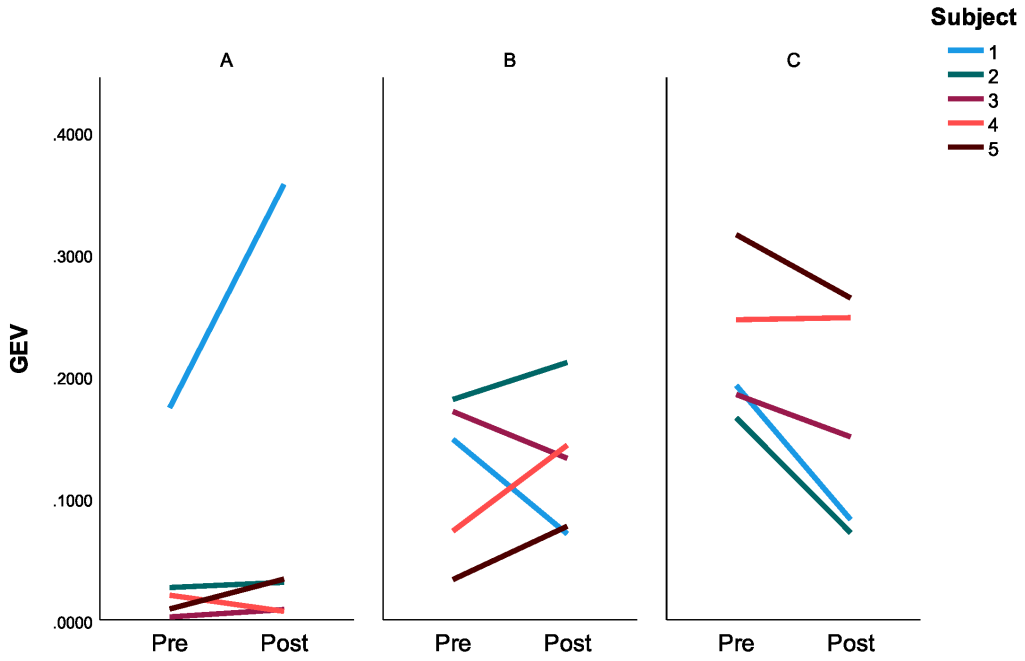

Figure 5.7: Microstate parameter: Changes in the GEV of resting state microstates A, B, and C from pre fatigue to post fatigue

Table 5.3: Paired sample t-test performed on parameters of Resting state microstate C. A significant decrease in coverage and GEV is observed with p<0.05.

Paired Samples Test									
		Paired Differences					t	df	Sig. (2-tailed)
		Mean	Std. Deviation	Std. Error Mean	95% Confidence Interval of the Difference				
					Lower	Upper			
Pair 1	Occurrence_Pre - Occurrence_Post	0.12000	1.19013	0.53224	-1.35774	1.59774	0.225	4	0.833
Pair 2	Duration_Pre - Duration_Post	72.05600	98.16792	43.90203	-49.83557	193.94757	1.641	4	0.176
Pair 3	Coverage_Pre - Coverage_Post	12.400	8.173	3.655	2.252	22.548	3.392	4	0.027
Pair 4	GEV_Pre - GEV_Post	0.05774	0.04506	0.02015	0.00179	0.11369	2.865	4	0.046

5.3.2 NHPT trial microstates

The microstates were found when a person performs the first peg transfer in trial 1 and trial 3. Trial 1 was the first trial when the participant is not fatigued yet. Trial 3 was the trial just after the fatiguing exercise and can therefore be called the post-fatigue trial. Three microstates were observed in the task EEG and named MS1, MS2 and MS3 in order to distinguish them from the resting state microstates. Just like for the resting state microstates here also the microstate parameters, occurrence, coverage, duration and GEV were calculated and tabulated. Table 5.4 details the pre-fatigue and post-fatigue values of the microstate parameters.

Table 5.4: Pre and post fatigue NHPT trial microstate parameters.

Subject	Microstates	Occurrence			Duration(ms)			Coverage(%)			GEV		
		Pre	Post	Change	Pre	Post	Change	Pre	Post	Change	Pre	Post	Change
1	MS1	0.81	1.52	↑	78.89	65.56	↓	6.40	10.00	↑	0.0023	0.02	↑
	MS2	1.08	1.28	↑	48.96	61.98	↑	5.30	8.82	↑	0.0035	0.01	↑
	MS3	2.16	3.31	↑	409.69	266.01	↓	88.30	81.19	↓	0.63	0.38	↓
2	MS1	0.29	0.67	↑	3.46*	1.76*	↓	100	98.29	↓	0.69	0.81	↑
	MS2	0	0.33	↑	0	25.69	↑	0	1.72	↑	0	0.0011	↑
	MS3	0	0		0	0		0	0		0	0	
3	MS1	1.86	1.00	↓	492.02	975.00	↑	91.68	97.79	↑	0.81	0.87	↑
	MS2	0.53	0.50	↓	75.42	44.17	↓	4.02	2.21	↓	0.0023	0.0015	↓
	MS3	1.06	0	↓	40.42	0	↓	4.30	0	↓	0.0054	0	↓
4	MS1	2.67	2.62	↓	154.72	399.78	↑	42.45	73.67	↑	0.30	0.61	↑
	MS2	2.67	2.24	↓	258.64	102.69	↓	49.31	24.67	↓	0.33	0.07	↓
	MS3	1.00	0.25	↓	69.21	33.13	↓	8.23	1.66	↓	0.02	0.0007	↓
5	MS1	3.92	1.31	↓	189.08	703.75	↑	74.13	92.45	↑	0.41	0.75	↑
	MS2	1.18	1.31	↑	39.72	57.50	↑	4.67	7.55	↑	0.01	0.01	↑
	MS3	3.92	0	↓	54.08	0	↓	21.20	0	↓	0.05	0	↓

↑and ↓ indicates increase and decrease of microstate parameters respectively
*Duration of MS1 for subject 2 is in seconds

For MS1 the occurrence increased with fatigue for two participants and decreased with fatigue for three participants. The Occurrence of MS2 increased with fatigue for three subjects and decreased with fatigue for two subjects. MS3 exhibited an increase in occurrence for one subject and a decrease in occurrence for three subjects. The changes in occurrence and duration while the participant transitions from a pre fatigue state to post fatigue state are presented in

Figure 5.8 and Figure 5.9.

The duration of MS1 increased with fatigue for three subjects and decreased for the other two. The coverage of MS1 increased for all subjects except one. The global explained variance of MS1 increased with fatigue for all subjects. For MS2 all the parameters increased with fatigue for three subjects and decreased with fatigue for two subjects. No MS3 was observed for subject 2. In the other four subjects, the duration, coverage and GEV decreased with fatigue for MS3. The alterations in coverage and GEV for trial microstates are illustrated in Figure 5.10 and Figure 5.11. A paired-sample t-test was conducted to assess potential differences in NHPT trial microstate parameters before and after fatigue. However, the analysis did not reveal any statistically significant differences.

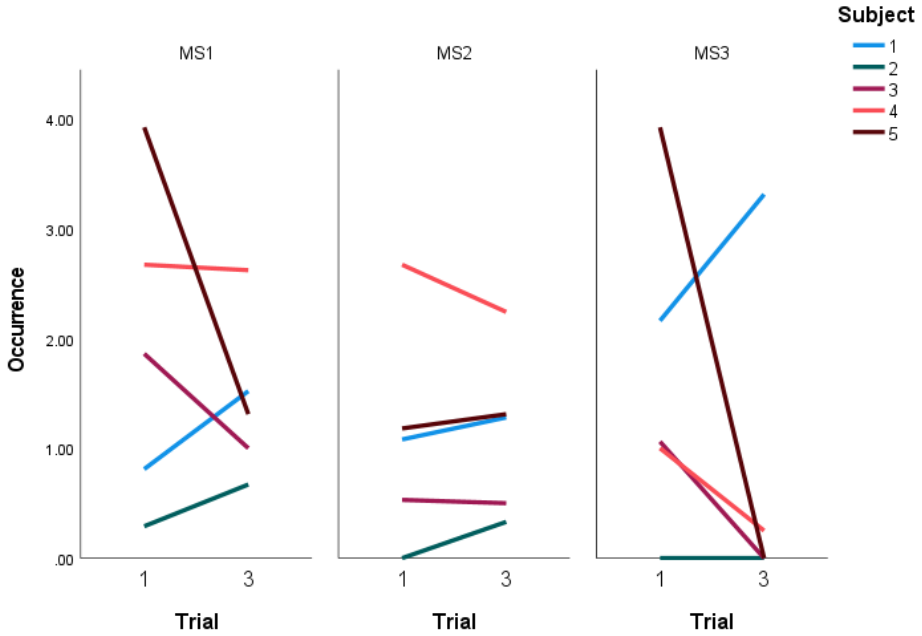

Figure 5.8: Microstate parameter: Changes in the occurrence of NHPT trial microstates from pre fatigue to post fatigue trials. Trial 1 is the pre fatigue trial and trial 3 is the post fatigue trial.

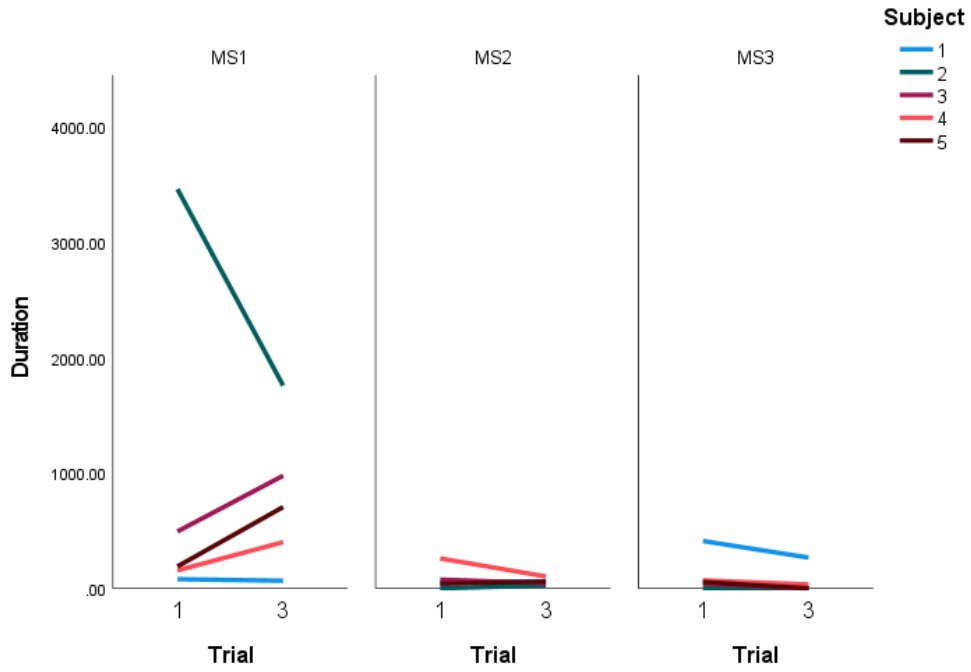

Figure 5.9: Microstate parameter: Changes in the duration of NHPT trial microstates from pre fatigue to post fatigue trials. Trial 1 is the pre fatigue trial and trial 3 is the post fatigue trial.

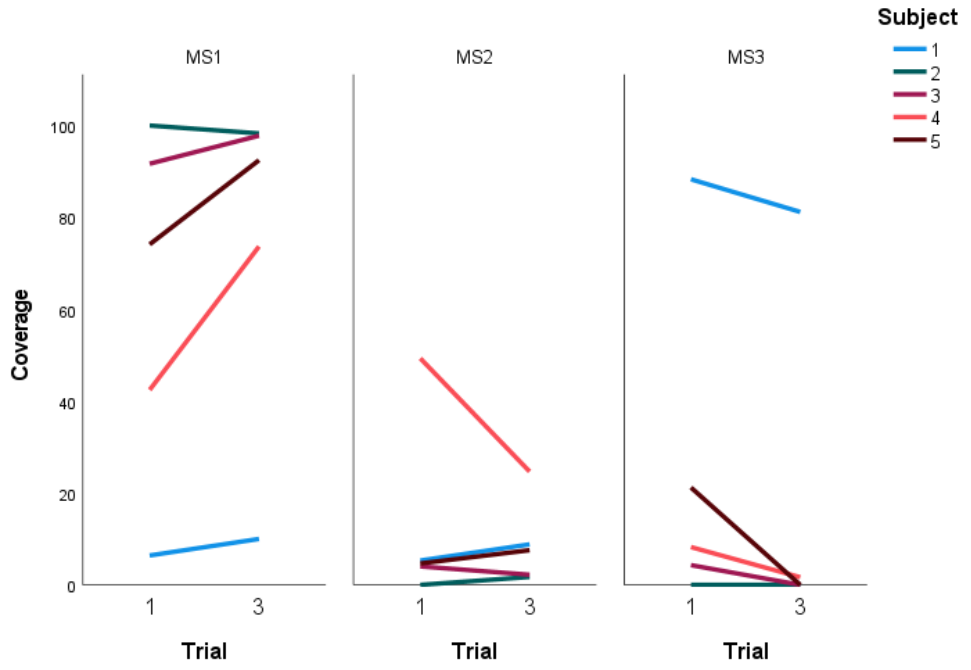

Figure 5.10: Microstate parameter: Changes in the coverage of NHPT trial microstates from pre fatigue to post fatigue trials. Trial 1 is the pre fatigue trial and trial 3 is the post fatigue trial.

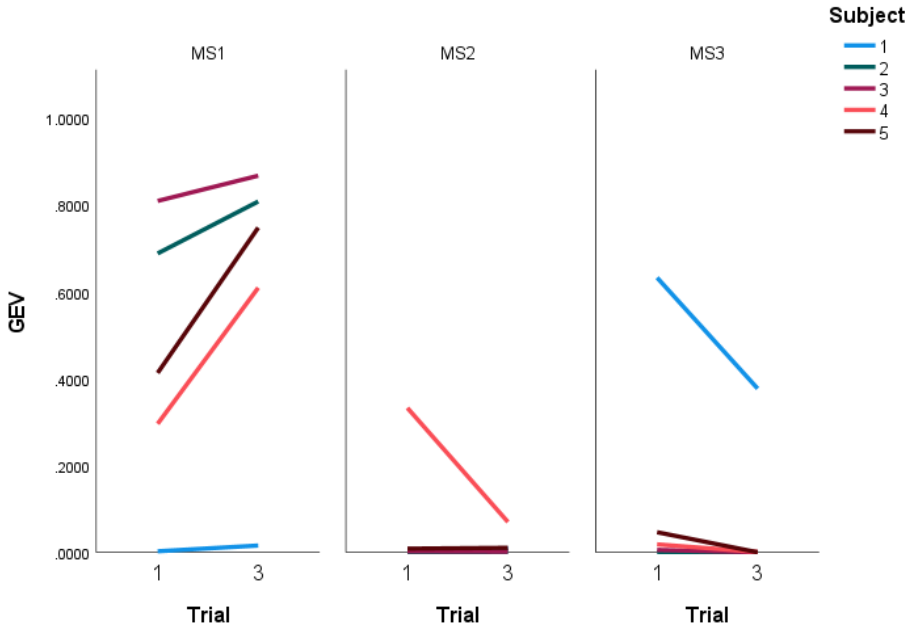

Figure 5.11: Microstate parameter: Changes in the GEV of NHPT trial microstates from pre fatigue to post fatigue trials. Trial 1 is the pre fatigue trial and trial 3 is the post fatigue trial.

5.3.3 Microstates while performing dumbbell exercise

After two trials of NHPT, the participants were asked to perform a dumbbell exercise involving flexion and extension of the wrist. The principal aim of this exercise was to induce muscle fatigue in the forearm. Each participant did three sets of repetitions with a 30 seconds break. The first set had 12 repetitions of flexion and extension of the wrist followed by 10 repetitions which in turn followed by 8 repetitions. It was expected that the participant would get fatigued by the third set of exercises. Since none of the participants reported fatigue after the three sets, they were asked to perform extra repetitions of flexion and extension until they felt fatigued. EEG data were collected throughout this entire duration.

Microstate analysis was performed on the EEG data collected during the first set of repetitions and the extra repetitions, that is, at the beginning and end of the exercise. Three microstates P, Q, and R were observed. The microstate parameters found at the beginning and end of the dumbbell exercise are tabulated in Table 5.5. The changes in microstate parameters while transitioning from the beginning of the exercise to the end of the exercise are presented in Figure 5.12, Figure 5.13, Figure 5.14 and Figure 5.15.

The microstate parameters observed at the start and end of the dumbbell exercise did not demonstrate any noticeable pattern. A paired-sample t-test was conducted to assess potential differences in microstate parameters at the start and end of the exercise. However, the analysis did not reveal any statistically significant differences. The coverage of microstate R for all participants except subject 4 decreased at the end of the exercise. Microstate R was not present

for subject 1 at the end of the exercise. In comparison to other participants, subject 4 exhibited a greater alteration in microstate parameters. A paired-sample t-test was conducted to assess any significant changes in the microstate parameters at the beginning and end of the exercise. However, the analysis did not reveal any statistically significant differences.

Table 5.5: Dumbbell microstate parameters at the beginning and end of the exercise.

Subject	Microstates	Occurrence			Duration(ms)			Coverage(%)			GEV		
		Start	End	Change	Start	End	Change	Start	End	Change	Start	End	Change
1	P	3.50	3.78	↑	198.55	165.01	↓	66.84	59.85	↓	0.365	0.307	↓
	Q	3.11	3.72	↑	107.47	118.02	↑	32.98	40.15	↑	0.188	0.218	↑
	R	0.06	0.00	↓	3.70	0.00	↓	0.19	0.00	↓	0	0	
2	P	1.44	1.50	↑	100.64	72.39	↓	11.82	12.85	↑	0.013	0.012	↓
	Q	2.67	2.50	↓	457.02	404.38	↓	79.43	79.07	↓	0.171	0.249	↑
	R	1.39	1.44	↑	47.10	49.68	↑	8.75	8.08	↓	0.006	0.005	↓
3	P	2.67	2.22	↓	109.89	123.98	↑	29.18	28.35	↓	0.034	0.043	↑
	Q	2.83	2.78	↓	109.94	162.68	↑	28.56	40.03	↑	0.037	0.067	↑
	R	3.11	2.78	↓	140.56	113.29	↓	42.26	31.62	↓	0.064	0.065	↑
4	P	1.33	0.39	↓	94.24	68.12	↓	14.43	5.67	↓	0.029	0.014	↓
	Q	2.78	0.78	↓	179.08	171.23	↓	42.80	15.88	↓	0.133	0.056	↓
	R	2.67	1.28	↓	207.06	658.60	↑	42.77	78.45	↑	0.222	0.463	↑
5	P	0.67	1.11	↑	38.43	47.50	↑	3.85	5.80	↑	0.001	0.005	↑
	Q	2.94	3.39	↑	179.13	153.87	↓	49.16	49.79	↑	0.142	0.132	↓
	R	3.17	3.33	↑	159.91	143.21	↓	46.99	44.41	↓	0.123	0.109	↓

↑and ↓ indicates increase and decrease of microstate parameters respectively

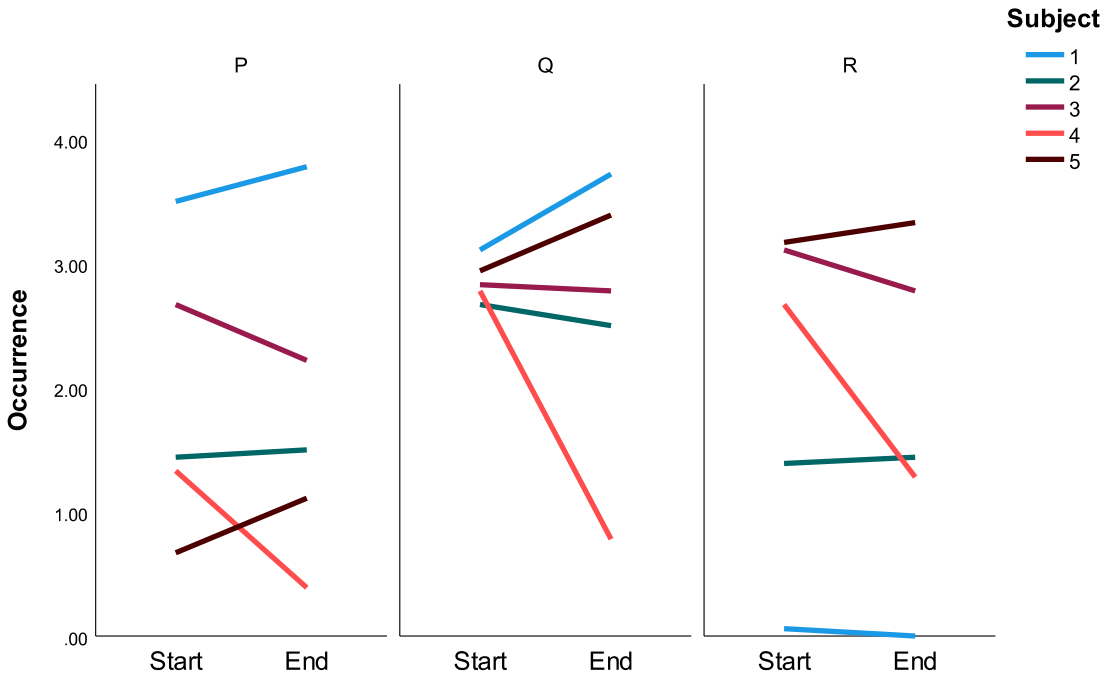

Figure 5.12: Microstate parameter: Changes in the occurrence of microstates P, Q, R from the beginning to the end of the dumbbell exercise.

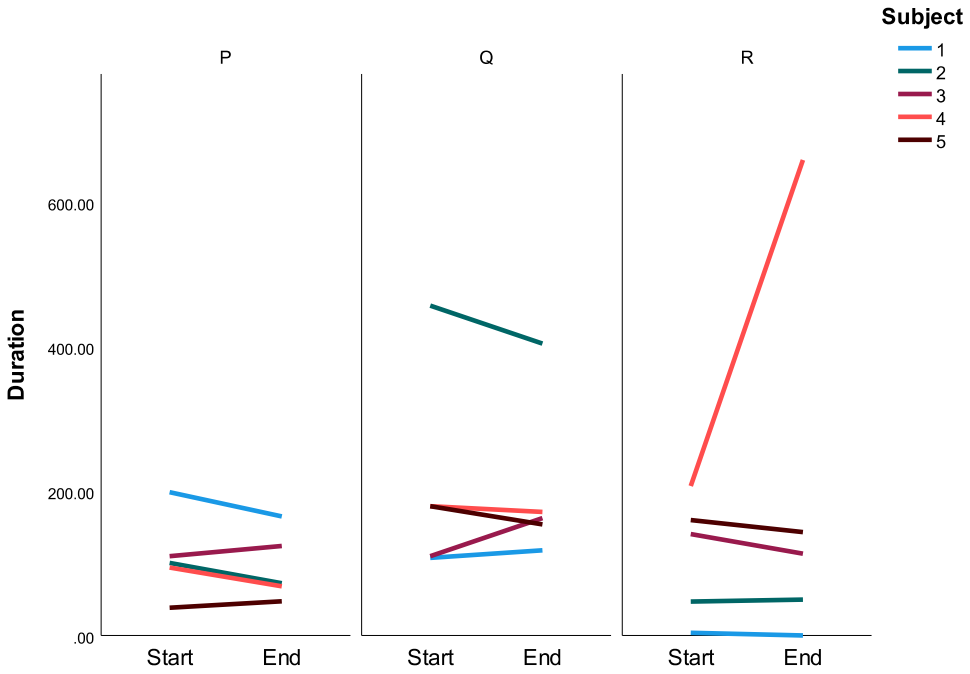

Figure 5.13: Microstate parameter: Changes in the duration of microstates P, Q, R from the beginning to the end of the dumbbell exercise.

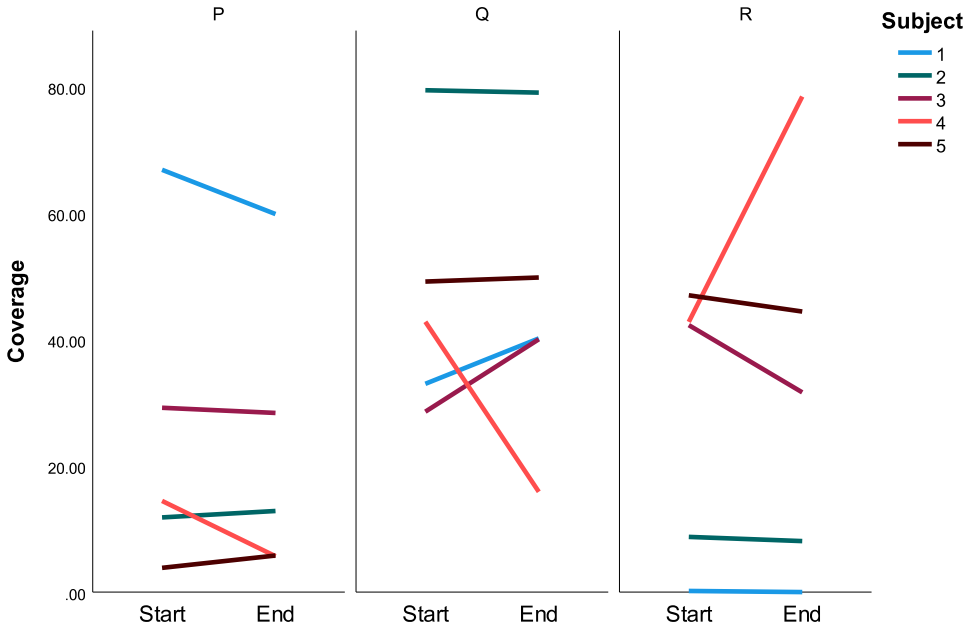

Figure 5.14: Microstate parameter: Changes in the coverage of microstates P, Q, R from the beginning to the end of the dumbbell exercise.

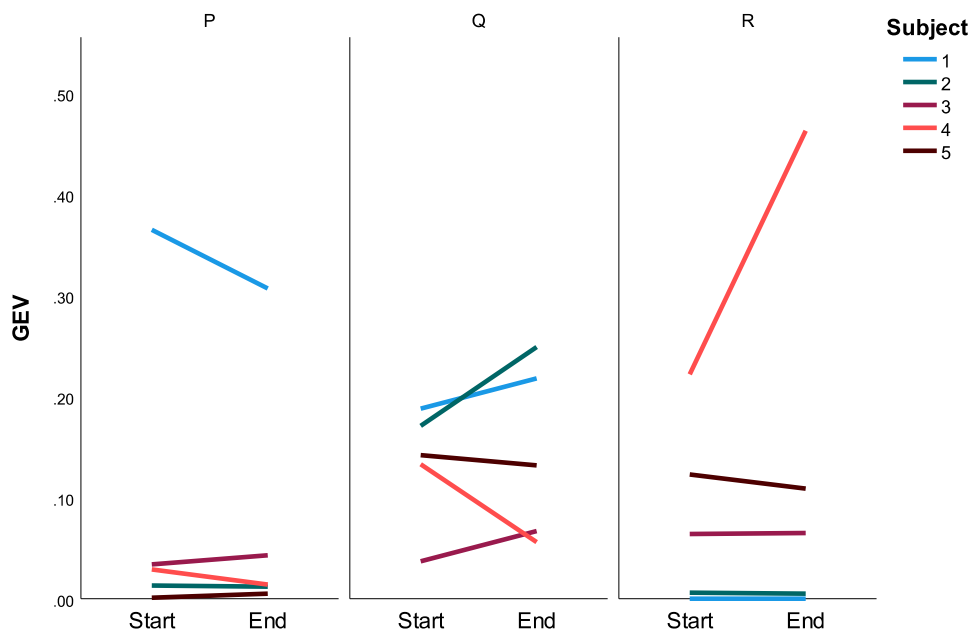

Figure 5.15: Microstate parameter: Changes in the GEV of microstates P, Q, R from the beginning to the end of the dumbbell exercise.

5.3.4 Subjective measures of fatigue and performance time

The forearm fatigue status of each participant was recorded during the experiment. Participants were asked to update their fatigue status on a scale of 1 (indicating not fatigued), to 10 (indicating extremely fatigued), before trial 1, after trial 2, before trial 3 and after trial 4. The fatigue score of each participant is shown in Table 5.6. This table shows that all participants reported fatigue after the dumbbell exercise, but the reduction of scores from before trial 3, to after trial 4, for participants 1, 3 and 5 could indicate an adjustment to the task complexity.

Table 5.6: Self-reported Fatigue status of each participant. The fatigue score is collected on a scale of 1-10 where 1 indicating not fatigued and 10 indicating extremely fatigued.

Subject	Before Trial1	After Trial2	Before Trial3	After Trial 4
1	1	2	8	7
2	1	1	8	8
3	1	1	8	6
4	1	4	9	9
5	1	2	8	7

Table 5.7 shows the time taken for each trial which was recorded with the help of Geomagic Touch API. A paired sample t-test was performed between trial 1 and trial 3 and it was found that the time taken for post fatigue trial is not statistically different from the time taken for

pre fatigue trial (p-value 0.608). However, given the small number of samples, looking at the individual values for trial 1 versus trial 3, two participants (Subject 1 and Subject 2) showed an increase in completion time while the remaining participants showed an improvement in the peg-placement and task completion.

Table 5.7: Time taken for each trial of NHPT in seconds

Subject	Trial1	Trial2	Trial3	Trial4
1	67	58	78	67
2	90	118	127	102
3	53	49	46	37
4	114	86	79	69
5	96	62	47	55
Mean (SD)	84 (21.59)	74.6 (27.85)	75.4 (32.99)	66 (23.81)

5.4 Discussion

Changes in EEG microstates when performing an embedded reality NHPT, pre and post fatigue were explored here. The analysis identified microstates during the performance of a NHPT and detailed the changes to these microstates after a fatiguing exercise. Here an attempt was made to explore how physical fatigue alters the microstate parameters like occurrence, coverage, duration and GEV.

Multiple studies in the field of microstates found that the optimal number of maps across subjects is four[116]. An overview article[116] discussing the application of EEG microstates to investigate the temporal dynamics of brain networks depicted the topography of the four microstate maps identified across various independent studies. They claim that numerous experimental and clinical studies adhered to the initially established number of clusters, which was four as determined by Koenig et al[90]. The rationale behind this choice was to maintain consistency with the prevailing approach adopted in the majority of earlier studies. However, in our study, the polarity invariant measures of global explained variance and cross validation were used to determine the optimum number of microstates. Three distinct microstates were found for resting state data and NHPT trial data. Microstates B and C found in this study resembled resting state microstates B and A in the literature[116][85].

It was found that with fatigue all the parameters of microstate A increased for all subjects except one. The coverage of microstate C decreased for all subjects, which implies that fatigue made microstate C less dominant and increased the occurrence of other microstates. It could be seen that reduction in coverage of microstate C was compensated by the increase in the coverage of microstate B or A. A study exploring the effect of acute exercise fatigue on large-scale brain functional networks[199] found that the duration and occurrence of a particular resting state

microstate (microstate C in the literature) were significantly higher after exhaustive exercise. This is in line with the result obtained for microstate A in the current research. The current research, however, centers on fatiguing exercise specifically targeting the forearm, in contrast to the study paradigm in the aforementioned research, which involved exercise on a treadmill. Also the methodology used in this study involves interaction with a robotic device.

Three microstates were observed in the EEG while performing NHPT trials. The microstate parameters were determined for transferring the first peg in pre-fatigue and post-fatigue trials (trial 1 and trial 3). MS3 was not present for one subject and, for all the other subjects, the coverage of MS3 decreased. This implies that new neural correlates were introduced with fatigue which reduced the coverage of MS3. While the coverage of MS3 decreased, the coverage of MS1 increased, which means that the fatigue caused changes in brain signals which created more MS1. A similar trend could also be seen in the GEV values. For MS1, GEV increased which was compensated by a decrease in GEV of MS3. The duration of MS1 was very high compared to the other microstates and it could be seen that its duration sometimes reached seconds. For subject 2 the duration of MS1 was in the order of seconds because only that particular microstate was present in the pre-fatigue trial, and in the post-fatigue trial, MS2 was present for a very short duration.

Looking at the microstates for the dumbbell exercise, it could be seen that the neural assemblies present for the fatiguing exercise are entirely different from those of the NHPT trial. This means the cognitive demand for NHPT introduces the activation of brain areas different from those of the dumbbell exercise. This observation is supported by the examination of subject scores for fatigue and completion times for pre and post fatigue trials. An analysis of microstates during the dumbbell exercise showed a reduction in coverage of microstate R for all participants except one. However, none of the other parameters showed any noticeable pattern. An interesting finding with dumbbell microstate parameters was that for subject 4 a greater alteration in microstate parameters was observed compared to other participants. From Table 5.1 it was observed that the BMI of subject 4 is well above that of other participants. The significant differences in microstate parameters observed for this participant could be related to their body mass index, as literature has shown an association between obesity and self-reported fatigue[144]. Participant 4 had offered a maximum subjective score of fatigue before NHPT trial 3, indicating that his high BMI potentially heightened his susceptibility to fatigue during the experiment.

Comparing the microstate analysis performed for three phases of the experiment, that is, resting state, NHPT trial and dumbbell exercise, it was observed that the coverage of some microstates is affected by fatigue in all the cases. The coverage of microstate C of resting state, MS3 of the NHPT trial and microstate R of dumbbell exercise all decreased as a result of fatigue. The GEV and duration followed a similar trend for resting state microstate C and NHPT trial microstate MS3. However, no noticeable trend was observed in dumbbell exercise microstates. A paired-sample t-test employed to assess the impact of fatigue on microstate parameters for

resting state, NHPT trial and dumbbell exercises found a statistically significant decrease in both the coverage ($p = 0.027$) and Global Explained Variance (GEV) of resting state microstate C ($p = 0.046$) suggesting the influence of fatigue on the observed alterations in coverage and GEV. None of the other microstate parameters showed any significant changes. Nevertheless, it is crucial to acknowledge that the limited sample size utilised in this study presents a hurdle in attaining statistical significance.

Subject scores for fatigue for participants 1, 3 and 5 were reduced after trial 4, and there was an improvement in NHPT performance from trial 3 to trial 4. From Table 5.6 it can be seen that NHPT alone induces fatigue for subjects 1,4 and 5 after trial 2. However, looking at the trial time there was a reduction in trial time for these subjects which indicates NHPT performance improvement. This could indicate that while participants worked harder, and perceived to work harder, they actually improved their performance score as indicated by the reduction in peg placement time.

When comparing the time between trial 1 and trial 3, it can be seen that participants 1 and 2 took more time to complete NHPT when fatigued. Completion time for trial 3 was less for participants 3, 4, and 5 compared to trial 1, despite reporting fatigue following the dumbbell exercise. These observations can indicate that physical fatigue alone does not impact NHPT performance. This could be because these participants did not find the NHPT task challenging and haptic/visual assistance given to these tasks provided a good medium for reducing their completion time despite fatigue in their wrists. It could also be possible that the NHPT task involves a different neural assembly compared to the assemblies needed for the wrist exercise. Furthermore, it is possible that the participants' fitness level could impact their recovery from fatigue. Participant 4 who had a higher BMI increased his fatigue level by performing NHPT alone compared to others. Comparing Table 5.1 and Table 5.6 it can be seen that participants with better BMI recovered soon from fatigue except for participant 2.

No MS3 was present for participant 2 while the NHPT trial time was more for each trial compared to others. Also, this participant struggled a lot to place the pegs in the hole during the experiment. This suggests that cognitive fatigue might also have an impact on MS3. Coverage of MS3 for all other participants decreased after fatiguing exercise which shows the impact of physical fatigue on microstates.

5.5 Chapter summary

This chapter investigated the changes in EEG microstates while a person performed a haptic Nine Hole Peg Test, before and after fatigue conditions. Also, EEG microstate analysis was performed on resting state EEG data and dumbbell exercise EEG. The main goal of the study was to observe differences in resting state and task performance microstates and to observe the changes due to a physically fatiguing dumbbell exercise. We observed these differences, as

highlighted by the topological maps, but also observed changes in the microstate parameters.

Although the experiment was conducted on healthy participants, we contend that our methodology has potential benefits in practical settings, such as with stroke patients who may have decreased physical and cognitive abilities as a result of their neurological condition. Our methodology yielded an assessment of fatigue and its associated neural correlates during the execution of a task designed to evaluate fine motor dexterity. An improvement in the performance of the NHPT task is observed with repetition. However, the situation may differ significantly for individuals who have suffered a stroke, as their medical condition may impose restrictions on both their physical and neural capabilities. Furthermore, a larger sample size for this experiment could have potentially provided stronger statistical evidence to support the results.

CHAPTER 6

CONCLUSIONS AND FUTURE WORK

6.1 Conclusions

Stroke rehabilitation is a comprehensive and multidisciplinary approach that plays a crucial role in the recovery process after a stroke. By focusing on physical, cognitive, emotional, and social aspects, rehabilitation aims to improve the overall quality of life for stroke survivors. Early intervention, repetitive and targeted interventions, and a holistic approach play an important role in the success of stroke rehabilitation. These approaches promote neuroplasticity and help individuals to regain their functional ability. Fatigue is often associated with chronic conditions such as stroke, and acts as a hindrance towards intensive and repetitive training.

Neural correlates of stroke often involve changes in the brain activity within the motor cortex, sensory regions, and areas responsible for motor planning and execution. Improvements in motor function and recovery have been associated with better sensory feedback modulation and better brain-muscle coordination. Based on the negative impact of fatigue, by exploring the neural correlates of fatigue, researchers can gain insights into the mechanisms underlying the formation of fatigue and its subsequent prevention in order to optimise recovery. As the study of neural correlates is performed at individual level, this allows for the development of more targeted and individualised rehabilitation approaches.

Rehabilitation robotics provides interactive tools with the aim to tailor the therapy to each individual's specific needs. It provides the opportunity for high-intensity and repetitive training, which has been shown to enhance motor re-learning and functional recovery. Robot-assisted rehabilitation helps in tracking and analysing a patient's performance during therapy sessions, providing personal feedback which can facilitate the recovery process. Combining knowledge of

fatigue with repetitive training is expected to provide an opportunity for a more intensive and personalised therapy, that can stimulate neuroplasticity and is expected to promote functional recovery.

Through an extensive review of the literature, as detailed in chapter 2, on EEG-EMG coherence and EEG microstates in the context of fatigue and stroke rehabilitation, the work in this thesis offered a comprehensive overview of the topic for present and future researchers in the field. The literature review revealed the research gap, that the neural correlates of fatigue in rehabilitation require further research. Moreover, to the author's knowledge, neural correlates related to the standardised assessment tool for fine motor control, the Nine Hole Peg Test (NHPT) have not yet been explored.

6.2 Key Findings

The main hypothesis behind this research was:

"Fatigue can be detected and assessed by analysing alterations in neurophysiological parameters during interaction with a robotic rig and physical exercise".

This led to two research questions and an experiment was designed and conducted with healthy participants to analyse the EEG-EMG coherence and EEG microstates while interacting with a robotic rig and physical exercise. The experiment allowed us to monitor EEG and EMG prior to, during and after two interactions consisting of a haptic dexterity test and a physical dumbbell exercise.

Research question 1 was formulated as:

"How does physical fatigue alter the coherence between EEG and EMG for healthy participants while performing a robot-assisted NHPT?"

To address this research question, EEG-EMG coherence was calculated between three EEG electrodes C1, C3 and CP3 and three upper limb muscles FCR, ECR and ED during pre fatigue and post fatigue trials of NHPT. Alterations in coherence specifically to the beta band and gamma band were explored. The analysis showed an increase in corticomuscular coupling with fatigue in both of these bands. This suggests that when a person becomes fatigued, there is a greater activation of neurons, leading to the recruitment of more motor units in order to compensate for the fatigue. This is in agreement with previous studies of corticomuscular coupling[66][190]. Conversely, a previous study reported weakening of functional coupling between the brain and muscles as a result of fatigue[194][140]. The difference in results may be due to the difference in methodologies and the muscles involved in the study[106]. Muscle dependency on EEG-EMG coherence is already explored in past and found that corticomuscular coherence differs among muscles[180]. Increased physical and mental effort is needed to sustain the task performance while performing NHPT after fatigue. The beta and gamma bands relate to the alert states of the human brain. The dominance of both beta band and gamma band coherence indicates their

potential importance in regulating motor tasks when confronted with fatigue.

FCR showed better coupling with EEG in both frequency bands after fatigue. Post fatigue coupling between ECR and EEG electrodes improved in the beta band whereas decreased in the gamma band. The coupling between ED and brain signals increased in both bands except with C1 in the beta band. Gamma band coherence values were much higher compared to beta band values. Past studies demonstrated a shift of corticomuscular coherence from beta band to gamma band under the influence of muscle fatigue[191]. The results suggest that when muscles get fatigued motor cortex enhances communication in the gamma band to cope with it. Also, the results highlight the frequency specificity of coherence measures and the role of different cortical regions in motor control and performance. All participants reported fatigue on their forearm after the dumbbell exercise. However, when considering NHPT completion time, except for three participants, all others completed NHPT trial 3 in less time compared to trial 1. A paired sample t-test performed between pre and post fatigue trial times found no statistically significant difference (p-value 0.366). This indicates that physical fatigue alone is not impacting the NHPT performance. Familiarisation with the haptic NHPT might have also helped the participants complete the task in a lesser time.

Research question 2 was formulated as:

"Does fatigue impact EEG microstate parameters while interacting with a robotic rig and physical exercise?"

EEG microstate analysis was performed on data collected during three stages of the experiment: one during rest, another during the performance of the NHPT task and a third during the dumbbell exercise. Three distinct sets of microstates were found for each of these stages. Two microstates observed during the resting state resembled that in the literature. Alterations in parameters were observed for resting state and task microstates. The coverage of microstate C, which is a resting state microstate, decreased for all the subjects with fatigue. All the parameters of microstate A increased for all subjects except one. The coverage of MS3, which is a microstate observed during the NHPT trial, decreased with fatigue for all subjects except one for whom MS3 was not present. GEV and duration followed a similar trend to that of coverage. Coverage of microstate R of dumbbell exercise decreased when moving from the beginning of the exercise to the end of the exercise. However, none of the other parameters for dumbbell microstates showed any noticeable patterns among the subjects. The coverage of microstates measures the percentage of the total time during which a specific microstate is dominant. It reflects the dominance of underlying neural generators[197]. Analysis of microstate parameters showed that coverage of certain microstates was impacted by fatigue in all the three stages under consideration ie. resting state, NHPT trial and dumbbell exercise. This implies that fatigue caused inhibition of neural activations in certain areas of the brain which in turn reduced the coverage of some microstates. This is in line with a previous study on the impact of exhaustive exercises on resting state large-scale brain networks[199].

A greater alteration in microstate parameters was observed with one participant who had a higher BMI compared to others. The literature already showed a positive correlation between BMI and self-reported fatigue[144] which highlight the fact that microstate parameters might differ in people with different BMI. Despite all the participants reporting fatigue on their forearm after dumbbell exercise, the performance time obtained from NHPT completion of some participants improved after fatigue. This could indicate that while participants worked harder, and perceived to work harder, they actually improved their performance score as indicated by the reduction in peg placement time. This suggests that physical fatigue had minimal influence on NHPT completion time.

The microstates observed for dumbbell exercise were different from those observed for the NHPT trial or resting state. This indicates variations in neural assemblies associated with different physical states of an individual. This suggests that specific patterns of neural connectivity and information processing are involved in the execution of different motor tasks or engagement in different physical states. These findings highlight the dynamic nature of the brain and its ability to adapt and reorganise its neural networks in response to different physical demands. This is in line with our observation in corticomuscular coherence where it was observed that increased neural recruitment happened in an effort to recruit additional motor units to cope with fatigue. The differences in microstates and increase in EEG-EMG coherence collectively suggest that fatigue induces changes in the neural assemblies and functional connectivity in the brain. These changes reflect the adaptive response of the brain to the increased physical and mental effort exerted by individuals to sustain motor task performance under fatigue.

6.3 Contribution to Knowledge

By researching the neurophysiological correlates of fatigue in the robot-assisted NHPT and physical exercise, this research aims to contribute to the development of more effective rehabilitation strategies. The findings of this study have the potential to help in the design and implementation of targeted interventions to alleviate fatigue and enhance motor function in clinical and rehabilitative settings. Analysis performed in chapter 4 suggested an enhancement in corticomuscular coupling with fatigue. The results demonstrated stronger coupling in the gamma band compared to the beta band. This leads to the conclusion that gamma band coherence has a better potential to identify fatigue in robot-assisted NHPT. This result can be further extended to robot-assisted training exercises too. The results also demonstrated the difference in coupling between different upper limb muscles and the motor cortex, in the context of the task set for this experiment. Upper limb muscle FCR demonstrated better coupling with the motor cortex which establishes the importance of this muscle in the functional coordination of fine motor activities.

Exploring the effect of fatigue on microstate parameters established the potential of microstate parameters as biomarkers of fatigue. Analysis in chapter 5 demonstrated that physical

fatigue did not affect the NHPT performance as some participants reporting physical fatigue improved performance during the NHPT trials. However, alterations in microstate parameters were observed after the physical fatigue. A decline in the coverage, duration and global explained variance of some microstates was observed as a result of fatigue. The findings also shed light on the compensatory mechanism that the brain uses to maintain motor function as fatigue sets in. The analysis also suggested a potential effect of BMI on microstate parameters while performing physical exercises as greater variations in microstate parameters were observed in a participant with high BMI.

The research work presented in this thesis has also contributed towards the following publications:

- Meethal, S.A., Steuber, V. and Amirabdollahian, F., "Analysis of EEG Microstates During Execution of a Nine Hole Peg Test". ACHI 2023, The Sixteenth International Conference on Advances in Computer-Human Interactions, Venice, Italy, April 24 -28, 2023
- Meethal, S.A., Steuber, V. and Amirabdollahian, F., "Evaluation of Cortico Muscular Coupling while Performing Haptic NHPT under Fatigue Conditions". (submitted to IEEE ROMAN 2023)
- Meethal, S.A., Steuber, V. and Amirabdollahian, F.," Impact of Fatigue on Neural Correlates during Robot-Assisted NHPT and Physical Exercise" (in preparation)

6.4 Limitations and Future Work

The study encountered several limitations due to the COVID-19 pandemic. The primary impact of COVID on the research was the need to halt the experiments due to safety concerns of the researcher as well as the participants. The experiment methodology required close interaction between the researcher and participants for collecting EEG and EMG data. The ongoing pandemic and associated limitations restricted the designing and implementation of further experiments. This led to a small sample size which constrained the possibility of considering statistical power and generalisation of our findings. Increasing the number of participants would allow for a more comprehensive understanding of the results obtained in this study.

The increase in EEG-EMG coherence with fatigue during robot-assisted NHPT highlights the complex interplay between the brain and muscles during prolonged periods of physical activity. Further research is needed to fully understand the mechanisms underlying these changes and to develop effective fatigue management strategies. Only sixteen electrodes were used for collecting EEG data from participants. Even though the literature established the reliability of microstate analysis using as less as eight electrodes, one possible limitation of this study is the absence of EEG signals collected from the parietal area. Expanding the number of electrodes will provide more detailed spatial information regarding brain activity which might benefit in better results

for microstates. Also, our methodology involved the utilisation of a virtual environment, which induced some cognitive load. However, we did not collect any subjective feedback regarding the level of mental exhaustion experienced during the experiment phases, thereby restricting our ability to draw definitive conclusions about the extent of cognitive fatigue. To improve the efficacy of the study, it would be beneficial to introduce distinct practical elements that induce physical and cognitive fatigue, respectively. This would permit a separate evaluation of the impact of each of these factors on the neural correlates indicated by microstate parameters.

This research showed that fatigue can be detected and assessed by analysing alterations in neurophysiological parameters during interaction with a robotic rig and physical exercise. The analysis and findings presented in this thesis lead to various potential directions of research. The present study looked at the neural correlates related to haptic NHPT and physical exercise. This concept can be further expanded to rehabilitation training involving robotic devices. The current study was performed with healthy participants. The methodology presented in this thesis can be extended to stroke patients who may have decreased physical and cognitive abilities as a result of their neurological condition. Previous studies show that the microstates parameters observed for patients with different neurological conditions like multiple sclerosis, stroke and Parkinson's disease differ from healthy controls[8] [63][42]. A recent study on cancer patients revealed the weakening of functional corticomuscular coupling during voluntary motor activity associated with cancer-related fatigue[75]. Alterations in corticomuscular coupling were suggested in stroke patients compared to healthy controls[93][61][50]. Our study was conducted with healthy participants who managed to recover from fatigue and demonstrated brain signal adaptation in response to increased physical demands. The logical next step is exploring the neural correlates in a sample of individuals recovering from stroke and other neurological conditions, but also in populations suffering from chronic fatigue, thus to observe how limitations imposed by chronic conditions impact neural correlates and to further formulate how these correlates can be used as indicators to direct therapy and treatment.

As the study focused on healthy participants, the methodology applies to diverse domains. The findings contribute to injury prevention by pinpointing and addressing potential risks linked to inappropriate exercise intensity. Furthermore, they facilitate the fine-tuning of training intensity, empowering runners to boost their fitness effectively while reducing the risk of injuries due to excessive exertion. A study explored the correlation between time-frequency domain indexes derived from surface electromyography (EMG) signals of specific muscles, heart rate, exercise intensity, and subjective fatigue found that the physiological indicators selected in that study are limited[28]. The findings from this research offer an improved indicator for the detection of fatigue. The methodology can also be extended to detect fatigue in older people since facilitating safe exercise is vital for the strength training in aged population.

A possible future study is to analyse the kinematic features of Geomagic Touch to detect the onset of fatigue. The neural correlates identified in this thesis can be used to design algorithms

which can help in adaptive upper limb rehabilitation training. The algorithm used for EEG-EMG coherence in this study has the potential to be used in adaptive rehabilitation training studies. However further works needs to be done to improve the algorithm for EEG microstate analysis, related to the extent of processing and preparation, to be used in an adaptive environment.

APPENDIX A

Research Questionnaire

Thank you for participating in the study. Please circle the corresponding fatigue level. The answers will be anonymous and will only be used for the experimental result analysis.

About you

1. **Subject ID:** _____
2. **Your name:** _____
3. **Age:** _____ years.
4. **Gender:** □ Male □ Female
5. **Dominant Arm:** □ Right Handed □ Left Handed

MVC measurement:

Hand Grip 1:

Hand Grip 2:

Hand Grip 3:

Hand Grip 4:

Before NHPT Rep1:

6. **Current Level of Muscle Fatigue on a scale of 1 to 10:**
(1:Not fatigued 10: extremely fatigued.)

1 2 3 4 5 6 7 8 9 10

After NHPT Rep2:

7. **Current Level of Muscle Fatigue on a scale of 1 to 10:**
(1:Not fatigued 10: extremely fatigued.)

1 2 3 4 5 6 7 8 9 10

Before NHPT Rep3:

8. **Current Level of Muscle Fatigue on a scale of 1 to 10:**
(1:Not fatigued 10: extremely fatigued.)

1 2 3 4 5 6 7 8 9 10

After NHPT Rep4:

9. **Current Level of Muscle Fatigue on a scale of 1 to 10:**
(1:Not fatigued 10: extremely fatigued.)

1 2 3 4 5 6 7 8 9 10

10. Would you like to write some more lines on how you felt about the experiment?. Do you have any suggestions on how to improve the experiment?

Experiment Measures (To be entered by the principal investigator)

11. **Height:** _____ cm.
12. **Weight:** _____ Kg.
13. **Body Mass Index:** _____ .
14. **Visceral Fat Classification:** _____ .
15. **Skeletal Muscle Percentage:** _____ .
16. **Body Fat Percentage:** _____.

APPENDIX B

Paired sample t-test on trial time for trial 1 and trial 3

Paired Samples Test

		Paired Differences					t	df	Sig. (2-tailed)
		Mean	Std. Deviation	Std. Error Mean	95% Confidence Interval of the Difference Lower	Upper			
Pair 1	Trial1 - Trial3	8.600	34.624	15.484	-34.391	51.591	.555	4	.608

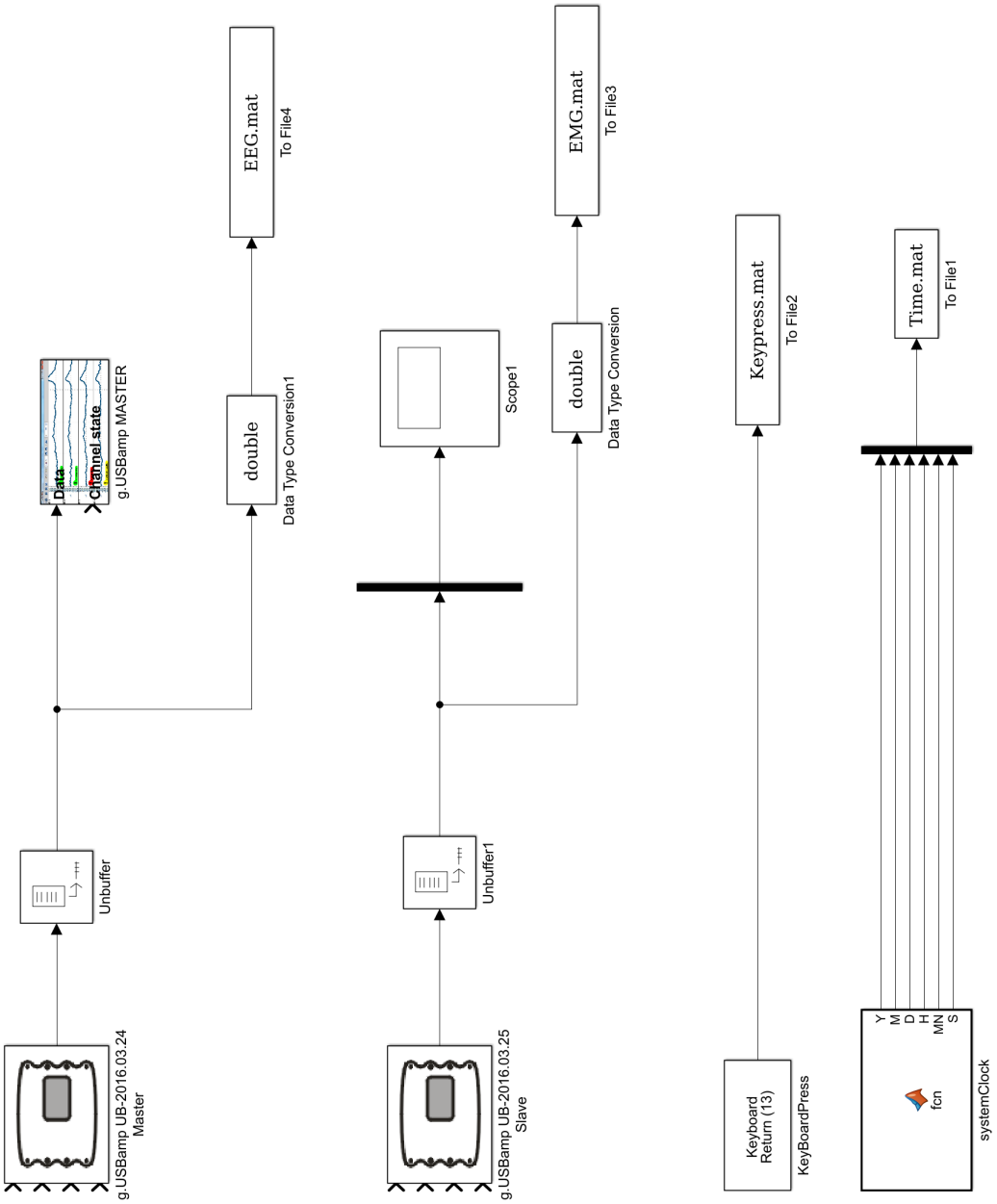

Figure B.1: Data acquisition MATLAB simulink model

Paired sample t-test on coherence in beta band

Paired Samples Test									
		Paired Differences					t	df	Sig. (2-tailed)
		Mean	Std. Deviation	Std. Error Mean	95% Confidence Interval of the Difference				
					Lower	Upper			
Pair 1	C3-FCR_trial1 - C3-FCR_trial3	-0.015163	0.027867	0.009853	-0.038460	0.0081353	-1.539	7	0.168
Pair 2	C3-ECR_trial1 - C3-ECR_trial3	-0.014250	0.027886	0.009859	-0.037563	0.0090631	-1.445	7	0.192
Pair 3	C3-ED_Trial1 - C3-ED_trial3	-0.009838	0.023885	0.008445	-0.029806	0.0101307	-1.165	7	0.282

Figure B.2: Paired sample t-test performed on pre and post fatigue coherence between C3 and muscles in beta band. Trial 1 corresponds to pre fatigue coherence and trial 3 corresponds to post fatigue trial. No significant difference in pre and post fatigue coherences.

Paired Samples Test									
		Paired Differences					t	df	Sig. (2-tailed)
		Mean	Std. Deviation	Std. Error Mean	95% Confidence Interval of the Difference				
					Lower	Upper			
Pair 1	CP3-FCR_trial1 - CP3-FCR_trial3	-0.017688	0.030977	0.010952	-0.043585	0.008210	-1.615	7	0.150
Pair 2	ECR_trial1 - ECR_trial3	-0.006638	0.034293	0.012124	-0.035307	0.022032	-0.547	7	0.601
Pair 3	CP3-ED_Trial1 - CP3-ED_trial3	-0.005688	0.025226	0.008919	-0.026777	0.015402	-0.638	7	0.544

Figure B.3: Paired sample t-test performed on pre and post fatigue coherence between CP3 and muscles in beta band. Trial 1 corresponds to pre fatigue coherence and trial 3 corresponds to post fatigue trial. No significant difference in pre and post fatigue coherences.

Paired sample t-test on coherence in gamma band

Paired Samples Test									
		Paired Differences					t	df	Sig. (2-tailed)
		Mean	Std. Deviation	Std. Error Mean	95% Confidence Interval of the Difference				
					Lower	Upper			
Pair 1	C1_FCR_trial1 - C1_FCR_trial3	-0.113143	0.278413	0.105230	-0.370632	0.144346	-1.075	6	0.324
Pair 2	C1_ECR_trial1 - C1_ECR_trial3	0.012357	0.058963	0.022286	-0.042175	0.066889	0.554	6	0.599
Pair 3	C1_ED_trial1 - C1_ED_trial3	-0.042300	0.102753	0.038837	-0.137331	0.052731	-1.089	6	0.318

Figure B.4: Paired sample t-test performed on pre and post fatigue coherence between C1 and muscles in the gamma band. Trial 1 corresponds to pre fatigue coherence and trial 3 corresponds to post fatigue trial. No significant difference in pre and post fatigue coherences.

Paired Samples Test									
		Paired Differences					t	df	Sig. (2-tailed)
		Mean	Std. Deviation	Std. Error Mean	95% Confidence Interval of the Difference				
					Lower	Upper			
Pair 1	C3_FCR_trial1 - C3_FCR_trial3	-0.094475	0.255468	0.090322	-0.308052	0.119102	-1.046	7	0.330
Pair 2	C3_ECR_trial1 - C3_ECR_trial3	0.022463	0.063133	0.022321	-0.030318	0.075243	1.006	7	0.348
Pair 3	C3_ED_trial1 - C3_ED_trial3	-0.032700	0.093164	0.032938	-0.110587	0.045187	-0.993	7	0.354

Figure B.5: Paired sample t-test performed on pre and post fatigue coherence between C3 and muscles in the gamma band. Trial 1 corresponds to pre fatigue coherence and trial 3 corresponds to post fatigue trial. No significant difference in pre and post fatigue coherences.

Paired Samples Test									
		Paired Differences					t	df	Sig. (2-tailed)
		Mean	Std. Deviation	Std. Error Mean	95% Confidence Interval of the Difference				
					Lower	Upper			
Pair 1	CP3_FCR_trial1 - CP3_FCR_trial3	-0.094238	0.264139	0.093387	-0.315063	0.126588	-1.009	7	0.347
Pair 2	CP3_ECR_trial1 - CP3_ECR_trial3	0.019100	0.057467	0.020318	-0.028944	0.067144	0.940	7	0.378
Pair 3	CP3_ED_trial1 - CP3_ED_trial3	-0.028188	0.089710	0.031717	-0.103187	0.046812	-0.889	7	0.404

Figure B.6: Paired sample t-test performed on pre and post fatigue coherence between CP3 and muscles in the gamma band. Trial 1 corresponds to pre fatigue coherence and trial 3 corresponds to post fatigue trial. No significant difference in pre and post fatigue coherences.

Paired Samples Test									
		Paired Differences					t	df	Sig. (2-tailed)
		Mean	Std. Deviation	Std. Error Mean	95% Confidence Interval of the Difference				
					Lower	Upper			
Pair 1	Occurrence_Pre - Occurrence_Post	-0.44400	0.68730	0.30737	-1.29739	0.40939	-1.445	4	0.222
Pair 2	Duration_Pre - Duration_Post	-11.39600	40.62725	18.16906	-61.84139	39.04939	-0.627	4	0.565
Pair 3	Coverage_Pre - Coverage_Post	-7.400	14.046	6.282	-24.841	10.041	-1.178	4	0.304
Pair 4	GEV_Pre - GEV_Post	-0.04088	0.08051	0.03600	-0.14084	0.05908	-1.135	4	0.320

Figure B.7: Paired sample t-test performed on parameters of Resting state microstate A. No significant difference in pre and post fatigue microstate parameters.

Paired Samples Test									
		Paired Differences					t	df	Sig. (2-tailed)
		Mean	Std. Deviation	Std. Error Mean	95% Confidence Interval of the Difference				
					Lower	Upper			
Pair 1	Occurrence_Pre - Occurrence_Post	-0.26200	0.91789	0.41049	-1.40171	0.87771	-0.638	4	0.558
Pair 2	Duration_Pre - Duration_Post	-3.15000	24.50813	10.96037	-33.58086	27.28086	-0.287	4	0.788
Pair 3	Coverage_Pre - Coverage_Post	-4.400	12.137	5.428	-19.470	10.670	-0.811	4	0.463
Pair 4	GEV_Pre - GEV_Post	-0.00564	0.06138	0.02745	-0.08185	0.07057	-0.205	4	0.847

Figure B.8: Paired sample t-test performed on parameters of Resting state microstate B. No significant difference in pre and post fatigue microstate parameters.

Paired Samples Test									
		Paired Differences					t	df	Sig. (2-tailed)
		Mean	Std. Deviation	Std. Error Mean	95% Confidence Interval of the Difference				
					Lower	Upper			
Pair 1	Occurrence_Pre - Occurrence_Post	0.48600	1.32493	0.59253	-1.15911	2.13111	0.820	4	0.458
Pair 2	Duration_Pre - Duration_Post	94.18400	922.63941	412.61689	-1051.42414	1239.79214	0.228	4	0.831
Pair 3	Coverage_Pre - Coverage_Post	-11.50800	13.24157	5.92181	-27.94958	4.93358	-1.943	4	0.124
Pair 4	GEV_Pre - GEV_Post	-0.1677400	0.1476667	0.0660386	-0.3510925	0.0156125	-2.540	4	0.064

Figure B.9: Paired sample t-test performed on parameters of NHPT task microstate MS1. No significant difference in pre and post fatigue microstate parameters.

Paired Samples Test									
		Paired Differences					t	df	Sig. (2-tailed)
		Mean	Std. Deviation	Std. Error Mean	95% Confidence Interval of the Difference				
					Lower	Upper			
Pair 1	Occurrence_Pre - Occurrence_Post	-0.04000	0.29309	0.13107	-0.40392	0.32392	-0.305	4	0.775
Pair 2	Duration_Pre - Duration_Post	26.14200	75.87089	33.93049	-68.06416	120.34816	0.770	4	0.484
Pair 3	Coverage_Pre - Coverage_Post	3.66600	11.90432	5.32377	-11.11516	18.44716	0.689	4	0.529
Pair 4	GEV_Pre - GEV_Post	0.0510400	0.1183414	0.0529239	-0.0959003	0.1979803	0.964	4	0.389

Figure B.10: Paired sample t-test performed on parameters of NHPT task microstate MS2. No significant difference in pre and post fatigue microstate parameters.

Paired Samples Test									
		Paired Differences					t	df	Sig. (2-tailed)
		Mean	Std. Deviation	Std. Error Mean	95% Confidence Interval of the Difference				
					Lower	Upper			
Pair 1	Occurrence_Pre - Occurrence_Post	0.91600	1.88280	0.84201	-1.42180	3.25380	1.088	4	0.338
Pair 2	Duration_Pre - Duration_Post	54.85200	53.52668	23.93786	-11.61015	121.31415	2.291	4	0.084
Pair 3	Coverage_Pre - Coverage_Post	7.83600	7.97860	3.56814	-2.07075	17.74275	2.196	4	0.093
Pair 4	GEV_Pre - GEV_Post	0.0649200	0.1080244	0.0483100	-0.0692100	0.1990500	1.344	4	0.250

Figure B.11: Paired sample t-test performed on parameters of NHPT task microstate MS3. No significant difference in pre and post fatigue microstate parameters.

Paired Samples Test									
		Paired Differences					t	df	Sig. (2-tailed)
		Mean	Std. Deviation	Std. Error Mean	95% Confidence Interval of the Difference				
					Lower	Upper			
Pair 1	Occurrence_Pre - Occurrence_Post	0.12200	0.56729	0.25370	-0.58239	0.82639	0.481	4	0.656
Pair 2	Duration_Pre - Duration_Post	12.95000	22.62481	10.11812	-15.14242	41.04242	1.280	4	0.270
Pair 3	Coverage_Pre - Coverage_Post	2.72000	4.85175	2.16977	-3.30425	8.74425	1.254	4	0.278
Pair 4	GEV_Pre - GEV_Post	0.012200	0.027124	0.012130	-0.021479	0.045879	1.006	4	0.371

Figure B.12: Paired sample t-test performed on parameters of Dumbbell exercise microstate P. No significant difference in pre and post fatigue microstate parameters.

Paired Samples Test									
		Paired Differences					t	df	Sig. (2-tailed)
		Mean	Std. Deviation	Std. Error Mean	95% Confidence Interval of the Difference				
					Lower	Upper			
Pair 1	Occurrence_Pre - Occurrence_Post	0.23200	1.04126	0.46567	-1.06089	1.52489	0.498	4	0.644
Pair 2	Duration_Pre - Duration_Post	4.49200	39.56823	17.69545	-44.63845	53.62245	0.254	4	0.812
Pair 3	Coverage_Pre - Coverage_Post	1.60200	14.96121	6.69085	-16.97479	20.17879	0.239	4	0.823
Pair 4	GEV_Pre - GEV_Post	-0.010200	0.057864	0.025877	-0.082047	0.061647	-0.394	4	0.714

Figure B.13: Paired sample t-test performed on parameters of Dumbbell exercise microstate Q. No significant difference in pre and post fatigue microstate parameters.

Paired Samples Test									
		Paired Differences					t	df	Sig. (2-tailed)
		Mean	Std. Deviation	Std. Error Mean	95% Confidence Interval of the Difference				
					Lower	Upper			
Pair 1	Occurrence_Pre - Occurrence_Post	0.31400	0.62843	0.28104	-0.46630	1.09430	1.117	4	0.326
Pair 2	Duration_Pre - Duration_Post	-81.29000	207.29866	92.70678	-338.68528	176.10528	-0.877	4	0.430
Pair 3	Coverage_Pre - Coverage_Post	-4.32000	18.02846	8.06257	-26.70529	18.06529	-0.536	4	0.620
Pair 4	GEV_Pre - GEV_Post	-0.045400	0.109514	0.048976	-0.181379	0.090579	-0.927	4	0.406

Figure B.14: Paired sample t-test performed on parameters of Dumbbell exercise microstate R. No significant difference in pre and post fatigue microstate parameters.

APPENDIX C

APPENDIX C

Pre and post fatigue coherence of participants

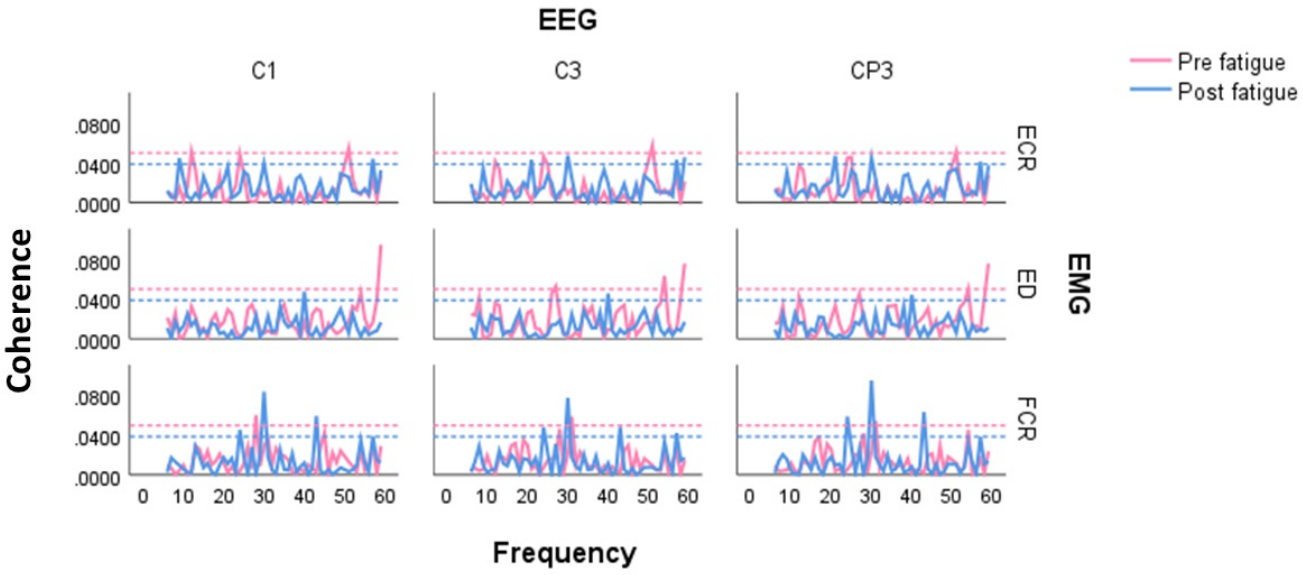

Figure C.1: Pre and post fatigue coherence for Subject 1. Pre fatigue coherence is plotted in pink colour and post fatigue coherence is plotted in blue colour. Dashed lines represent significant coherences.

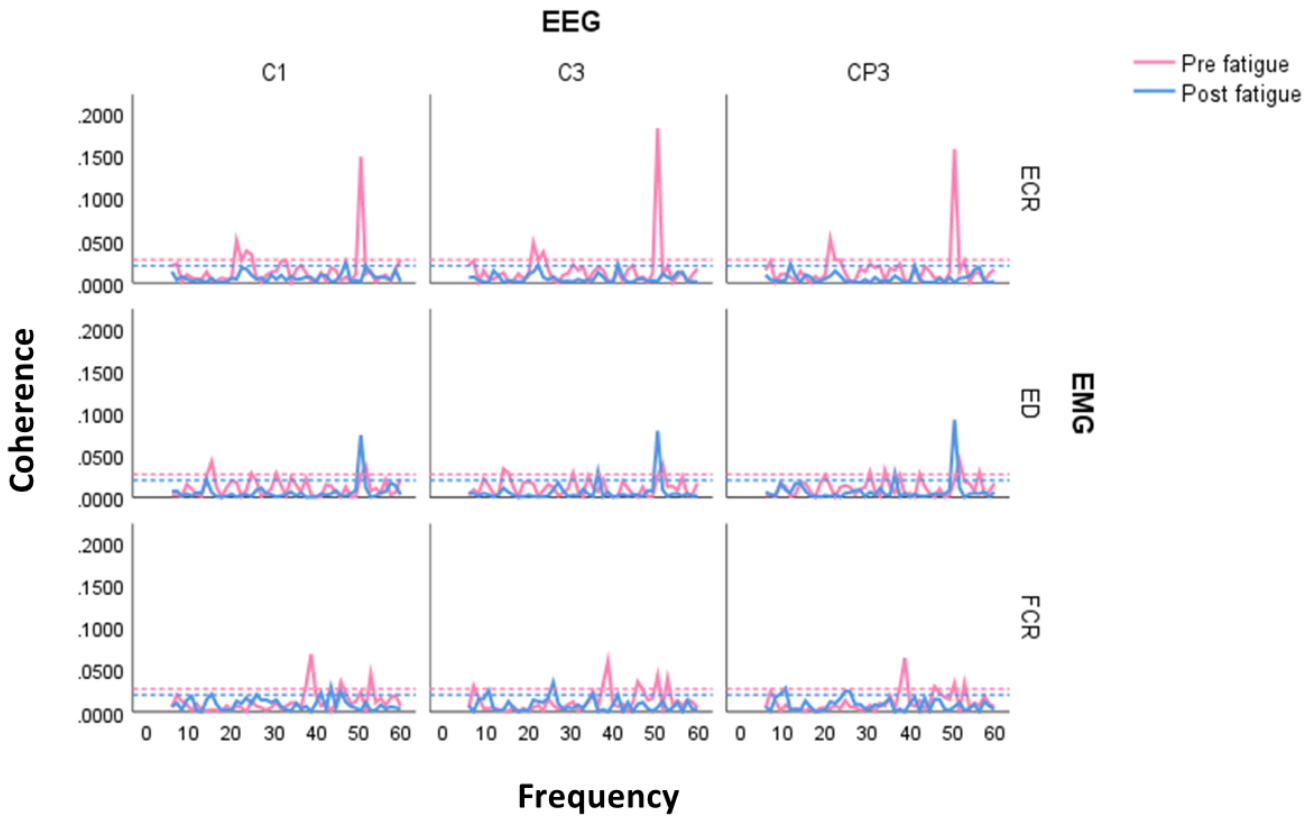

Figure C.2: Pre and post fatigue coherence for Subject 2. Pre fatigue coherence is plotted in pink colour and post fatigue coherence is plotted in blue colour. Dashed lines represent significant coherences.

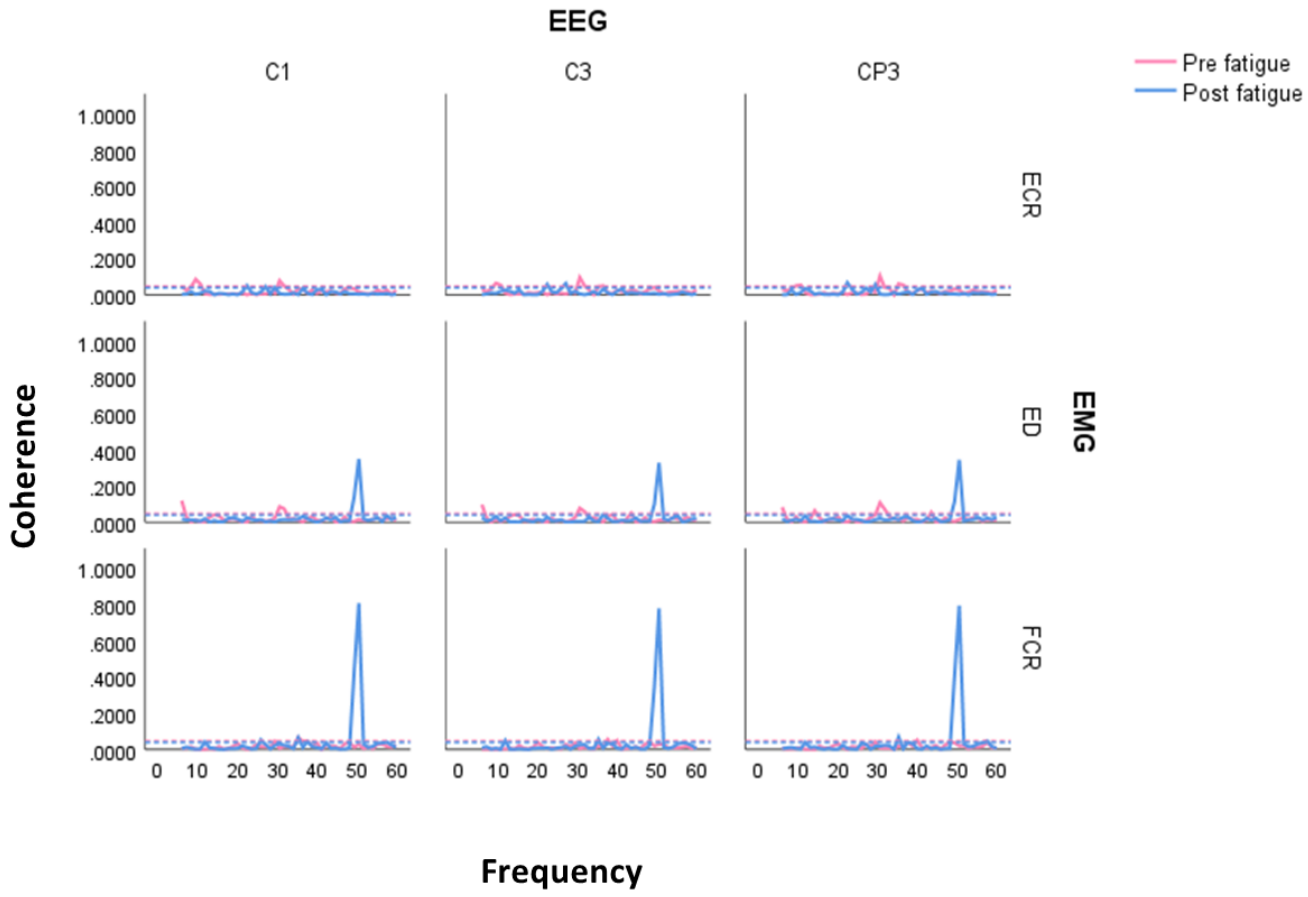

Figure C.3: Pre and post fatigue coherence for Subject 3. Pre fatigue coherence is plotted in pink colour and post fatigue coherence is plotted in blue colour. Dashed lines represent significant coherences.

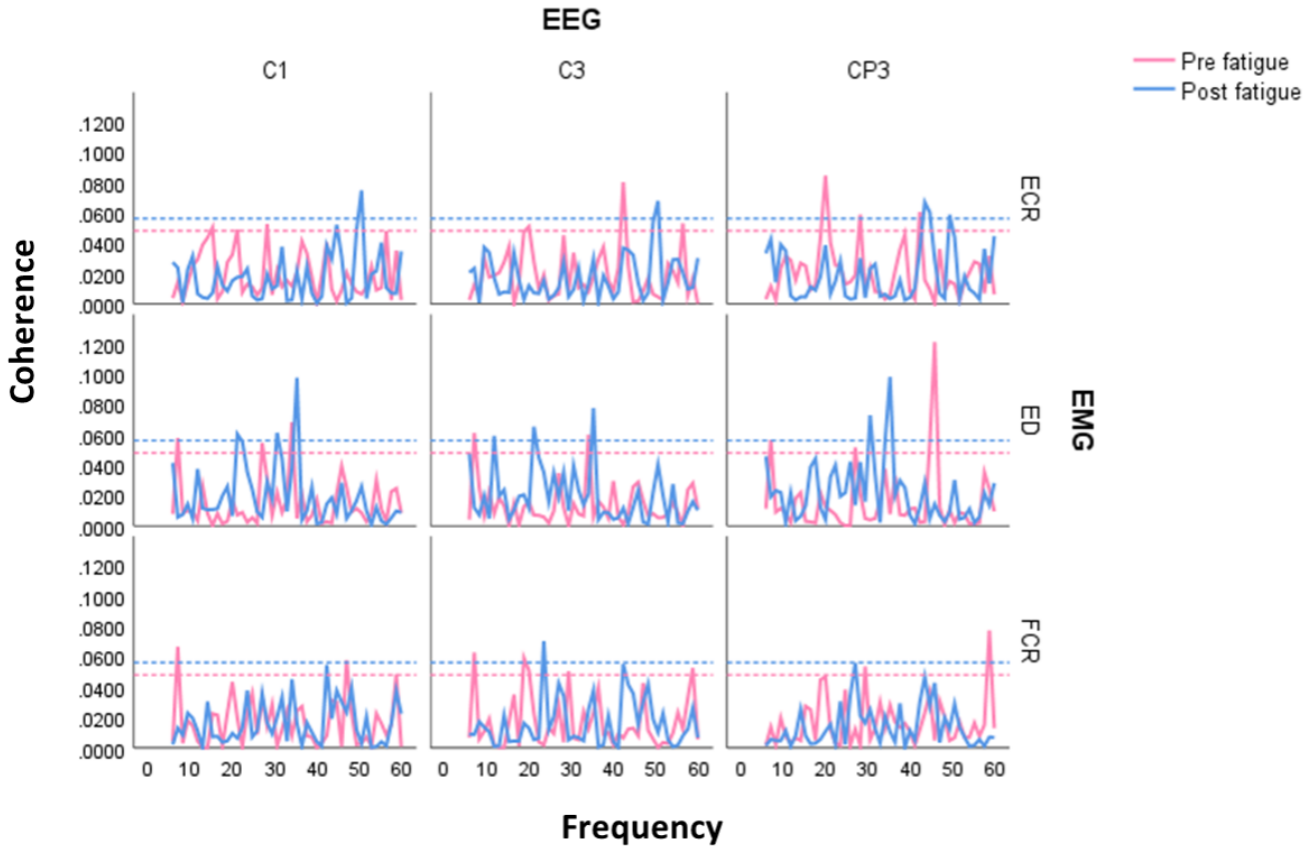

Figure C.4: Pre and post fatigue coherence for Subject 4. Pre fatigue coherence is plotted in pink colour and post fatigue coherence is plotted in blue colour. Dashed lines represent significant coherences.

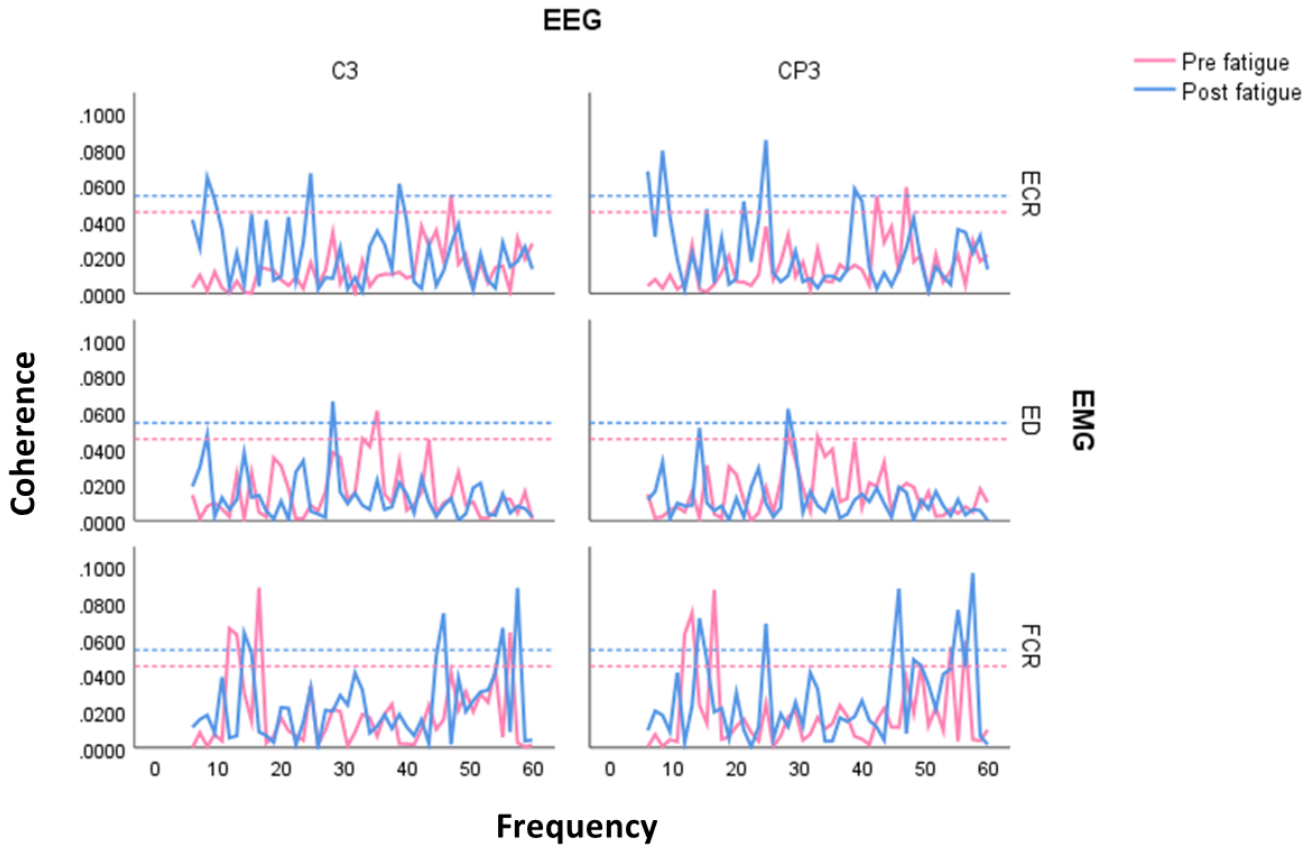

Figure C.5: Pre and post fatigue coherence for Subject 5. Pre fatigue coherence is plotted in pink colour and post fatigue coherence is plotted in blue colour. Dashed lines represent significant coherences.

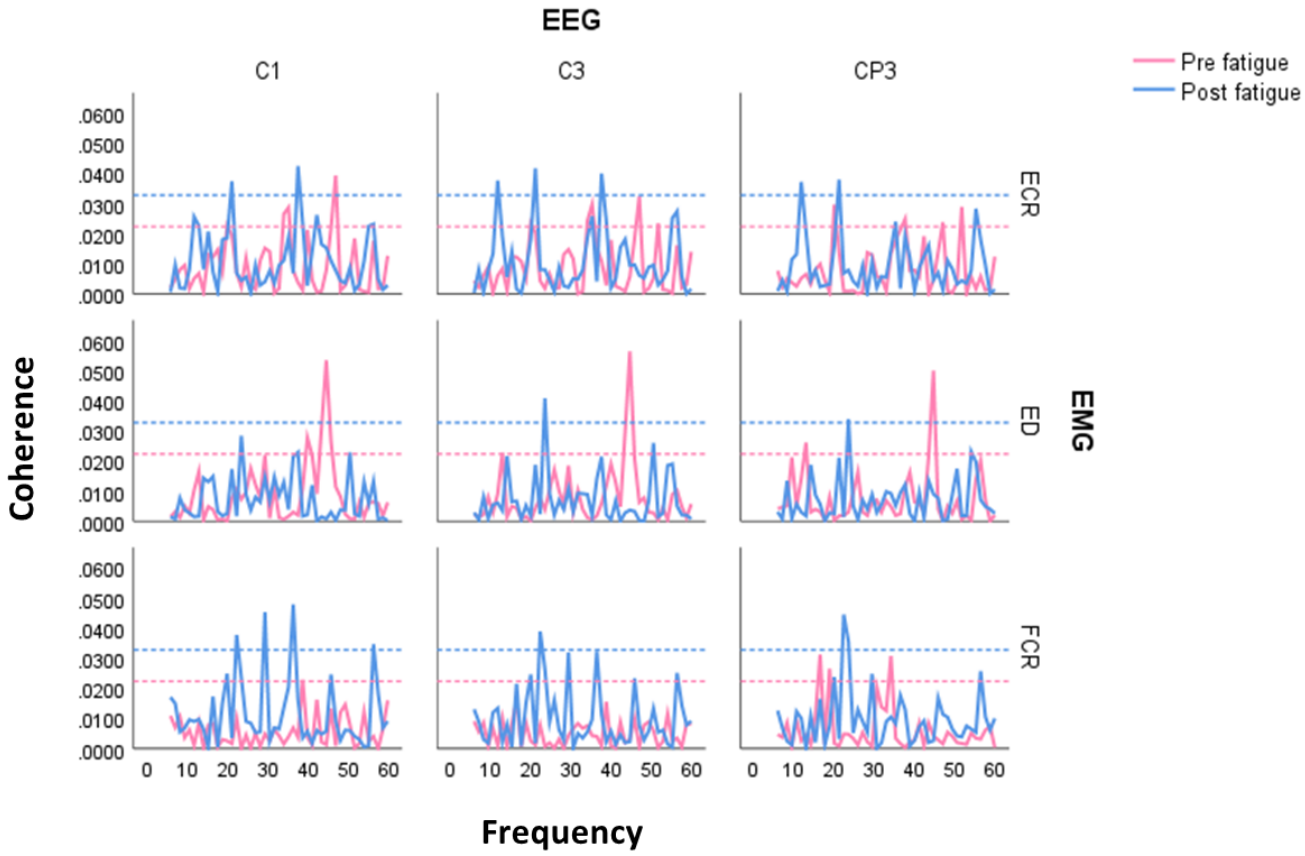

Figure C.6: Pre and post fatigue coherence for Subject 6. Pre fatigue coherence is plotted in pink colour and post fatigue coherence is plotted in blue colour. Dashed lines represent significant coherences.

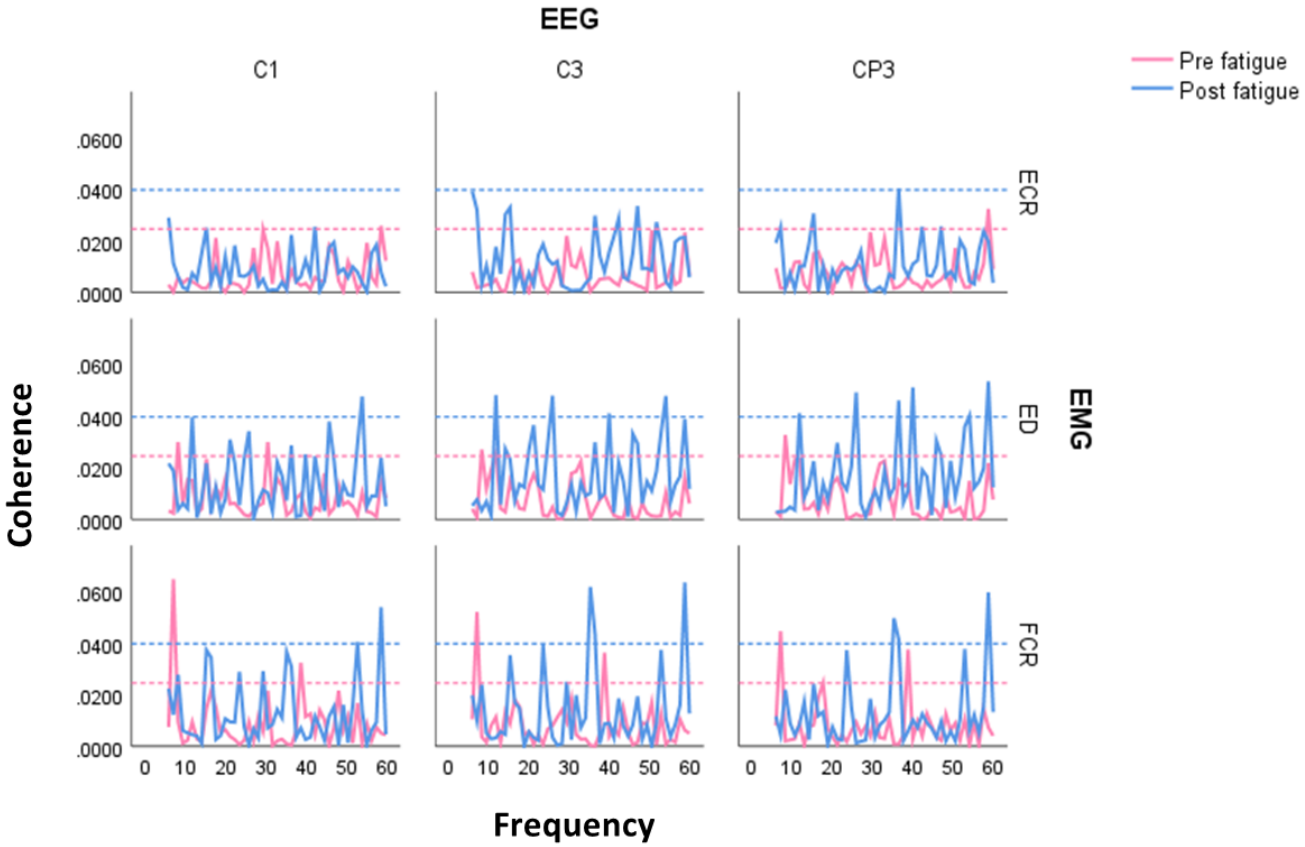

Figure C.7: Pre and post fatigue coherence for Subject 8. Pre fatigue coherence is plotted in pink colour and post fatigue coherence is plotted in blue colour. Dashed lines represent significant coherences.

8

BIBLIOGRAPHY

[1] Abhang, P. A., Gawali, B. W. and Mehrotra, S. C. [2016], 'Technical aspects of brain rhythms and speech parameters', *Introduction to EEG-and speech-based emotion recognition* pp. 51–79.

[2] Ali, A. A. L., Cosic, I., Kumar, D. K., Polus, B. and Costa, C. D. [2004], Power changes of eeg signals associated with muscle fatigue: The root mean square analysis of eeg bands, pp. 531–534.

[3] Amirabdollahian, F., Ates, S., Basteris, A., Cesario, A., Buurke, J., Hermens, H., Hofs, D., Johansson, E., Mountain, G., Nasr, N. et al. [2014], 'Design, development and deployment of a hand/wrist exoskeleton for home-based rehabilitation after stroke-script project', *Robotica* **32**(8), 1331–1346.

[4] Amirabdollahian, F. and Johnson, G. [2011], 'Analysis of the results from use of haptic peg-in-hole task for assessment in neurorehabilitation', *Applied Bionics and Biomechanics* **8**(1), 1–11.

[5] Antonova, I., Bänninger, A., Dierks, T., Griskova-Bulanova, I., Koenig, T. and Kohler, A. [2015], 'Differential recruitment of brain networks during visuospatial and color processing: evidence from erp microstates', *Neuroscience* **305**, 128–138.

[6] Anwer, S., Waris, A., Gilani, S. O., Iqbal, J., Shaikh, N., Pujari, A. N. and Niazi, I. K. [2022], Rehabilitation of upper limb motor impairment in stroke: A narrative review on the prevalence, risk factors, and economic statistics of stroke and state of the art therapies, *in* 'Healthcare', Vol. 10, MDPI, p. 190.

[7] Aprile, I., Germanotta, M., Cruciani, A., Loreti, S., Pecchioli, C., Cecchi, F., Montesano, A., Galeri, S., Diverio, M., Falsini, C. et al. [2020], 'Upper limb robotic rehabilitation after stroke: a multicenter, randomized clinical trial', *Journal of Neurologic Physical Therapy* **44**(1), 3–14.

[8] Baldini, S., Morelli, M. E., Sartori, A., Pasquin, F., Dinoto, A., Bratina, A., Bosco, A. and Manganotti, P. [2023], 'Microstates in multiple sclerosis: an electrophysiological signature of altered large-scale networks functioning?', *Brain Communications* **5**(1), fcac255.

[9] Balestra, N., Sharma, G., Riek, L. M. and Busza, A. [2021], 'Automatic identification of upper extremity rehabilitation exercise type and dose using body-worn sensors and machine learning: a pilot study', *Digital Biomarkers* **5**(2), 158–166.

[10] Ballester, B. R., Ward, N. S., Brander, F., Maier, M., Kelly, K. and Verschure, P. F. [2022], 'Relationship between intensity and recovery in post-stroke rehabilitation: a retrospective analysis', *Journal of Neurology, Neurosurgery & Psychiatry* **93**(2), 226–228.

[11] Baradits, M., Bitter, I. and Czobor, P. [2020], 'Multivariate patterns of eeg microstate parameters and their role in the discrimination of patients with schizophrenia from healthy controls', *Psychiatry Research* **288**, 112938.

[12] Basteris, A., Nijenhuis, S. M., Stienen, A. H., Buurke, J. H., Prange, G. B. and Amirabdollahian, F. [2014], 'Training modalities in robot-mediated upper limb rehabilitation in stroke: a framework for classification based on a systematic review', *Journal of neuroengineering and rehabilitation* **11**, 1–15.

[13] Bayram, M. B., Siemionow, V. and Yue, G. H. [2015], 'Weakening of corticomuscular signal coupling during voluntary motor action in aging', *Journals of Gerontology Series A: Biomedical Sciences and Medical Sciences* **70**(8), 1037–1043.

[14] Biasiucci, A., Chavarriaga, R., Hamner, B., Leeb, R., Pichiorri, F., Fallani, F. D. V., Mattia, D. and Millán, J. d. R. [2011], Combining discriminant and topographic information in bci: preliminary results on stroke patients, *in* '2011 5th international ieee/embs conference on neural engineering', IEEE, pp. 290–293.

[15] Blinowska, K. and Durka, P. [2006], 'Electroencephalography (eeg)', *Wiley encyclopedia of biomedical engineering* .

[16] Bowers, L., Bowler, M. and Amirabdollahian, F. [2013], 'Haptic cues for vision impaired art makers: 'Seeing' through touch', *Proceedings - 2013 IEEE International Conference on Systems, Man, and Cybernetics, SMC 2013* pp. 547–552.

[17] Bowler, M., Amirabdollahian, F. and Dautenhahn, K. [2011], 'Using an embedded reality approach to improve test reliability for NHPT tasks', *IEEE International Conference on Rehabilitation Robotics* .

[18] Bowler, M. E. [2019], Interactive Haptics for Remote and On-Site Assessment of Arm Function Following a Stroke, PhD thesis, University of Hertfordshire.

[19] Brambilla, C., Pirovano, I., Mira, R. M., Rizzo, G., Scano, A. and Mastropietro, A. [2021], 'Combined use of emg and eeg techniques for neuromotor assessment in rehabilitative applications: a systematic review', *Sensors* **21**(21), 7014.

[20] Bréchet, L. and Michel, C. M. [2022], 'Eeg microstates in altered states of consciousness', *Frontiers in Psychology* **13**.

[21] Britton, J. W., Frey, L. C., Hopp, J. L., Korb, P., Koubeissi, M. Z., Lievens, W. E., Pestana-Knight, E. M. and St Louis, E. [2016], 'Electroencephalography (eeg): An introductory text and atlas of normal and abnormal findings in adults, children, and infants'.

[22] Brown, P., Salenius, S., Rothwell, J. C. and Hari, R. [1998], 'Cortical correlate of the piper rhythm in humans', *Journal of neurophysiology* **80**(6), 2911–2917.

[23] Bruce, J. M., Bruce, A. S. and Arnett, P. A. [2010], 'Response variability is associated with self-reported cognitive fatigue in multiple sclerosis.', *Neuropsychology* **24**(1), 77.

[24] Caglar, A., Gurses, H., Mutluay, F. and Kiziltan, G. [2005], 'Effects of home exercises on motor performance in patients with parkinson's disease', *Clinical rehabilitation* **19**(8), 870–877.

[25] Calcagno, A., Coelli, S., Tacchino, G., Baratto, M., Molteni, F., Guanziroli, E., Puttilli, C. and Bianchi, A. M. [2020], Arte project: Eeg analysis during robotic rehabilitation, *in* 'XV Mediterranean Conference on Medical and Biological Engineering and Computing–MEDICON 2019: Proceedings of MEDICON 2019, September 26-28, 2019, Coimbra, Portugal', Springer, pp. 755–760.

[26] Cao, L., Hao, D., Rong, Y., Zhou, Y., Li, M. and Tian, Y. [2015], 'Investigating the modulation of brain activity associated with handgrip force and fatigue', *Technology and Health Care* **23**(s2), S427–S433.

[27] Carey, J. R., Kimberley, T. J., Lewis, S. M., Auerbach, E. J., Dorsey, L., Rundquist, P. and Ugurbil, K. [2002], 'Analysis of fmri and finger tracking training in subjects with chronic stroke', *Brain* **125**(4), 773–788.

[28] Chai, G., Wang, Y., Wu, J., Yang, H., Tang, Z. and Zhang, L. [2019], Study on the recognition of exercise intensity and fatigue on runners based on subjective and objective information, *in* 'Healthcare', Vol. 7, MDPI, p. 150.

[29] Charles, D., Pedlow, K., McDonough, S., Shek, K. and Charles, T. [2014], 'Close range depth sensing cameras for virtual reality based hand rehabilitation', *Journal of Assistive Technologies* **8**(3), 138–149.

[30] Chemuturi, R., Amirabdollahian, F. and Dautenhahn, K. [2013], 'Adaptive training algorithm for robot-assisted upper-arm rehabilitation, applicable to individualised and therapeutic human-robot interaction', *Journal of neuroengineering and rehabilitation* **10**, 1–18.

[31] Chen, X., Xie, P., Zhang, Y., Chen, Y., Cheng, S. and Zhang, L. [2018], 'Abnormal functional corticomuscular coupling after stroke', *NeuroImage: Clinical* **19**(November 2017), 147–159.

[32] Choudhary, A., Gulati, S., Kabra, M., Singh, U. P., Sankhyan, N., Pandey, R. M. and Kalra, V. [2013], 'Efficacy of modified constraint induced movement therapy in improving upper limb function in children with hemiplegic cerebral palsy: A randomized controlled trial', *Brain and Development* **35**(9), 870–876.

[33] Chrvala, C. A. [n.d.], 'The Role of Robotic-assisted Therapy in Stroke Rehabilitation'.
URL: *https://www.medpagetoday.com/resource-centers/spotlight-on-ischemic-stroke/role-robotic-assisted-therapy-stroke-rehabilitation/1528*

[34] Cisotto, G., Guglielmi, A. V., Badia, L. and Zanella, A. [2018], 'Classification of grasping tasks based on EEG-EMG coherence', *2018 IEEE 20th International Conference on e-Health Networking, Applications and Services (Healthcom)* pp. 1–6.

[35] Cohen, M. X. [2017], 'Where does eeg come from and what does it mean?', *Trends in neurosciences* **40**(4), 208–218.

[36] Colombo, R., Pisano, F., Micera, S., Mazzone, A., Delconte, C., Carrozza, M. C., Dario, P. and Minuco, G. [2005], 'Robotic techniques for upper limb evaluation and rehabilitation of stroke patients', *IEEE transactions on neural systems and rehabilitation engineering* **13**(3), 311–324.

[37] Comani, S., Velluto, L., Schinaia, L., Cerroni, G., Serio, A., Buzzelli, S., Sorbi, S. and Guarnieri, B. [2015], 'Monitoring neuro-motor recovery from stroke with high-resolution eeg, robotics and virtual reality: a proof of concept', *IEEE Transactions on Neural Systems and Rehabilitation Engineering* **23**(6), 1106–1116.

[38] Constantin-Teodosiu, D. and Constantin, D. [2021], 'Molecular mechanisms of muscle fatigue', *International Journal of Molecular Sciences* **22**(21), 11587.

[39] Copaci, D., Arias, J., Gómez-Tomé, M., Moreno, L. and Blanco, D. [2022], 'semg-based gesture classifier for a rehabilitation glove', *Frontiers in Neurorobotics* **16**.

[40] Crabbe, J. B. and Dishman, R. K. [2004], 'Brain electrocortical activity during and after exercise: A quantitative synthesis'.

[41] D'Croz-Baron, D. F., Baker, M., Michel, C. M. and Karp, T. [2019], 'Eeg microstates analysis in young adults with autism spectrum disorder during resting-state', *Frontiers in human neuroscience* **13**, 173.

[42] de Carvalho Costa, T. D., da Silva Machado, C. B., Segundo, R. P. L., dos Santos Silva, J. P., Silva, A. C. T., de Souza Andrade, R., Rosa, M. R. D., Smaili, S. M., Morya, E., Costa-Ribeiro, A. et al. [2023], 'Are the eeg microstates correlated with motor and non-motor parameters in patients with parkinson's disease?', *Neurophysiologie Clinique* **53**(1), 102839.

[43] De Pascalis, V. [2004], 'On the psychophysiology of extraversion', *On the psychobiology of personality: Essays in honor of Marvin Zuckerman* pp. 295–327.

[44] de Sousa, D. G., Harvey, L. A., Dorsch, S. and Glinsky, J. V. [2018], 'Interventions involving repetitive practice improve strength after stroke: a systematic review', *Journal of physiotherapy* **64**(4), 210–221.

[45] Delorme, A. and Makeig, S. [2004], 'EEGLAB: An open source toolbox for analysis of single-trial EEG dynamics including independent component analysis', *Journal of Neuroscience Methods* **134**(1), 9–21.

[46] Dias, M. P. F., Silva Santos, A. T., Calixto-Júnior, R., De Oliveira, V. A., Kosour, C. and Silva Vilela Terra, A. M. [2022], 'Is there a relation between brain and muscle activity after virtual reality training in individuals with stroke? a cross-sectional study', *International Journal of Environmental Research and Public Health* **19**(19), 12705.

[47] Dissanayake, U. C., Steuber, V. and Amirabdollahian, F. [2022], 'Eeg spectral feature modulations associated with fatigue in robot-mediated upper limb gross and fine motor interactions', *Frontiers in Neurorobotics* **15**, 192.

[48] *EEG Signal Quality in Wet Versus Dry Electrodes* [n.d.], `https://https://sapienlabs.org/lab-talk/eeg-signal-quality-in-wet-versus-dry-electrodes/`. Accessed: 2023-03-29.

[49] Enoka, R. M. and Duchateau, J. [2008], 'Muscle fatigue: what, why and how it influences muscle function', *The Journal of physiology* **586**(1), 11–23.

[50] Fang, Y., Daly, J. J., Sun, J., Hvorat, K., Fredrickson, E., Pundik, S., Sahgal, V. and Yue, G. H. [2009], 'Functional corticomuscular connection during reaching is weakened following stroke', *Clinical neurophysiology* **120**(5), 994–1002.

[51] Fisk, J. D., Ritvo, P. G., Ross, L., Haase, D. A., Marrie, T. J. and Schlech, W. F. [1994], 'Measuring the functional impact of fatigue: initial validation of the fatigue impact scale', *Clinical Infectious Diseases* **18**(Supplement_1), S79–S83.

[52] Flynn, N., Froude, E., Cooke, D. and Kuys, S. [2022], 'Repetitions, duration and intensity of upper limb practice following the implementation of robot assisted therapy with subacute stroke survivors: an observational study', *Disability and Rehabilitation: Assistive Technology* **17**(6), 675–680.

[53] Freeman, C. T., Rogers, E., Hughes, A.-M., Burridge, J. H. and Meadmore, K. L. [2012], 'Iterative learning control in health care: Electrical stimulation and robotic-assisted upper-limb stroke rehabilitation', *IEEE Control Systems Magazine* **32**(1), 18–43.

[54] French, B., Thomas, L. H., Coupe, J., McMahon, N. E., Connell, L., Harrison, J., Sutton, C. J., Tishkovskaya, S. and Watkins, C. L. [2016], 'Repetitive task training for improving functional ability after stroke', *Cochrane database of systematic reviews* (11).

[55] Gandevia, S., Allen, G. M., Butler, J. E. and Taylor, J. L. [1996], 'Supraspinal factors in human muscle fatigue: evidence for suboptimal output from the motor cortex.', *The Journal of physiology* **490**(2), 529–536.

[56] Gärtner, M., Brodbeck, V., Laufs, H. and Schneider, G. [2015], 'A stochastic model for eeg microstate sequence analysis', *Neuroimage* **104**, 199–208.

[57] Gary Kamen, D. A. [2009], *Essentials of Electromyography*, Human Kinetics.

[58] Gemperline, J. J., Allen, S., Walk, D. and Rymer, W. Z. [1995], 'Characteristics of motor unit discharge in subjects with hemiparesis', *Muscle & Nerve: Official Journal of the American Association of Electrodiagnostic Medicine* **18**(10), 1101–1114.

[59] Guerrero-Mendez, C. D. and Ruiz-Olaya, A. F. [2022], 'Coherence-based connectivity analysis of eeg and emg signals during reach-to-grasp movement involving two weights', *Brain-Computer Interfaces* **9**(3), 140–154.

[60] Gui, P., Jiang, Y., Zang, D., Qi, Z., Tan, J., Tanigawa, H., Jiang, J., Wen, Y., Xu, L., Zhao, J. et al. [2020], 'Assessing the depth of language processing in patients with disorders of consciousness', *Nature neuroscience* **23**(6), 761–770.

[61] Guo, Z., Qian, Q., Wong, K., Zhu, H., Huang, Y., Hu, X. and Zheng, Y. [2020], 'Altered corticomuscular coherence (cmcoh) pattern in the upper limb during finger movements after stroke', *Frontiers in Neurology* **11**, 410.

[62] Halaki, M. and Ginn, K. [2012], 'Normalization of emg signals: to normalize or not to normalize and what to normalize to', *Computational intelligence in electromyography analysis-a perspective on current applications and future challenges* **10**, 49957.

[63] Hao, Z., Zhai, X., Cheng, D., Pan, Y. and Dou, W. [2022], 'Eeg microstate-specific functional connectivity and stroke-related alterations in brain dynamics', *Frontiers in Neuroscience* **16**, 617.

[64] Havlikova, E., Rosenberger, J., Nagyova, I., Middel, B., Dubayova, T., Gdovinova, Z., Van Dijk, J. P. and Groothoff, J. W. [2008], 'Impact of fatigue on quality of life in patients with parkinson‚Äôs disease', *European Journal of Neurology* **15**(5), 475–480.

[65] Heller, A., Wade, D. T., Wood, V. A., Sunderland, A., Hewer, R. L. and Ward, E. [1987], 'Arm function after stroke: measurement and recovery over the first three months.', *Journal of Neurology, Neurosurgery & Psychiatry* **50**(6), 714–719.

[66] Hsu, L.-I., Lim, K.-W., Lai, Y.-H., Chen, C.-S. and Chou, L.-W. [2023], 'Effects of muscle fatigue and recovery on the neuromuscular network after an intermittent handgrip fatigue task: Spectral analysis of electroencephalography and electromyography signals', *Sensors* **23**(5), 2440.

[67] *https://www.world-stroke.org/component/content/article/16-forpatients/84-facts-and-figures-about-stroke* [n.d.].
URL: *https://www.world-stroke.org/component/content/article/16-forpatients/84-facts-and-figures-about-stroke*

[68] Huo, C., Xu, G., Sun, A., Xie, H., Hu, X., Li, W., Li, Z. and Fan, Y. [2023], 'Cortical response induced by task-oriented training of the upper limb in subacute stroke patients as assessed by functional near-infrared spectroscopy', *Journal of Biophotonics* **16**(3), e202200228.

[69] Ivanitsky, A. M., Nikolaev, A. R. and Ivanitsky, G. A. [1999], 'Electroencephalography', *Modern techniques in neuroscience research* pp. 971–995.

[70] James, L. M., Halliday, D. M., Stephens, J. A. and Farmer, S. F. [2008], 'On the development of human corticospinal oscillations: age-related changes in eeg–emg coherence and cumulant', *European Journal of Neuroscience* **27**(12), 3369–3379.

[71] Jasper, H. H. [1958], 'Report of the committee on methods of clinical examination in electroencephalography', *Electroencephalography and Clinical Neurophysiology* **10**, 370–375.

[72] Jasper, H. H. and Andrews, H. L. [1938], 'Brain potentials and voluntary muscle activity in man', *Journal of Neurophysiology* **1**(2), 87–100.

[73] Jawabri, K. H. and Sharma, S. [2021], 'Physiology, cerebral cortex functions', *StatPearls [internet]* .

[74] Jia, X. and Kohn, A. [2011], 'Gamma rhythms in the brain', *PLoS biology* **9**(4), e1001045.

[75] Jiang, C., Yang, Q., Chen, T., Siemionow, V., Ranganathan, V. K., Yan, A. F. and Yue, G. H. [2019], 'Functional corticomuscular signal coupling is weakened during voluntary motor action in cancer-related fatigue', *Neural plasticity* **2019**.

[76] Jiang, X., Bian, G. B. and Tian, Z. [2019], 'Removal of artifacts from EEG signals: A review', *Sensors (Switzerland)* **19**(5), 1–18.

[77] JJ, B.-R. B. W. [1984], 'Changes in muscle contractile properties and neural control during human muscular fatigue', *Muscle Nerve* **7**(9), 691.

[78] Johari, K. and Behroozmand, R. [2020], 'Event-related desynchronization of alpha and beta band neural oscillations predicts speech and limb motor timing deficits in normal aging', *Behavioural brain research* **393**, 112763.

[79] Johnson, S. K., Frederick, J., Kaufman, M. and Mountjoy, B. [1999], 'A controlled investigation of bodywork in multiple sclerosis', *The Journal of Alternative and Complementary Medicine* **5**(3), 237–243.

[80] Jung, T. P., Makeig, S., Humphries, C., Lee, T. W., Mckeown, M. J., Iragui, V. and Sejnowski, T. J. [2000], 'Removing electroencephalographic artifacts by blind source separation', *Psychophysiology* **37**.

[81] Kaiser, J. and Lutzenberger, W. [2003], 'Induced gamma-band activity and human brain function', *Neuroscientist* **9**, 475–484.

[82] Kalavina, R. [2019], 'The challenges and experiences of stroke patients and their spouses in blantyre, malawi', *Malawi Medical Journal* **31**(2), 112–117.

[83] Kan, P., Huq, R., Hoey, J., Goetschalckx, R. and Mihailidis, A. [2011], 'The development of an adaptive upper-limb stroke rehabilitation robotic system', *Journal of neuroengineering and rehabilitation* **8**(1), 1–18.

[84] Khanna, A., Pascual-Leone, A. and Farzan, F. [2014], 'Reliability of resting-state microstate features in electroencephalography', *PLoS ONE* **9**(12), 1–21.

[85] Khanna, A., Pascual-Leone, A., Michel, C. M. and Farzan, F. [2015], 'Microstates in resting-state eeg: current status and future directions', *Neuroscience & Biobehavioral Reviews* **49**, 105–113.

[86] Kilner, J. M., Baker, S. N., Salenius, S., Hari, R. and Lemon, R. N. [2000], 'Human cortical muscle coherence is directly related to specific motor parameters', *Journal of Neuroscience* **20**(23), 8838–8845.

[87] Kim, B., Kim, L., Kim, Y. H. and Yoo, S. K. [2017], 'Cross-association analysis of EEG and EMG signals according to movement intention state', *Cognitive Systems Research* **44**, 1–9.

[88] Kimberley, T. J., Samargia, S., Moore, L. G., Shakya, J. K. and Lang, C. E. [2010], 'Comparison of amounts and types of practice during rehabilitation for traumatic brain injury and stroke'.

[89] Knorr, S., Ivanova, T., Doherty, T., Campbell, J. and Garland, S. [2011], 'The origins of neuromuscular fatigue post-stroke', *Experimental brain research* **214**, 303–315.

[90] Koenig, T., Lehmann, D., Merlo, M. C., Kochi, K., Hell, D. and Koukkou, M. [1999], 'A deviant eeg brain microstate in acute, neuroleptic-naive schizophrenics at rest', *European archives of psychiatry and clinical neuroscience* **249**, 205–211.

[91] Koenig, T., Tomescu, M. I., Rihs, T. A. and Koukkou, M. [2017], 'Eeg indices of cortical network formation and their relevance for studying variance in subjective experience and behavior', *In Vivo Neuropharmacology and Neurophysiology* pp. 17–35.

[92] Konrad, P. [2005], 'The abc of emg,a practical introduction to kinesiological electromyography', **1**(2005), 30–5.

[93] Krauth, R., Schwertner, J., Vogt, S., Lindquist, S., Sailer, M., Sickert, A., Lamprecht, J., Perdikis, S., Corbet, T., Millán, J. d. R. et al. [2019], 'Cortico-muscular coherence is reduced acutely post-stroke and increases bilaterally during motor recovery: a pilot study', *Frontiers in neurology* **10**, 126.

[94] Kristeva-Feige, R., Fritsch, C., Timmer, J. and Lücking, C.-H. [2002], 'Effects of attention and precision of exerted force on beta range eeg-emg synchronization during a maintained motor contraction task', *Clinical Neurophysiology* **113**(1), 124–131.

[95] Lambercy, O., Fluet, M.-C., Lamers, I., Kerkhofs, L., Feys, P. and Gassert, R. [2013], Assessment of upper limb motor function in patients with multiple sclerosis using the virtual peg insertion test: a pilot study, *in* '2013 IEEE 13th international conference on rehabilitation robotics (ICORR)', IEEE, pp. 1–6.

[96] Lang, C. E., Bland, M. D., Bailey, R. R., Schaefer, S. Y. and Birkenmeier, R. L. [2013], 'Assessment of upper extremity impairment, function, and activity after stroke: foundations for clinical decision making', *Journal of Hand Therapy* **26**(2), 104–115.

[97] Langhorne, P., Bernhardt, J. and Kwakkel, G. [2011], 'Stroke rehabilitation', *The Lancet* **377**(9778), 1693–1702.

[98] Laut, J., Porfiri, M. and Raghavan, P. [2016], 'The present and future of robotic technology in rehabilitation', *Current physical medicine and rehabilitation reports* **4**, 312–319.

[99] Lawrence, E. S., Coshall, C., Dundas, R., Stewart, J., Rudd, A. G., Howard, R. and Wolfe, C. D. [2001], 'Estimates of the prevalence of acute stroke impairments and disability in a multiethnic population', *Stroke* **32**(6), 1279–1284.

[100] Lee, J. H., Whittington, M. A. and Kopell, N. J. [2013], 'Top-down beta rhythms support selective attention via interlaminar interaction: a model', *PLoS computational biology* **9**(8), e1003164.

[101] Lehmann, D. [1990], Brain electric microstates and cognition: the atoms of thought, *in* 'Machinery of the Mind', Springer, pp. 209–224.

[102] Lehmann, D., Pascual-Marqui, R. D. and Michel, C. [2009], 'Eeg microstates', *Scholarpedia* **4**(3), 7632.

[103] Li, M., He, B., Liang, Z., Zhao, C.-G., Chen, J., Zhuo, Y., Xu, G., Xie, J. and Althoefer, K. [2019], 'An attention-controlled hand exoskeleton for the rehabilitation of finger extension and flexion using a rigid-soft combined mechanism', *Frontiers in neurorobotics* **13**, 34.

[104] Li, W., Cheng, S., Wang, H. and Chang, Y. [2023], 'Eeg microstate changes according to mental fatigue induced by aircraft piloting simulation: An exploratory study', *Behavioural Brain Research* **438**, 114203.

[105] Liepert, J., Graef, S., Uhde, I., Leidner, O. and Weiller, C. [2000], 'Training-induced changes of motor cortex representations in stroke patients', *Acta neurologica scandinavica* **101**(5), 321–326.

[106] Liu, J., Sheng, Y. and Liu, H. [2019], 'Corticomuscular coherence and its applications: A review', *Frontiers in Human Neuroscience* **13**.

[107] Louis, E. and Frey, L. [n.d.], Electroencephalography,Äîan introductory text and atlas of normal and abnormal findings in adults, children, and infants; american epilepsy society: Chicago, il, usa, 2016, Technical report, ISBN 13-978-0-9979756-0-4.

[108] Loureiro, R., Amirabdollahian, F., Topping, M., Driessen, B. and Harwin, W. [2003], 'Upper limb robot mediated stroke therapy,Äîgentle/s approach', *Autonomous Robots* **15**, 35–51.

[109] Lundbye-Jensen, J. and Nielsen, J. B. [2008], 'Central nervous adaptations following 1 wk of wrist and hand immobilization', *Journal of applied physiology* **105**(1), 139–151.

[110] Malmivuo, J., Plonsey, R. et al. [1995], *Bioelectromagnetism: principles and applications of bioelectric and biomagnetic fields*, Oxford University Press, USA.

[111] Masiero, S. and Carraro, E. [2008], 'Upper limb movements and cerebral plasticity in post-stroke rehabilitation', *Aging clinical and experimental research* **20**, 103–108.

[112] Mathiowetz, V., Weber, K., Kashman, N. and Volland, G. [1985], 'Adult norms for the nine hole peg test of finger dexterity', *The Occupational Therapy Journal of Research* **5**(1), 24–38.

[113] Maura, R. M., Rueda Parra, S., Stevens, R. E., Weeks, D. L., Wolbrecht, E. T. and Perry, J. C. [2023], 'Literature review of stroke assessment for upper-extremity physical function via eeg, emg, kinematic, and kinetic measurements and their reliability', *Journal of NeuroEngineering and Rehabilitation* **20**(1), 1–32.

[114] Merletti, R. and Parker, P. J. [2004], *Electromyography: physiology, engineering, and non-invasive applications*, Vol. 11, John Wiley & Sons.

[115] Miao, Q., Zhang, M., McDaid, A., Peng, Y. and Xie, S. Q. [2020], 'A robot-assisted bilateral upper limb training strategy with subject-specific workspace: A pilot study', *Robotics and Autonomous Systems* **124**, 103334.

[116] Michel, C. M. and Koenig, T. [2018], 'Eeg microstates as a tool for studying the temporal dynamics of whole-brain neuronal networks: a review', *Neuroimage* **180**, 577–593.

[117] Michel, C. M., Koenig, T. and Brandeis, D. [2009], Electrical neuroimaging in the time domain, *in* C. M. Michel, T. Koenig, D. Brandeis, L. R. R. Gianotti and J. Wackermann, eds, 'Electrical Neuroimaging', Cambridge University Press, pp. 111–144.

[118] Mima, T., Hallett, M. and Shibasaki, H. [2003], Coherence, cortico-muscular, *in* 'Handbook of Clinical Neurophysiology', Vol. 1, Elsevier, pp. 87–94.

[119] Mima, T., Ohara, S. and Nagamine, T. [2002], Cortical–muscular coherence, *in* 'International Congress Series', Vol. 1226, Elsevier, pp. 109–119.

[120] Mima, T., Toma, K., Koshy, B. and Hallett, M. [2001], 'Coherence between cortical and muscular activities after subcortical stroke', *Stroke* **32**(11), 2597–2601.

[121] Mistry, K. S., Pelayo, P., Anil, D. G. and George, K. [2018], An ssvep based brain computer interface system to control electric wheelchairs, *in* '2018 IEEE International Instrumentation and Measurement Technology Conference (I2MTC)', IEEE, pp. 1–6.

[122] Moran, G., Fletcher, B., Feltham, M., Calvert, M., Sackley, C. and Marshall, T. [2014], 'Fatigue, psychological and cognitive impairment following transient ischaemic attack and minor stroke: a systematic review', *European journal of neurology* **21**(10), 1258–1267.

[123] *Muscles of the Anterior Forearm - Flexion - Pronation - TeachMeAnatomy* [n.d.].
URL: *https://teachmeanatomy.info/upper-limb/muscles/anterior-forearm/*

[124] *Muscles of the Posterior Forearm - Superficial - Deep - TeachMeAnatomy* [n.d.].
URL: *https://teachmeanatomy.info/upper-limb/muscles/posterior-forearm/*

[125] Naik, G. R., Al-Timemy, A. H. and Nguyen, H. T. [2015], 'Transradial amputee gesture classification using an optimal number of semg sensors: an approach using ica clustering', *IEEE Transactions on Neural Systems and Rehabilitation Engineering* **24**(8), 837–846.

[126] Nakano, H. [2020], Eeg measurement as a tool for rehabilitation assessment and treatment, *in* 'Electroencephalography-From Basic Research to Clinical Applications', IntechOpen.

[127] Nakayashiki, K., Saeki, M., Takata, Y., Hayashi, Y. and Kondo, T. [2014], 'Modulation of event-related desynchronization during kinematic and kinetic hand movements', *Journal of neuroengineering and rehabilitation* **11**(1), 1–9.

[128] Nuwer, M. R., Comi, G., Emerson, R., Fuglsang-Frederiksen, A., Guérit, J.-M., Hinrichs, H., Ikeda, A., Luccas, F. J. C. and Rappelsburger, P. [1998], 'Ifcn standards for digital recording of clinical eeg', *Electroencephalography and clinical Neurophysiology* **106**(3), 259–261.

[129] Orekhova, E., Stroganova, T., Posikera, I. and Elam, M. [2006], 'Eeg theta rhythm in infants and preschool children', *Clinical neurophysiology* **117**(5), 1047–1062.

[130] Oxford Grice, K., Vogel, K. A., Le, V., Mitchell, A., Muniz, S. and Vollmer, M. A. [2003], 'Adult norms for a commercially available nine hole peg test for finger dexterity', *The American journal of occupational therapy* **57**(5), 570–573.

[131] Paciaroni, M. and Acciarresi, M. [2019], 'Poststroke fatigue', *Stroke* **50**(7), 1927–1933.

[132] Page, S., Gater, D. and Bach-Y-Rita, P. [2004], 'Reconsidering the motor recovery plateau after stroke', *Arch Phys Med Rehabil* **85**, 1377–81.

[133] Pan, L., Zhao, L., Song, A., Yin, Z. and She, S. [2019], 'A novel robot-aided upper limb rehabilitation training system based on multimodal feedback', *Frontiers in Robotics and AI* **6**, 102.

[134] Pascual-Marqui, R. D., Michel, C. M. and Lehmann, D. [1995], 'Segmentation of brain electrical activity into microstates: model estimation and validation', *IEEE Transactions on Biomedical Engineering* **42**(7), 658–665.

[135] Patel, A., Biso, G. M. N. R. and Fowler, J. B. [2021], Neuroanatomy, temporal lobe, *in* 'StatPearls [Internet]', StatPearls Publishing.

[136] Perez, M. A., Lundbye-Jensen, J. and Nielsen, J. B. [2006], 'Changes in corticospinal drive to spinal motoneurones following visuo-motor skill learning in humans', *The Journal of physiology* **573**(3), 843–855.

[137] Pinegger, A., Wriessnegger, S. C., Faller, J. and Müller-Putz, G. R. [2016], 'Evaluation of different eeg acquisition systems concerning their suitability for building a brain–computer interface: case studies', *Frontiers in neuroscience* **10**, 441.

[138] Poulsen, A. T., Pedroni, A., Langer, N. and Hansen, L. K. [2018], 'Microstate eeglab toolbox: An introductory guide', *bioRxiv* p. 289850.
URL: *https://www.biorxiv.org/content/10.1101/289850v1 https://www.biorxiv.org/content/10.1101/289850v1.abstract*

[139] Poyil, A. T., Steuber, V. and Amirabdollahian, F. [2020], 'Influence of muscle fatigue on electromyogram–kinematic correlation during robot-assisted upper limb training', *Journal of Rehabilitation and Assistive Technologies Engineering* **7**, 2055668320903014.

[140] Qi, Y., Siemionow, V., Yao, W., Sahgal, V. and Yue, G. H. [2010], 'Single-Trial EEG-EMG Coherence Analysis Reveals Muscle Fatigue-Related Progressive Alterations in Corticomuscular Coupling', *IEEE Transactions on Neural Systems and Rehabilitation Engineering* **18**(2), 97–106.

[141] Qiu, Q., Cao, L., Hao, D., Yang, L., Hillstrom, R. and Zheng, D. [2018], 'Muscle Extremely Low Frequency Magnetic Stimulation Eliminates the Effect of Fatigue on EEG-EMG Coherence during the Lateral Raise Task: A Pilot Quantitative Investigation', *BioMed Research International* **2018**.

[142] Raimona Zadry, H., Dawal, S. Z. M. and Taha, Z. [2011], 'The relation between upper limb muscle and brain activity in two precision levels of repetitive light tasks', *International Journal of Occupational Safety and Ergonomics* **17**(4), 373–384.

[143] Reaz, M. B. I., Hussain, M. S. and Mohd-Yasin, F. [2006], 'Techniques of emg signal analysis: detection, processing, classification and applications', *Biological procedures online* **8**, 11–35.

[144] Resnick, H. E., Carter, E. A., Aloia, M. and Phillips, B. [2006], 'Cross-sectional relationship of reported fatigue to obesity, diet, and physical activity: results from the third national health and nutrition examination survey', *Journal of Clinical Sleep Medicine* **2**(02), 163–169.

[145] Resnik, L., Huang, H., Winslow, A., Crouch, D. L., Zhang, F. and Wolk, N. [2018], 'Evaluation of emg pattern recognition for upper limb prosthesis control: a case study in comparison with direct myoelectric control', *Journal of neuroengineering and rehabilitation* **15**, 1–13.

[146] Reyes, A., Laine, C. M., Kutch, J. J. and Valero-Cuevas, F. J. [2017], 'Beta band corticomuscular drive reflects muscle coordination strategies', *Frontiers in computational neuroscience* **11**, 17.

[147] Rossiter, H. E., Eaves, C., Davis, E., Boudrias, M.-H., Park, C.-h., Farmer, S., Barnes, G., Litvak, V. and Ward, N. S. [2013], 'Changes in the location of cortico-muscular coherence following stroke', *NeuroImage: Clinical* **2**, 50–55.

[148] Saeid Sanei, J. [2007], 'Eeg signal processing', *JA Saeid Sanei, EEG signal processing. Wiley* .

[149] Sailer, M., Sweeney-Reed, C. M. and Lamprecht, J. [2017], 'Robot-assisted and device-based rehabilitation of the upper extremity', *Neurology International Open* **1**(03), E242–E246.

[150] Schlegel, F., Lehmann, D., Faber, P. L., Milz, P. and Gianotti, L. R. [2012], 'Eeg microstates during resting represent personality differences', *Brain topography* **25**, 20–26.

[151] Schnitzler, A., Gross, J. and Timmermann, L. [2000], 'Synchronised oscillations of the human sensorimotor cortex', *Acta neurobiologiae experimentalis* **60**(2), 271–288.

[152] Schomer, D. L. and Lopes da Silva, F. H. [2017], *Niedermeyer's Electroencephalography: Basic Principles, Clinical Applications, and Related Fields*, Oxford University Press. **URL:** *https://doi.org/10.1093/med/9780190228484.001.0001*

[153] Seeber, M., Cantonas, L.-M., Hoevels, M., Sesia, T., Visser-Vandewalle, V. and Michel, C. M. [2019], 'Subcortical electrophysiological activity is detectable with high-density eeg source imaging', *Nature communications* **10**(1), 753.

[154] Sengupta, A., Tiwari, A. and Routray, A. [2017], Analysis of cognitive fatigue using eeg parameters, *in* '2017 39th Annual International Conference of the IEEE Engineering in Medicine and Biology Society (EMBC)', IEEE, pp. 2554–2557.

[155] Shibasaki, H. and Nagamine, T. [2003], Eeg (meg)/emg correlation, *in* 'Handbook of Clinical Neurophysiology', Vol. 1, Elsevier, pp. 15–29.

[156] Shusong, X. and Xia, Z. [2010], Emg-driven computer game for post-stroke rehabilitation, *in* '2010 IEEE Conference on Robotics, Automation and Mechatronics', IEEE, pp. 32–36.

[157] Siemionow, V., Yue, G. H., Ranganathan, V. K., Liu, J. Z. and Sahgal, V. [2000], 'Relationship between motor activity-related cortical potential and voluntary muscle activation', *Experimental brain research* **133**, 303–311.

[158] Siswoyo, A., Arief, Z. and Sulistijono, I. A. [2017], 'Application of artificial neural networks in modeling direction wheelchairs using neurosky mindset mobile (eeg) device', *EMITTER International Journal of Engineering Technology* **5**(1), 170–191.

[159] Smith, Y. A., Hong, E. and Presson, C. [2000], 'Normative and validation studies of the nine-hole peg test with children', *Perceptual and motor skills* **90**(3), 823–843.

[160] Soufineyestani, M., Dowling, D. and Khan, A. [2020], 'Electroencephalography (eeg) technology applications and available devices', *Applied Sciences* **10**(21), 7453.

[161] Spicer, R., Anglin, J., Krum, D. M. and Liew, S.-L. [2017], Reinvent: A low-cost, virtual reality brain-computer interface for severe stroke upper limb motor recovery, *in* '2017 IEEE Virtual Reality (VR)', IEEE, pp. 385–386.

[162] Spring, J. N., Bourdillon, N. and Barral, J. [2018], 'Resting eeg microstates and autonomic heart rate variability do not return to baseline one hour after a submaximal exercise', *Frontiers in neuroscience* **12**, 460.

[163] Spring, J. N., Sallard, E. F., Trabucchi, P., Millet, G. P. and Barral, J. [2022], 'Alterations in spontaneous electrical brain activity after an extreme mountain ultramarathon', *Biological Psychology* **171**, 108348.

[164] Steinisch, M., Tana, M. G. and Comani, S. [2013], 'A post-stroke rehabilitation system integrating robotics, vr and high-resolution eeg imaging', *IEEE Transactions on Neural Systems and Rehabilitation Engineering* **21**(5), 849–859.

[165] Suviseshamuthu, E. S., Handiru, V. S., Allexandre, D., Hoxha, A., Saleh, S. and Yue, G. H. [2022], 'Corrigendum: Eeg-based spectral analysis showing brainwave changes related to modulating progressive fatigue during a prolonged intermittent motor task', *Frontiers in Human Neuroscience* **16**.

[166] Tacchino, G., Gandolla, M., Coelli, S., Barbieri, R., Pedrocchi, A. and Bianchi, A. M. [2016], 'Eeg analysis during active and assisted repetitive movements: evidence for differences in neural engagement', *IEEE Transactions on Neural Systems and Rehabilitation Engineering* **25**(6), 761–771.

[167] Takemi, M., Masakado, Y., Liu, M. and Ushiba, J. [2013], 'Event-related desynchronization reflects downregulation of intracortical inhibition in human primary motor cortex', *Journal of neurophysiology* **110**(5), 1158–1166.

[168] Tatum IV, W. O. [2021], *Handbook of EEG interpretation*, Springer Publishing Company.

[169] Teasell, R. W., Fernandez, M. M., McIntyre, A. and Mehta, S. [2014], 'Rethinking the continuum of stroke rehabilitation', *Archives of physical medicine and rehabilitation* **95**(4), 595–596.

[170] Tecchio, F., Porcaro, C., Zappasodi, F., Pesenti, A., Ercolani, M. and Rossini, P. M. [2006], 'Resear ch ar tic le cortical short-term fatigue effects assessed via rhythmic brain-muscle coherence', *Exp Brain Res* **174**, 144–151.

[171] Thacham Poyil, A., Steuber, V. and Amirabdollahian, F. [2020], 'Adaptive robot mediated upper limb training using electromyogram-based muscle fatigue indicators', *Plos one* **15**(5), e0233545.

[172] *The Central Nervous System - Cerebral Cortex and Brain Lobes* [2023], `https://bio.libretexts.org/Bookshelves/Introductory_and_General_Biology/Book%3A_General_Biology_%28Boundless%29/35%3A_The_Nervous_System/35.10%3A_The_Central_Nervous_System_-_Cerebral_Cortex_and_Brain_Lobes`. Accessed: 2023-03-24.

[173] Thuraisingham, R. A., Tran, Y., Craig, A., Wijesuriya, N. and Nguyen, H. [2009], 'Using microstate intensity for the analysis of spontaneous EEG: Tracking changes from alert to the fatigue state', *Proceedings of the 31st Annual International Conference of the IEEE Engineering in Medicine and Biology Society: Engineering the Future of Biomedicine, EMBC 2009* pp. 4982–4985.

[174] Timmermans, A. A., Seelen, H. A., Willmann, R. D. and Kingma, H. [2009], 'Technology-assisted training of arm-hand skills in stroke: concepts on reacquisition of motor control and therapist guidelines for rehabilitation technology design', *Journal of neuroengineering and rehabilitation* **6**(1), 1–18.

[175] Tomasevic, L., Zito, G., Pasqualetti, P., Filippi, M. M., Landi, D., Ghazaryan, A., Lupoi, D. and Porcaro, C. [2012], 'Cortico-muscular coherence as an index of fatigue in multiple sclerosis'.

[176] *Touch-Haptic device* [2023].
Accessed: 2023-05-15.
URL: *https://www.3dsystems.com/haptics-devices/touch*

[177] Trejo, L. J., Kochavi, R., Kubitz, K., Montgomery, L. D., Rosipal, R. and Matthews, B. [2005], 'EEG-based Estimation of Cognitive Fatigue', *Proceedings of SPIE : Bio-monitoring for physiological and cognitive performance during military operations* **5797**(May 2014), 105–115.

[178] Usakli, A. B. et al. [2010], 'Improvement of eeg signal acquisition: An electrical aspect for state of the art of front end', *Computational intelligence and neuroscience* **2010**.

[179] Ushiyama, J., Katsu, M., Masakado, Y., Kimura, A., Liu, M. and Ushiba, J. [2011], 'Muscle fatigue-induced enhancement of corticomuscular coherence following sustained submaximal isometric contraction of the tibialis anterior muscle', *Journal of Applied Physiology* **110**(5), 1233–1240.

[180] Ushiyama, J., Takahashi, Y. and Ushiba, J. [2010], 'Muscle dependency of corticomuscular coherence in upper and lower limb muscles and training-related alterations in ballet dancers and weightlifters', *Journal of applied physiology* **109**(4), 1086–1095.

[181] Vaca Benitez, L. M., Tabie, M., Will, N., Schmidt, S., Jordan, M. and Kirchner, E. A. [2013], 'Exoskeleton technology in rehabilitation: Towards an emg-based orthosis system for upper limb neuromotor rehabilitation', *Journal of Robotics* **2013**.

[182] van Duinen, H., Renken, R., Maurits, N. M. and Zijdewind, I. [2008], 'Relation between muscle and brain activity during isometric contractions of the first dorsal interosseus muscle', *Human brain mapping* **29**(3), 281–299.

[183] von Carlowitz-Ghori, K., Bayraktaroglu, Z., Hohlefeld, F. U., Losch, F., Curio, G. and Nikulin, V. V. [2014], 'Corticomuscular coherence in acute and chronic stroke', *Clinical Neurophysiology* **125**(6), 1182–1191.

[184] Von Wegner, F. and Laufs, H. [2018], 'Information-theoretical analysis of eeg microstate sequences in python', *Frontiers in Neuroinformatics* **12**, 30.

[185] Wade, D. [n.d.], *Measurement in Neurological Rehabilitation*, Oxford medical publications, Oxford University Press.

[186] Wallmann, H. W. [2007], Chapter 5 - muscle fatigue, *in* R. Donatelli, ed., 'Sports-Specific Rehabilitation', Churchill Livingstone, Saint Louis, pp. 87–95.
URL: *https://www.sciencedirect.com/science/article/pii/B9780443066429500083*

[187] Wang, C., Trongnetrpunya, A., Samuel, I. B. H., Ding, M. and Kluger, B. M. [2016], 'Compensatory neural activity in response to cognitive fatigue', *Journal of neuroscience* **36**(14), 3919–3924.

[188] Wang, J. [2018], 'Using Corticomuscular Coherence to Reflect Function Recovery of Paretic Upper Limb after Stroke : A Case Study', **8**(January), 1–6.

[189] Wang, Z., Liu, Z., Chen, L., Liu, S., Xu, M., He, F. and Ming, D. [2022], 'Resting-state electroencephalogram microstate to evaluate post-stroke rehabilitation and associate with clinical scales', *Frontiers in Neuroscience* **16**.

[190] Witte, M., Patino, L., Andrykiewicz, A., Hepp-Reymond, M.-C. and Kristeva, R. [n.d.], 'Modulation of human corticomuscular beta-range coherence with low-level static forces'.

[191] Xi, X., Pi, S., Zhao, Y.-B., Wang, H. and Luo, Z. [2021], 'Effect of muscle fatigue on the cortical-muscle network: a combined electroencephalogram and electromyogram study', *Brain Research* **1752**, 147221.

[192] Xu, R., Wang, Y., Wang, K., Zhang, S., He, C. and Ming, D. [2018], 'Increased corticomuscular coherence and brain activation immediately after short-term neuromuscular electrical stimulation', *Frontiers in Neurology* **9**, 886.

[193] Xu, R., Zhang, C., He, F., Zhao, X., Qi, H. and Zhou, P. [2018], 'How Physical Activities Affect Mental Fatigue Based on EEG Energy , Connectivity , and Complexity', *Frontiers in Neurology* **9**(October), 1–13.

[194] Yang, Q., Fang, Y., Sun, C. K., Siemionow, V., Ranganathan, V. K., Khoshknabi, D., Davis, M. P., Walsh, D., Sahgal, V. and Yue, G. H. [2009], 'Weakening of functional corticomuscular coupling during muscle fatigue', *Brain Research* **1250**, 101–112.

[195] Yap, H. K., Ang, B. W., Lim, J. H., Goh, J. C. and Yeow, C.-H. [2016], A fabric-regulated soft robotic glove with user intent detection using emg and rfid for hand assistive application, *in* '2016 IEEE International Conference on Robotics and Automation (ICRA)', IEEE, pp. 3537–3542.

[196] Zanesco, A. P., King, B. G., Skwara, A. C. and Saron, C. D. [2020], 'Within and between-person correlates of the temporal dynamics of resting eeg microstates', *Neuroimage* **211**, 116631.

[197] Zappasodi, F., Croce, P., Giordani, A., Assenza, G., Giannantoni, N. M., Profice, P., Granata, G., Rossini, P. M. and Tecchio, F. [2017], 'Prognostic value of eeg microstates in acute stroke', *Brain topography* **30**, 698–710.

[198] Zhang, K., Shi, W., Wang, C., Li, Y., Liu, Z., Liu, T., Li, J., Yan, X., Wang, Q., Cao, Z. et al. [2021], 'Reliability of eeg microstate analysis at different electrode densities during propofol-induced transitions of brain states', *NeuroImage* **231**, 117861.

[199] Zhao, S., Lin, H., Chi, A. and Gao, Y. [2023], 'Effects of acute exercise fatigue on the spatiotemporal dynamics of resting-state large-scale brain networks', *Frontiers in neuroscience* **17**.

[200] Zheng, Y., Peng, Y., Xu, G., Li, L. and Wang, J. [2018], 'Using corticomuscular coherence to reflect function recovery of paretic upper limb after stroke: a case study', *Frontiers in neurology* **8**, 728.

[201] Zwarts, M., Bleijenberg, G. and Van Engelen, B. [2008], 'Clinical neurophysiology of fatigue', *Clinical neurophysiology* **119**(1), 2–10.